DESIGN AND CHARACTERIZATION OF COMPUTATIONALLY OPTIMIZED BROADLY REACTIVE ANTIGEN (COBRA) VACCINES AGAINST HUMAN SEASONAL INFLUENZA A(H3N2) VIRUSES

by

JAMES D. ALLEN

(Under the Direction of Ted M. Ross)

ABSTRACT

Influenza viruses (*Orthomyxoviridae*) cause acute respiratory diseases in humans that inflict a significant amount of morbidity and mortality every year around the world. Currently, vaccination is the most effective means of preventing seasonal influenza virus infections. However, traditional inactivated wild-type (WT) vaccines often have difficulty preventing illness caused by antigenically drifted strains. This is particularly true for influenza vaccines targeting H3N2 influenza viruses. Methodologies for generating broadly reactive influenza vaccines exist, and offer potential solutions to this problem, but over time the protection offered by these vaccines may wane as influenza viruses naturally evolve to evade host immunity. Thus, developing a method to update broadly reactive vaccine antigens to better protect against antigenically drifted co-circulating viral variants is of great importance. Building upon the computationally optimized broadly reactive antigen (COBRA) methodology for designing influenza hemagglutinin (HA) vaccines, this study describes a next-generation COBRA design methodology that utilizes current seasonal surveillance information, in combination with consensus-based layered sequence

building approaches, to produce broadly reactive influenza HA vaccine candidates that can be updated in real time to keep pace with the ever-changing H3N2 viral landscape. Using this next-generation COBRA design methodology, multiple H3 HA vaccine antigens were generated on a seasonal basis from 2002-2019, and tested in influenza naive mice and pre-immune ferrets for their ability to elicit broadly reactive antibodies against historical H3N2 WT vaccine strain isolates as well as antigenically drifted co-circulating H3N2 strains. The H3 COBRA HA antigens were superior to WT HA vaccine antigens at eliciting sero-protective hemagglutination inhibition (HAI) reactive antibodies against historical and antigenically drifted H3N2 viruses from the last 15 years, and also displayed the ability to neutralize infections from newly emerging H3N2 isolates. The lead H3 COBRA HA candidates were then mixed with an H1 COBRA HA antigen, and they were administered together as a bivalent HA vaccine to mice that were pre-immune to both H1N1 and H3N2 influenza viruses. The bivalent mixtures of COBRA H1+H3 antigens outperformed bivalent mixtures of WT H1+H3 HA antigens by eliciting sero-protective HAI antibody titers against all of the H1N1 and H3N2 historical vaccine strain isolates from 2009-2019.

INDEX WORDS: Influenza, vaccine, H3N2, hemagglutinin, universal, broadly reactive, HA, pre-immunity, original antigenic sin, next-generation, COBRA, computationally optimized broadly reactive antigen

DESIGN AND CHARACTERIZATION OF COMPUTATIONALLY OPTIMIZED BROADLY REACTIVE ANTIGEN (COBRA) VACCINES AGAINST HUMAN SEASONAL INFLUENZA A(H3N2) VIRUSES

by

JAMES D. ALLEN

BS, Louisiana State University, 2010

MS, University of Miami, 2013

A Dissertation Submitted to the Graduate Faculty of The University of Georgia in Partial Fulfillment of the Requirements for the Degree

DOCTOR OF PHILOSOPHY

ATHENS, GEORGIA

2021

DESIGN AND CHARACTERIZATION OF COMPUTATIONALLY OPTIMIZED BROADLY REACTIVE ANTIGEN (COBRA) VACCINES AGAINST HUMAN SEASONAL INFLEUZNA A(H3N2) VIRUSES

by

JAMES D. ALLEN

Major Professor:	Ted M. Ross
Committee:	Donald Harn
	Jarrod Mousa
	Jeff Hogan
	Daniela de Souza Rajao

Electronic Version Approved:

Ron Walcott
Vice Provost for Graduate Education and Dean of the Graduate School
The University of Georgia
December 2021

DEDICATION

To my father, Dr. Douglas S. Allen, for instilling a love of science and a curiosity for research in me from a very young age. I will never forget our time spent together, and I will carry your memory with me always.

ACKNOWLEDGEMENTS

I would like to thank my advisor and mentor, Dr. Ted Ross, for his continual guidance and support. His undying dedication and passion for science is a continual source of inspiration, and I am very fortunate to have him as a role model. I would also like to thank the other members of my graduate committee, Dr. Don Harn, Dr. Jarrod Mousa, Dr. Jeff Hogan, and Dr. Daniela de Souza Rajao for their invaluable advice and insight in regards to my research during my graduate studies.

I would also like to thank the past and present members of the Ross lab for their roles in assisting with my research and my development as a scientist. I appreciate you all for treating me as both a peer and a collaborator. I would like to thank all of my undergraduate student workers, John Ingram, Arnel Sicam, Carswell Leis, Ummar Jamal, and Alexandra Abu-Shmais for all of their assistance in performing the science necessary for completing this thesis work. I would also like to thank the other graduate students in the lab, Naoko Uno, Michael Carlock, Ivette Nunez, Beau Reneer, Amanda Skarlupka, Pedro Sanchez, Pan Ge, Robert Richardson, and Spencer Pierce for their assistance with my benchwork as well as my animal studies. I would like to thank the post docs and researchers, Dr. Greg Kirchenbaum, Dr. Rodrigo Abreu, Dr. Giuseppe Sautto, Dr. Hyesun Jang, Dr. Ying Huang, Dr. David Forgacs, Jeff Ecker, and Robert Cooper for their assistance with assay development, animal work, protein production, and for their moral support. I am truly honored to have worked with so many brilliant and wonderful people during my time in the Ross lab.

I would also like to thank my family for their constant love and support throughout this process, especially my wife Elizabeth, and my daughter Christina. I could not have done this without you both. I would also like to thank my mother, Kathy, and my brother, Brian, for their continued love and constant support to always follow my dreams. I could not have done all of this work without you, and I love you all.

TABLE OF CONTENTS

Page

LIST OF TABLES

Page

LIST OF FIGURES

Page

CHAPTER 1

INTRODUCTION

Influenza A viruses (Orthomyxoviridae) from the H1N1 and H3N2 subtypes currently circulate in humans and infect 5-15% of the world's population annually. The World Health Organization estimates that these infections result in 250,000 to 500,000 deaths every year. In general, influenza seasons in which H3N2 viruses are prevalent tend to be more severe with a greater number of hospitalizations and deaths [1]. The 2017-2018 influenza season, dominated by H3N2 virus circulation, was particularly severe and saw the third most outpatient visits for influenza like illnesses in the last 20 years [2]. Additionally, during the 2018-2019 flu season, the H3N2 component of the influenza vaccine exhibited a poor protective efficacy of approximately 22% at preventing infection against co-circulating strains [3]. Currently wild-type influenza strains are chosen annually for inclusion in seasonal vaccines, but these antigens can be limited in the amount of antigenic breadth that they induce in their recipients [4]. Therefore, there is a need to design more broadly reactive H3N2 influenza seasonal vaccine antigens capable of generating antibodies that are reactive against drift variants as well as the dominant strains in circulation. Changing the way that we generate vaccine antigens could ultimately help bring vaccine design into the modern era. The studies described herein aim to update and industrialize previously published methods for generating computationally optimized broadly reactive antigens (COBRAs) for use as influenza vaccines by modifying their design approach to focus on seasonal H3N2 influenza drift variants present in the human population over the most recent seasons of circulation,

and characterize the antibody responses elicited by these antigens in both influenza naïve and pre-immune animal models.

The concept of developing a method to industrialize the design of broadly reactive COBRA vaccines on a seasonal basis is indeed innovative. Updating broadly reactive vaccine antigens based on influenza drift variants from the most recent seasons of circulation allows the natural evolution of the pathogen to dictate intelligent vaccine design. Additionally, most pre-clinical vaccines are only tested in naïve animal models which may not accurately represent the immune status of most adult humans [5]. Testing these next generation H3 hemagglutinin (HA) vaccine candidates in both naïve and pre-immune animal models will provide valuable information on how these antigens are likely to perform in the human population before they ever reach the clinic. These studies will advance the process of vaccine design and how vaccines are evaluated in the pre-clinical setting.

Annual seasonal influenza vaccines are composed of two wild-type influenza A strains representing the H1N1 and H3N2 subtypes, and two influenza B strains representing the Victoria and Yamagata lineages [6, 7]. Strains from these Influenza A and Influenza B subtypes currently co-circulate in humans posing a threat to their health and wellbeing [8]. In particular, influenza A H3N2 outbreaks have caused widespread illness to humans many times throughout history. The worst such documented outbreak occurred in 1968 when an avian reassortant virus of the H3N2 subtype was introduced into the human population causing a global pandemic associated with more than one million deaths world-wide. Prior to this outbreak there was no documentation of H3N2 viruses circulating in humans [4]. Further examination of this virus, A/Hong Kong/1/1968, provided evidence that the HA and PB1 fragments of previously circulating avian H3N2 viruses,

and the NA from the H2N2 pandemic strain of 1957 recombined into a new viral strain of H3N2 that possessed the ability to infect and transmit between humans [9].

Since their introduction in 1968, H3N2 influenza viruses have undergone extensive genetic and antigenic evolution leading to numerous seasonal epidemics, exemplified by the WHO recommending 29 H3N2 vaccine strain changes over the last 50 years [10]. The rapid evolution of influenza viruses often creates difficulties for experts to recognize and predict current and future epidemiological threats [6,7]. Typically, the strains that are chosen for use in the vaccine are viruses that are most prevalent in clinics around the world, but this method can often lead to the selection of strains that provide limited protection against co-circulating viral variants [11, 12].

To address the need for more broadly reactive influenza A vaccines, the Ross lab has previously reported on a methodology of antigen design, termed COBRA, which utilizes multiple rounds of layered consensus building to generate influenza vaccine hemagglutinin (HA) immunogens. COBRA HA antigens are capable of eliciting broadly reactive HA-specific antibody responses that can protect against both seasonal and pandemic influenza strains that have undergone genetic drift [13]. Overall, the goal of this research is to develop a new COBRA design methodology that generates H3 HA vaccine antigens that are suitable for individuals with diverse influenza pre-immune backgrounds, effective against 75% of influenza strains in a given season, and induce durable protection that lasts at least one year into the future. This is based on the central hypothesis that the COBRA H3 HA antigens generated through the next generation methodology will elicit broadly reactive antibodies capable of inducing more robust HAI and infection neutralizing titers than historical vaccine strains when tested against panels of historical, co-circulating, and future drifted influenza A(H3N2) viruses.

To test the COBRA vaccine antigens, the following specific aims were pursued:

Specific Aim 1: Design, generate, and evaluate next generation H3 COBRA HA influenza vaccines in an influenza naïve mouse model.

The working hypothesis is that the next generation COBRA H3 virus like particle (VLP) vaccinated mice will generate broadly reactive hemagglutination inhibition (HAI) antibodies against more H3N2 strains in circulation during 2004-2016 than those vaccinated with wild-type (WT) H3N2 antigens.

Specific Aim 2: Evaluate H3 COBRA HA vaccines in ferrets that are both naïve and pre-immune to H3N2 viruses from specific influenza antigenic eras.

The working hypothesis is that pre-immune animals that receive next generation COBRA H3 vaccinations will elicit antibodies against more strains in an H3N2 HAI breadth panel than those that receive WT vaccines, and these responses will vary based on the animal's prior H3N2 antigenic exposure.

Specific Aim 3: Evaluate bivalent mixtures of H1 and H3 COBRA HA vaccine antigens for expansion of immunologic breadth in mice that are pre-immune to both H1N1 and H3N2 influenza viruses.

The working hypothesis is that pre-immune animals vaccinated with bivalent formulations of H1 and H3 COBRA HA's will elicit broadly reactive antibodies against more H1N1 and H3N2 historical vaccine strains in an HAI breadth panel, and in neutralization assays than those that receive bivalent mixtures of WT HA vaccines.

CHAPTER 2

LITERATURE REVIEW[1]

[1]Allen, James D. and Ross, Ted M. *H3N2 Influenza Viruses in Humans: Viral Mechanisms, Evolution, and Evaluation.* Human Vaccines & Immunotherapeutics. 2018, **14**(8):1840–1847. Reprinted here with permission of the publisher. This is an Accepted Manuscript of an article published by Taylor & Francis in Journal of Human Vaccines & Immunotherapeutics on March 2018, available online: doi:10.1080/21645515.2018.1462639.

Introduction

Influenza is a respiratory illness that infects between 5-15% of the global population annually. The World Health Organization (WHO) estimates that these infections result in 250,000 to 500,000 deaths every year [1]. Those suffering from an influenza infection commonly display symptoms such as fever, sore throat, coughing, nasal discharge, headache, and myalgia. More severe cases can also lead to the development of conditions such as bronchitis or pneumonia [14]. Influenza outbreaks have caused widespread illness to humans many times throughout history. In 1968 an avian reassortant virus of the H3N2 subtype was introduced into the human population that caused a global pandemic associated with more than one million deaths world-wide [4]. More recently in 2009 an influenza pandemic caused by a novel strain of H1N1 resulted in millions of infections in more than 214 countries [15]. Since their introduction in 1968, H3N2 influenza viruses have undergone extensive genetic and antigenic evolution leading to numerous seasonal epidemics, exemplified by the WHO recommending 28 vaccine strain changes over that period of time. H3N2 influenza viruses have also altered their receptor binding properties over the last half century, and are beginning to display a reduced affinity for oligosaccharide analogues of cell surface receptors [10]. Recent H3N2 influenza vaccine effectiveness studies in the U.S. and in Europe from the 2016/2017 season in people showed a poor efficacy (~28-42%) for all age groups [16]. The rapid evolution of influenza viruses creates difficulties for experts to recognize and predict current and future epidemiological threats [17]. The WHO meets twice a year to recommend strains that will be included in the seasonal influenza vaccine. This is based primarily from results of hemagglutination inhibition (HAI) assays that compare antibody titers of reference ferret antiserum to currently circulating influenza isolates [18]. The HAI assay detects antibodies that bind to the viral hemagglutinin and prevent the virus-mediated agglutination of erythrocytes

[19]. However recent studies have demonstrated that most modern H3N2 strains have gained the ability to agglutinate red blood cells through neuraminidase-sialic acid interactions [20]. Therefore, many researchers have modified existing assays and developed new ways to characterize these modern H3N2 influenza viruses. One of the more common modifications includes the addition of Oseltamivir carboxylate, a neuraminidase inhibitor, into the HAI assay in order to ablate neuraminidase binding prior to host entry [21]. This review seeks to investigate these recent changes in modern H3N2 viruses and explore the methods that researchers are currently developing to analyze this ever-adapting pathogen.

Viral Life Cycle

There are currently three types of influenza viruses: A, B, and C [15]. Influenza and other members of the family Orthomyxoviridae are enveloped viruses characterized by having segmented, negative-sense RNA genomes [22, 23]. Influenza A viruses (IAV) can infect humans, birds, pigs, horses and other animals while influenza B and C viruses are only found in humans [1]. IAV are subtyped according to their surface glycoproteins hemagglutinin (HA) and neuraminidase (NA) [24, 25]. Currently there are 18 known subtypes of HA (H1-18) and 11 of NA (N1-11), but only a limited number of these i.e., H1N1 and H3N2 currently circulate in humans [14, 26]. HA is a trimeric glycoprotein that is typically classified in two groups: group 1 contains H1, H2, H5, H6, H8, H9, H11, H12, H13, and H16 while group 2 includes H3, H4, H7, H10, H14, H15. Recently two more HA subtypes, H17 and H18, have been discovered in bats. NA is a tetrameric glycoprotein that is divided into three groups: group 1 (N1, N4, N5, and N8), group 2 (N2, N3, N6, N7, N9), and group 3, which contain NA from B influenza viruses. N10 and N11 have only recently been discovered and primarily circulate in bats [27]. The IAV surface is

composed of a host cell derived lipid membrane that is studded with glycoprotein projections of HA and NA at a ratio around 4:1 respectively [28]. Also present on the outer membrane of IAV are a number of smaller matrix (M2) ion channels, which aid in viral un-coating, and M1 proteins which form a matrix that encloses the viral core [22]. The viral core houses the eight viral RNA segments. Two of the segments encode pre-mRNA that is eventually spliced to produce the nuclear export protein (NEP or NS1) as well as M1 and M2. The other six segments consist of mRNA that are translated into nucleoprotein (NP), polymerase subunit (PA, PB1, or PB2), HA, and NA [14].

The influenza infection cycle begins when HA on the viral surface binds to sialic-acid (SA) containing glycan receptors on the host cell surface [20]. SAs are commonly found on the surface of many cells located in the respiratory tract such as epithelial cells, dendritic cells, and alveolar macrophages [14]. The efficiency of the binding to SA depends both on the type of SA, and the type of linkage that connects the SA residue with the oligosaccharide of the receptor molecule. It has been shown that human influenza viruses preferentially bind to SA attached to galactose by an α2,6 linkage, while equine and avian viruses prefer α2,3 linked SA molecules [25, 29, 30]. After binding to SA, the virus is then internalized by the host cell through the process of endocytosis, and the virus is encapsulated in an endosome. The endosome possesses a low pH around 5 to 6 which triggers the fusion of the viral membrane with the endosome [20]. For membrane fusion to occur the HA precursor (HA_0) must be cleaved into two polypeptides, HA_1 and HA_2, which are linked by a disulphide bond [17]. This exposes a fusion peptide on HA_2 that mediates the merging of the viral envelope with the endosomal membrane. Meanwhile the M2 ion channel provides a route for hydrogen ions to diffuse into the virus particle which disrupts the internal protein-protein

interactions, and allows the viral RNPs to be released from the viral matrix into the host cell cytoplasm [22].

Once the viral RNPs have been released they are directed into the host nucleus with the help of viral localization signals [15]. In the nucleus, negative sense viral RNA is transcribed into positive sense mRNA using viral polymerase. The polymerase snatches 5' caps from cellular RNA and 3' RNA is polyadenylated in order to make viral pre-mRNA [14]. Also synthesized from the viral RNA is complementary RNA that RNA polymerase uses to transcribe more copies of negative–sense genomic viral RNA allowing the virus to efficiently replicate its genomic material [22]. Once the viral mRNA is capped and polyadenylated it is ready to be exported out of the nucleus and translated into proteins by the host ribosomes. The newly assembled proteins are then transported to the apical side of the cell membrane where the virions are assembled [14]. At this point discrete packaging signals on all viral RNA segments ensure that a full genome and the surface proteins HA, NA, and M2 are properly incorporated into the newly formed virus particles [22]. The mature HA protein is composed of three pairs of the HA_1/HA_2 subunits comprising a trimer, while NA is assembled as a tetramer [31].

Viral release from the host cell is initiated by an accumulation of M1 at the cytoplasmic side of the cell membrane. When budding is complete the HA continues to bind the SA on the host cell until it is cleaved by the sialidase activity of the NA protein [22]. This facilitates the release of progeny virions from the host cell. Additionally sialidase activity of NA is able to remove SA residues from the viral surface helping prevent newly assembled viruses from aggregating near the cell surface and enhancing infectivity [15]. Influenza viruses have a relatively simple replication cycle. However, their segmented genome, and their error-prone RNA-dependent RNA polymerases enable them to evade adaptive immune responses in a range of host

species. Therefore developing a long lasting vaccine against these viruses can be very challenging [22].

H3N2 Introduction & Evolution in Humans

H3N2 is responsible for one of the three major influenza pandemics that occurred in the last century. In 1968, a novel strain of H3N2 influenza virus emerged in Hong Kong (A/Hong Kong/1/1968 [HK/68]) that quickly led to a global epidemic that was associated with more than one million deaths world-wide [4]. Prior to this outbreak there was no documentation of H3N2 viruses circulating in humans. Most likely, circulating human H2N2 viruses re-assorted with avian H3N2 influenza viruses that resulted in a novel H3N2 viral strain that possessed the ability to infect and transmit between humans [23, 32]. Further examination of this virus provided evidence that the HA and PB1 fragments of avian H3N2, and the NA from the H2N2 pandemic strain of 1957 combined into a new viral strain of H3N2 [4, 27]. H2N2 and H2N3 viruses continued to co-circulate in humans until 1971 when H2N2 viruses began to wane from human circulation. However since 1968 H3N2 IAVs have circulated seasonally in the human population resulting in numerous epidemics, significant morbidity, and substantial mortality [23].

Hemagglutinin proteins on the surface of pandemic influenza viruses typically differ from their avian precursors by at least one or two mutations in the receptor binding site (RBS) that alter viral receptor specificity from preferentially binding to α2,3 linked SAs with α2,6 SAs. A combination of five amino acid substitutions in the HA of the Hong Kong 1968 H3N2 isolates were associated with the bird-to-human adaptation and pandemic emergence of these viruses [32]. Reassortment between influenza viruses, mutations, and genomic evolution are some of the ways for the virus to increase diversity in viral protein sequences, escape antibody pressure, and evade

the host's immune system [23]. IAVs typically evade the host immune response by changing the antigenicity of HA and NA, both gradually through antigenic drift, and abruptly through what is known as antigenic shift [26]. Groundbreaking work in the 1980s identified 131 amino acid positions in five antigenic sites (A-E) in the globular head of H3 near the RBS as the main targets for specific antibodies, and suggested that antigenic drift is likely caused by substitutions in these sites [33].

The virus can also escape immune pressure through the addition of N-linked glycosylation sites on the globular head of its glycoproteins. These sites support the attachment of sugar molecules to the side chain amide nitrogen of Asn (N) found in the sequon Asn-X-Ser/Thr where X may represent any amino acid except Pro [4]. The N-glycosylations of the HA and NA act to mask antigenic epitopes, limit binding to host antibodies, and protect the enzymatic sites of NA [24]. To date there has been no O-linked glycosylation (e.g., attachment of a sugar molecule to the hydroxyl group of Ser or Thr on the polypeptide chain) reported for IAVs. The globular head of HK/68 contained two N-glycosylation sites at residues 81 and 165. Since introduction into the human population, H3N2 viruses have evolved and gained up to 7 additional N-glycosylation sites on the HA globular head, and 5 on the HA stem region [4, 30]. The HA of the most recent H3N2 vaccine strain, A/Hong Kong/4801/2014, has 11 N-glycosylation sites, while the NA contains 8 motifs [24]. N-glycans are beneficial to the virus because they can physically interfere with the binding of antibodies to antigenic sites, but they may also be detrimental to viral fitness since these glycans may mask the RBS and reduce the receptor binding activity [34-36]. The receptor binding properties of HA are determined not only by amino acid residues forming the RBS, but also by glycan interactions with HA residues near the binding pocket [4]. This progressive accumulation

of N-glycosylation sites allows for the virus to escape antibody-mediated responses, thus playing a role in antigenic drift [37].

In addition to gaining N-glycosylation sites H3 HAs have also increased their overall electric potential. The net charge of the HA molecule is an important feature that effects viral antigenicity and receptor binding affinity. During viral adsorption a higher positive charge could promote the binding of HA to its negatively charged host cell sialic acid receptors. Since 1968 the net number of positively charged amino acids in the H3 HA molecule has increased on average from +7 to +17.8 [24]. These charged amino acid changes raise the avidity of the virus possibly allowing it to bind to the host cell receptor before recognition by antibodies. The change in the positive charge of H3 HA appears to parallel the addition of N-glycosylation sites on the molecule. Therefore, the positive charge of HA may have increased to compensate for the deleterious effects of gaining more N-glycosylations during the evolution of the human H3N2 virus [34].

Since its introduction to the human population in 1968, H3N2 has been constantly evolving to evade host immune pressures. Escape is primarily achieved through the addition of N-glycosylation sites, antigenic drift, and charged amino acid substitutions near the RBS. Adaptations of H3 IAVs have appeared so quickly that since 1968 the WHO has recommended 28 vaccine strain changes [10]. In the last ten years alone there have been six suggested H3N2 influenza vaccine strain changes. This is primarily due to the emergence of novel clades and sub-clades of H3N2 IAVs. Clades are typically defined by amino acid substitutions that occur as the virus progeny diversify from parental strains. These substitutions can be functionally relevant as they may influence the antigenicity and susceptibility to neutralizing antibodies induced by infection with other lineages of H3N2 [38]. The rapid mutation rate of human H3N2 IAVs results in the appearance of antigenically novel viruses every 2 to 5 years [39]. Sequence evolution within

these periods can confine antigenic drift of the virus to a group of sequence variants with similar antigenic properties, which is referred to as an antigenic clade [17]. Currently the majority of H3N2 IAVs in circulation belong to clades 3C.2a and 3c.3a [40]. WHO reference laboratories suggest that the strains in the A (H3N2) clades, 3c.2a and 3c.3a were diversified from 3c.2 and 3c.3, respectively and thereafter the 3c.2a clade dominated over 3c.3a [10, 31]. This is exemplified by the WHO choosing a representative of clade 3c.2a, A/Hong Kong/4801/2014 (HK/14), to be included in the northern hemisphere vaccine for the 2016/2017 and 2017/2018 seasons [16].

H3N2 IAVs belonging to clade 3c.2a first emerged during the 2014/2015-influenza season [31]. These viruses differed from the previous vaccine strain, A/Texas/50/2012 (Tx/12) (Clade 3c.1), by ~10-12 amino acids. Notably substitutions F159Y and K160T occurred at antigenic site B together with an existing N at site 158 represented the potential gain of a glycosylation site that is likely to mask viral epitopes and reduce antibody access to the antigenic site (Fig. 1)[40, 41]. These mutations in antigenic site B significantly decrease the binding of ferret, sheep, and human antibodies elicited by the Tx/12 vaccine strain. During the same influenza season another A (H3N2) clade, 3c.3a, also co-circulated in humans [31]. Both clade 3c.2a and 3c.3a viruses were determined to be antigenically distinct from Tx/12, and therefore the WHO recommended that the 2015/2016 H3N2 component of the northern hemisphere influenza vaccine be updated with an A/Switzerland/9715293/2013-like (Sz/13)(clade 3c.3a) virus [41]. However antigenic site B of clades 3c.2a and 3c.3a viruses differ due to the glycosylation at site 159 found on 3c.2a viruses, and by early 2015 the 3c.3a viruses began to wane from human circulation (Fig. 1)[31, 41]. It is possible that the additional glycosylation site conferred a selective evolutionary advantage that allowed 3c.2a viruses to be more efficient at human-to-human transmission than 3c.3a viruses [31]. As a result, the WHO once again recommended a vaccine strain change for the northern

hemisphere to include a clade 3c.2a representative, A/Hong Kong/4801/2014 (HK/14), for the 2016/2017 season [16, 40].

Clade 3c.2a viruses can currently be divided into sub-clades 3c.2a1 and 3c.3a2 both of which carry the mutation N121K which separates them from clade 3c.2a (Fig. 2.1) [38]. Viruses belonging to 3c.2a1 carry a signature amino acid substitution N171K located on antigenic site D. These viruses can be further characterized by substitutions D122N and T135K in antigenic site A that each cause the loss of N-linked glycosylation sites [16]. Clade 3c.2a2 viruses belong to a newly emerging group that is not yet recognized as an official clade by the WHO [16, 38]. Viruses from this clade are distinguished by the S144K substitution, which is located in an antigenic site flanking the RBS. 3c.2a2 viruses can be further categorized into two clusters. Cluster I possesses substitutions I58V and S219Y, and cluster II contains N122D and S262N substitutions, with N122D resulting in the loss of a potential N-linked glycosylation site (Fig. 2.1) [38]. Influenza surveillance and vaccine efficacy studies from the 2016/2017 influenza season in Greece, London, Canada, and Japan have all linked recent A (H3N2) epidemics to newly emerged clade 3c.2a viruses [16, 31, 38, 40]. The recommendation by the WHO to include the same H3N2 vaccine virus, HK/14, in the 2017/2018 vaccines indicates that the viruses of the newly emerged sub-clades are antigenically similar to HK/14. Nevertheless, there is an increased level of genetic diversification observed among circulating 3c.2a1 viruses, leading the WHO to once again recommend another vaccine strain change for the upcoming 2018/2019 season to a clade 3c.2a1 virus, A/Singapore/INFIMH-16-0019/2016 (Sing/16)(Fig 2.1) [16, 42]. Therefore, as new H3N2 strains emerge and spread, the genetic composition of these viruses is closely monitored due to the frequency of antigenic drift variants emerging and escaping vaccine induced protection.

Hemagglutination of Modern H3N2 Viruses

Assays that detect serum antibody concentrations are often used as correlates of protection for influenza virus infections. One of the most common assays for quantifying serum antibody titers is the hemagglutination inhibition assay (HAI). The HAI assay identifies antibodies that can prevent the agglutination of erythrocytes by the HA of an influenza virus [18]. The antibody concentration can then be quantified by taking the reciprocal of the highest serum dilution that completely inhibits the binding of the virus to the red blood cells (RBCs). An HAI titer ≥40 is associated with a 50% or higher protection against influenza infection compared to an HAI titer <10 [19, 43, 44]. However, this correlate of protection has been established from studies performed in healthy adults, and is not appropriate for predicting protection in children [19, 44].

The HAI assay also faces a few technical challenges, such as variations among erythrocytes from different species and inconsistencies between batches of erythrocytes from the same species [19]. The binding efficiency of influenza HA to the host SA is dependent on both the type of SA and the type of linkage that connects the SA with the oligosaccharide of the receptor molecule [29]. RBCs from different mammalian and avian species express surface SAs of various linkages, which make selecting the optimal RBCs to perform HAI assays challenging [36]. Equine and bovine RBCs display mainly α2,3 linked SA molecules, while avian and human RBCs display both α2,3 and α2,6 linked SA molecules. Typically, human influenza viruses agglutinate human, guinea pig, and avian RBCs, but not RBCs from horses or cows. However, H3N2 viruses from 2005 to present no longer agglutinate avian RBCs, but retain the ability to agglutinate guinea pig and human RBCs [29, 45]. Guinea pig and human RBCs display nearly threefold more α2,6 than α2,3 linked SA molecules when compared to avian RBCs indicating that modern H3N2 viruses may preferentially bind to α2,6 linked SA molecules [29, 36]. Surface biolayer interferometry

(BLI) assays analyzing H3N2 viral binding to polyacrylamide-linked polyvalent receptor analogues of α2,3-sialyl lactosamine and α2,6-sialyl lactosamine show a similar trend of recent H3N2 viruses preferentially binding to α2,6-linked molecules [25, 36, 45, 46]. As a result, many researchers now use guinea pig RBCs as targets in their HAI assays when analyzing recent H3N2 viruses [46, 47].

Viral Growth and Propagation

The ability to isolate and propagate H3N2 IAVs is essential to perform annual surveillance of circulating viruses as well as to determine the antigenic and antiviral sensitivity of different strains. Traditionally, IAVs are propagated in embryonated chicken eggs, and many manufacturers still use this medium to produce their vaccines today. Immortalized mammalian cell lines have also been used to propagate and isolate IAVs in scientific laboratories since the 1960's. The process is a relatively simple, sensitive, and cost-effective method [36, 48]. Numerous cell lines such as BHK-21, SPJL, LLC-MK2, and Vero cells have been successfully used for viral growth, but Madin-Darby canine kidney (MDCK) cells are the most reliable, sensitive, and easy to handle cell line. Influenza viruses isolated from MDCK cell cultures retain the same HA sequence as the original virus isolated from influenza infected subjects, whereas viruses propagated in embryonated chicken eggs occasionally mutate and display a different HA from the original source [29, 35].

MDCK cells express both α2,3 and α2,6-linked SA receptors on their surface allowing both human and avian influenza viruses to be isolated from MDCK cultures with high hemagglutination (HA) titers [29, 48]. However, in recent years most H3N2 IAV isolates have exhibited poor growth in MDCK cultures, and display a preferential binding to α2,6-linked SA molecules [29, 30, 35,

36]. When compared to human respiratory cells the amount of α2,6-linked SA receptors on MDCK cells are relatively low, and thus, MDCK cells may no longer be the ideal medium for viral propagation of modern human H3N2 viruses.

To circumvent this development, researchers have engineered a novel cell line, MDCK SIAT1, to overexpress α2,6-linked SA receptors on their surface [48, 49]. Increasing the amount of α2,6-linked SA receptors on the cell surface increases the number of potential interactions between influenza virions and the MDCK SIAT1 cells allowing this modified cell line to be useful for the propagation of recent human H3N2 viruses [25, 48]. MDCK SIAT1 cells are produced by stable transfection of MDCK cells with human CMP-N-acetylneuraminate: β-galactoside α2,6-sialtransferase, an enzyme that catalyzes the α2,6-sialylation of galactose moieties on glycoproteins or glycolipids [48, 49]. Unlike H3N2 viruses isolated from 1968 to 2001, viruses that have emerged after 2001 have decreased ratios of infection in MDCK cells when compared with MDCK SIAT1 cells [10, 47, 48]. As a result, MDCK SIAT1 cells are currently the preferred medium for propagation of modern H3N2 viruses because of their ability to maintain the faithful replication and infectivity of the virus, while avoiding the generation of defective viruses [10]. This shift towards propagating recent H3N2 viruses in cell cultures is further evidenced by the inclusion of cell propagated H3N2 viruses in the recommended list of vaccine viruses for the 2017/18 influenza season [16].

NA Binding in Modern H3N2 Viruses

Traditionally the roles of HA and NA during the influenza life cycle are associated with viral entry and release from the host cell respectively. However, the roles of these proteins in modern H3N2 IAVs may not be so clearly partitioned [28]. The NA glycoproteins of recent H3N2

viruses can facilitate viral entry into target cells during infection [15, 20, 21, 28]. Oseltamivir carboxylate, rather than increasing HA titers by inhibiting viral release from RBCs actually repressed the hemagglutination of both turkey and guinea pig RBCs [21]. In addition to its role in viral release, NA promotes viral access to target cells in airways through mucous degradation, aiding in the removal of decoy receptors on mucins, cilia, and cellular glycocalyx, which would impede viral access to the receptors on host cell surfaces [15, 20, 50].

The SA receptor binding activity of NA is associated with amino acid residue 151. A D151G mutation in the active catalytic site of NA causes the protein to bind to SA with increased affinity without cleaving sialic acid moieties [15, 20, 21, 28, 51]. The active site of NA consists of 8 functional residues (R118, D151, R152, R224, E276, R292, R371, and Y406) and 11 framework residues (E119, R165, W178, S179, D198, I222, E227, H274, E277, N294, and E425). These residues are highly conserved among all NA subtypes [15, 52]. Thus, a mutation in one of the functional residues at site 151 could be responsible for a change in the function of NA. The location of residue 151 at the edge of the NA active site, and its sensitivity to oseltamivir suggest that D151 is a critical residue involved in the catalytic activity of NA [20, 21, 30]. Residue D151 may function in wild-type NA to cleave the virus from the SA receptor, but once it is replaced by glycine the NA gains the ability to bind to SA receptors on RBCs [15].

The ability of NA to initiate viral binding to host cells is not unique to N2 subtypes. The G147R mutation in N1 NA also induces receptor-binding activity on the NA in the lab adapted H1N1 strain A/WSN/33. Site 147 is located near the NA active site, and it slightly decreases the sialidase activity of the NA [15, 28]. The G147R N1 mutation has been found in a small number of sequences including some human 2009 pandemic H1N1 strains, human seasonal strains, and chicken H5N1 isolates of various lineages [28]. NAs with the D151G or G147R mutations not

only bind to SA receptors, but they are also sensitive to neuraminidase inhibitors such as oseltamivir and zanamivir [15, 21, 28, 51]. Due to this observation, many researchers are now recommending that 20nM oseltamivir carboxylate be added to the HAI assay protocols when using guinea pig RBCs to inhibit the NA-dependent agglutination caused by modern H3N2 IAVs [15, 21].

H3N2 Neutralization Assays

The current issues occurring with the H3 HAI assay have raised interest in the use of alternative assays to antigenically characterize H3 IAVs [53]. In addition to the HAI, the micro-neutralization (MN) assay is another commonly used technique for determining the immune response induced by influenza vaccines [19]. Ideally in these assays a standard number of infectious units (*e.g.,* 100 50% tissue culture infectious doses ($TCID_{50}$)) is incubated with serial dilutions of serum samples in 96-well plates containing monolayers of MDCK cells. The infection of these cells are commonly assessed by either measuring cytopathic effects (CPE), detecting viral protein synthesis using enzyme-linked immunosorbent assay (ELISA), or by immunostaining virus-infected cells [53]. MN assays can be used to measure both the infectivity of an influenza virus, and the ability of antibodies in serum to neutralize virus replication in MDCK cells [54]. Neutralizing antibodies are generally accepted as primary mediators of immunity against influenza virus infection. The quantity of the antibodies in the MN assay is expressed as the reciprocal of the highest serum dilution that induces at least a 50% reduction in the cytopathic effect of an influenza virus on mammalian cell cultures [43]. As opposed to the HAI assay, to date no correlate of protection has been established for the MN assay [19]. MN assays are commonly used as an alternative to HAI assays because they can overcome non-antigenic effects due to affinity changes

in the receptor binding of different influenza viruses, which can complicate the interpretation of HAI results [54].

Until recently, most MN assays were based on CPE or ELISA assays, but in the 1990s MNs based on focus and plaque reduction that rely on counting visible plaques to quantify infectivity were developed. However, visual counting only captures larger plaques that are resolvable by the human eye, and excludes smaller plaques that are produced by many currently circulating H3N2 viruses [54]. Variation in plaque size and non-uniform morphology can also complicate visual quantification leading to disparity among the examiners, and between experiments leading to incomparable results [55]. In order to alleviate these issues, many researchers are now quantifying viral infection with flatbed scanners and counting software that provides users with a high throughput alternative for enumerating viral plaques [54, 55]. Conventional neutralization assays based on the inhibition of CPE in MDCK cells are also laborious and time-consuming. MN assays that utilize micro-titer plates and a downstream ELISA to detect infected cells is faster than conventional assays and can produce results in as little as two days [44].

The widespread use of multi-well plate assays along with advances in flatbed scanning technology now allow researchers to perform quantitative MN assays suitable for the antigenic characterization of large numbers of viruses, as well as a means for measuring the antiviral activities of neutralizing antibodies [54]. MN assays of this type allow users to measure virus infections on the cellular level, regardless of size, leading to a more sensitive assay that possesses the ability to characterize viruses with low infectivity [54, 55]. Additionally, the automation of the plaque enumerating process allows users to obtain results quickly, while also making their results more comparable between laboratories. Variations in measurements of the same sample

were less than 3%, which correlates to the uncertainty introduced during the image acquisition process [55]. This level of error can be further reduced by averaging images of the same well from multiple scans, but the current level of reproducibility is sufficient to provide data for many virological studies [54, 55]. Although no correlate of protection exists for these assays, their results have generally been consistent with those results obtained through HAI. These assays are also capable of examining the effects of a wider range of antibodies than HAI, making them an interesting tool for characterizing antigenic similarities or differences between H3N2 viruses and vaccines [54].

Conclusion

Since their introduction to humans in 1968, H3N2 IAVs have been rapidly evolving both genetically and antigenically in an attempt to escape host immune pressures. As a result, these viruses have altered themselves in many ways, including the addition of numerous N-linked glycans, increases to the overall net charge of the HA molecule, changes to preferences in receptor binding from α2,3 to α2,6-linked SA receptors, and the ability of NA to agglutinate RBCs prior to host entry. In order to adapt to this constantly changing viral landscape, researchers have been modifying existing assays that are commonly used for the antigenic characterization of H3N2 IAVs. The use of guinea pig red blood cells and the addition of 20nM oseltamivir carboxylate to the HAI assay allows investigators to assess modern H3N2 viruses using traditionally accepted techniques with known correlates of protection. Additionally, advances in MN assays allows for an additional method for assessing H3N2 viruses that can further support the results obtained from the HAI assay, while also providing more information about neutralizing antibodies that interfere with infection. The adaptations acquired by modern H3N2 IAVs create difficulties in recognizing

and predicting current and future epidemiological threats. However, adopting changes to the standard methods used to analyze H3N2 viruses would allow researchers to continue to study and better understand this ever-changing subtype of influenza viruses.

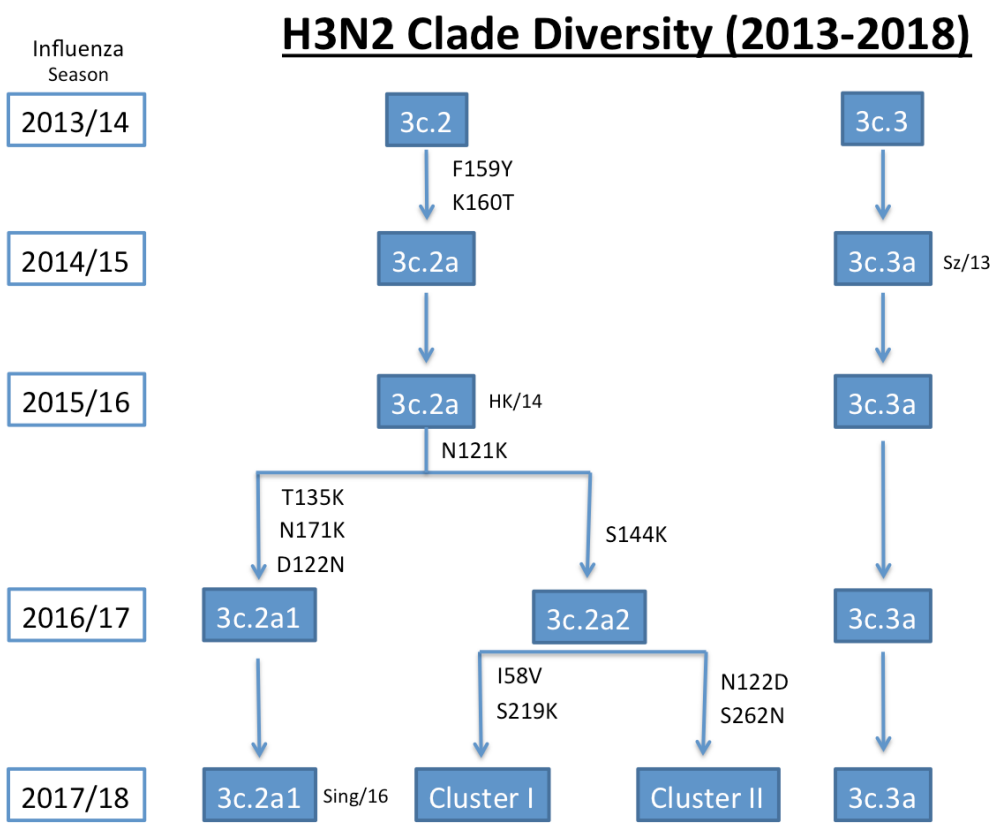

Figure 2.1. An overview of H3N2 IAV clade diversity from 2013-2018. During the 2013/14 season clades 3c.2 and 3c.3 represented the majority of H3N2 strains in human circulation. In the 2014/15 season, 2 new clades began to emerge, 3c.2a, which is characterized by F159Y and K160T mutations, that lead to a potential gain of a glycosylation site, and 3c.3a, from which the vaccine strain A/Switzerland/9715293/2013 emerged. By the 2015/16 season 3c.3a viruses began to wane from circulation resulting in another vaccine strain change to A/Hong Kong/4801/2014 (HK/14), which belongs to clade 3c.2a. In the 2016/17 season clade 3c.2a began diverging into two new clades, 3c.2a1, possessing the characteristic amino acid changes T135K, N171K, and D122N, which resulted in the loss of a glycosylation site, and 3c.2a2, which possess the mutations N121K and S144K. In the 2017/18 season clade 3c.2a2 began to split into cluster I, which is defined by

the I58V and S219K mutations, and cluster II, which contains N122D and S262N mutations, with the N122D mutation representing the potential loss of a glycosylation site. Clades 3c.2a1 of which A/Singapore/INFIMH-16-0019/2016 (Sing/16) belongs, and 3c.3a were also still in circulation during the 2017/18 season.

CHAPTER 3

NEXT GENERATION METHODOLOGY FOR UPDATING HA VACCINES AGAINST EMERGING HUMAN SEASONAL INFLUENZA A(H3N2) VIRUSES[1]

[1]Allen, James D. & Ross, Ted M. *Next Generation Methodology for Updating HA Vaccines Against Emerging Human Seasonal Influenza A (H3N2) Viruses*. Scientific Reports. 2021 Mar 2, **11**(1):1-4. Reprinted here with permission from Springer Nature. This is an Accepted Manuscript of an article published in Scientific Reports on March 2021, available online: doi:10.1038/s41598-020-79590-7.

Abstract

While vaccines remain the best tool for preventing influenza virus infections, they have demonstrated low to moderate effectiveness in recent years. Seasonal influenza vaccines typically consist of HA and NA of wild-type influenza A and B viruses that are limited in their ability to elicit protective immune responses against co-circulating influenza virus variant strains. Improved influenza virus vaccines need to elicit protective immune responses against multiple influenza virus drift variants within each season. Broadly reactive vaccine candidates potentially provide a solution to this problem, but may begin to wane as influenza viruses naturally mutate through processes that mediates drift. Thus, it is necessary to develop a method that commercial vaccine manufacturers can use to update broadly reactive vaccine antigens to better protect against future and currently circulating viral variants. Building upon the COBRA technology, nine next-generation H3N2 influenza hemagglutinin (HA) vaccines were designed using a next generation algorithm and design methodology. These next-generation broadly reactive COBRA H3 HA vaccines were superior to wild-type HA vaccines at eliciting antibodies with high HAI activity against a panel of historical and co-circulating H3N2 influenza viruses isolated over the last 15 years, as well as the ability to neutralize future emerging H3N2 isolates.

Introduction

Influenza A viruses (Orthomyxoviridae) from the A(H1N1) pdm09 and A(H3N2) subtypes currently circulate in humans and cause severe illness in 3-5 million people annually. The World Health Organization (WHO) estimates that these severe infections result in 290,000 to 650,000 respiratory related deaths every year [56, 57]. In general, since 1968 when A(H3N2) viruses emerged in the human population, influenza seasons in which A(H3N2) viruses are prevalent, tend to be more severe with a greater number of hospitalizations and deaths [1]. The 2017-2018 influenza season, dominated by A(H3N2) virus circulation, was particularly severe and led to the third most outpatient visits for influenza virus-like illnesses in the last 20 years, causing over 900,000 hospitalizations and 80,000 deaths [2, 58]. Influenza virus vaccine effectiveness estimates vary across seasons and between different age groups, but they are typically higher against influenza A(H1N1)pdm09 and influenza B than they are against A(H3N2) viruses [59]. During the 2018-2019 influenza season, the A(H3N2) component elicited immune responses that only protected individuals against ~9% of A(H3N2) virus infections [12, 60].

Despite low vaccine effectiveness, vaccination remains the cornerstone to prevent influenza virus infection [61]. Annual seasonal influenza virus vaccines in the United States are typically composed of two influenza A strains representing the A(H1N1) and A(H3N2) subtypes and either one or two influenza B strains representing the Victoria and Yamagata lineages [6, 7]. In some countries trivalent forms of the vaccine containing one H1N1, H3N2, and influenza B strain are still used. Strains from these Influenza A and Influenza B subtypes currently co-circulate and pose a threat to human health and well-being [8]. In particular, influenza A(H3N2) viruses are associated throughout recent history with widespread influenza virus induced illness [4, 27, 62, 63].

Since their introduction to the human population in 1968, A(H3N2) influenza viruses have undergone extensive genetic drift and antigenic evolution leading to numerous seasonal epidemics, exemplified by the WHO recommending 29 A(H3N2) vaccine strain changes over the last 50 years [10]. The rapid evolution of influenza A(H3N2) viruses creates difficulties for experts to recognize and predict current and future epidemiological threats [10, 27, 58]. Typically, the strains that are chosen for use in the vaccine are selected based on predictions of predominant or emerging clades of influenza viruses derived from global surveillance information, but this method can often lead to the selection of antigenically mismatched strains that induce limited antibody protection against co-circulating viral variants [12, 56]. Antigenic mismatches between the chosen vaccine strain and currently circulating viruses often lead to reduced vaccine effectiveness, requiring influenza vaccines to be updated frequently [64].

Designing an influenza virus vaccine that induces both broad antibody reactivity against co-circulating strains and neutralization across multiple future influenza virus seasons is a pivotal challenge for the development of new influenza vaccines [65]. In order to address the need for more broadly reactive influenza A vaccines, a previously reported methodology for enhanced antigen design, computationally optimized broadly reactive antigen (COBRA), which utilizes multiple rounds of layered consensus building to generate influenza vaccine HA immunogens for H1, H3, and H5 influenza subtypes has shown great promise [13, 65-71]. COBRA HA antigens are capable of eliciting broadly reactive HA-specific antibody responses that can protect against both seasonal and pandemic influenza strains that have undergone genetic drift [13, 65, 69]. These vaccine antigens have also been shown to inhibit viral infection and virus induced pathogenesis in various animal models including mice, ferrets, and non-human primates [68, 72-74].

Adapting a broadly reactive influenza virus vaccine design technology, such as COBRA, to industrial settings would be extremely beneficial for both manufacturers and consumers. Aside from potentially reducing the need to update vaccines on an annual basis, technologies like the COBRA methodology provide a promising solution to increase the protection offered by seasonal vaccines against currently co-circulating strains as well as future emerging isolates. The current vaccine manufacturing process takes about 6-8 months from strain selection to vaccine availability and any delays in strain recommendation or antigenic characterization can lead to devastating reductions in the vaccine supply [11, 75]. Thus, having a broadly reactive vaccine candidate, that has already been antigenically characterized, optimized for production, and is "shelf-ready" would save manufacturers a considerable amount of stress and time, while allowing for year-round production of more doses of vaccine.

Previous COBRA design methodologies focused on developing antigens that are broadly reactive against historical and contemporary influenza vaccine strains [13, 68, 71]. However, since A(H3N2) viruses evolve so rapidly through genetic mutation and reassortment, it is likely that the protection offered by a broadly reactive vaccine candidate designed using historical isolates, antigenic eras, and outbreak groups will eventually begin to decline due to the diversity of newly emerging surface epitopes present in the circulating A(H3N2) viral population [13, 76] . Therefore, there is a need to develop a method for updating these broadly reactive vaccines on a seasonal basis to better reflect the diversity present in the population of currently circulating viruses. The method described herein utilizes recent seasonal surveillance information, in combination with novel consensus-based sequence building approaches to provide a unique method for updating broadly reactive influenza virus vaccines designs to better protect people against co-circulating viruses.

In an effort to improve upon the COBRA methodology and enhance vaccine coverage within current and into future influenza A(H3N2) virus seasons, nine next-generation H3 HA antigens were designed utilizing two different scenarios of multi-consensus layering sequence alignment techniques that are unique to this method. These nine next-generation H3 COBRA HA antigens were expressed on the surface of virus like particles (VLP) and used to vaccinate immunologically naïve mice in a prime, boost, boost regimen. Serum samples collected from vaccinated mice were tested against a panel of historical and co-circulating A(H3N2) influenza viruses in both hemagglutination inhibition (HAI) and neutralization assays. Seven of the nine next-generation H3 COBRA HA vaccine candidates outperformed wild-type H3 HA antigens from historical influenza vaccine strains, and displayed the ability to elicit protective HAI antibody titers against numerous co-circulating and future drifted influenza virus variants. The next-generation H3 COBRA HA vaccine antigens also elicited high neutralizing antibody titers against A(H3N2) influenza viruses across a timeframe where 4 different wild-type A(H3N2) vaccine strains were selected as seasonal influenza vaccine candidates. Overall, the H3 HA vaccine antigens produced utilizing this next-generation COBRA methodology were effective at eliciting protective antibody titers against historical, co-circulating, and future drifted strains of A(H3N2) influenza viruses.

Materials and Methods

Antigen construction and synthesis

Full length wild-type influenza A(H3N2) HA protein amino acid sequences, residues 1-566 (starting with Methionine as the first amino acid), from 22,144 human H3N2 virus infections collected from January 1, 2002 to December 31, 2015 were downloaded from the Global Initiative on Sharing Avian Influenza Data (GISAID) EpiFlu online database and organized by their date of

collection. Unlike the traditional COBRA antigen design method, where input sequences are separated based upon the year in which they were collected, this next generation methodology separates isolates based on the representative influenza "season" in which they were collected [13, 66, 71]. In this approach, the downloaded sequences were separated into periods of time representing the "Northern" and "Southern" Hemisphere influenza seasons spanning from 2002-2015. The "Southern Hemisphere" season was defined to include sequences from all over the globe isolated from 5/1/XX – 9/30/XX of a given year, and each "Northern Hemisphere" season was defined to include sequences from around the world that were isolated from 10/1/XX - 4/30/XY of the following year. For example, sequences included in the 2009 "Southern Hemisphere" collection timeframe included those isolated between 5/1/2009 – 9/30/2009, and the isolates included in the 2009-2010 "Northern Hemisphere" collection contains sequences that were isolated between 10/1/2009 – 4/30/2010, regardless of where the sequences were isolated geographically. The HA amino acid sequences for each season were then aligned using Geneious bioinformatics software (Biomatters, Ltd. Auckland, New Zealand), and separated into multiple distinct clusters, which were then used to generate "primary" consensus sequences. The primary sequence clusters were derived using a 99% identity cutoff, which correlates to approximately 5 amino acid differences in the HA molecule. This cutoff was chosen based on the suggestion that influenza virus strains with more than 4 amino acid differences in their HA proteins are of epidemiological importance [77, 78]. This approach differs from the traditional influenza subtype specific COBRA antigen design approach that builds the primary level of consensus sequences from either outbreak groups, antigenic eras, or historical isolates, rather than from the most recent seasons of influenza circulation [13, 66, 71].

For each round of primary consensus generation, a multiple-sequence alignment was performed using the Geneious MUSCLE 3.8.425 alignment algorithm, and phylogenetic trees were constructed using the Jukes-Cantor genetic distance model and a neighbor-joining tree building method, such that trees were rooted to the oldest sequences collected. The full-length HA sequences were then aligned and clustered based on 99% identity. Then the most common amino acid residues found among each designated cluster of viruses was used to generate a primary consensus sequence. The multiple primary consensus sequences from each 6-month season were then aligned, phylogenetically analyzed using the previously described method, and clustered into groups based on phylogenetic similarity from which "secondary" level consensus amino acid sequences were generated. The secondary level sequences were then input into 2 different COBRA consensus building scenarios, which is unique to this next-generation COBRA methodology (Fig. 3.1). Both scenarios start by collecting the secondary sequences from 2.5 years, representing 5 consecutive influenza seasons, aligning them, and using those generate a "backbone" consensus sequence. The first scenario moves forward with time in such a way that the secondary sequences derived from the most recent 6-month period are added to the backbone and the secondary sequences from the oldest season of the now 3-year period are removed (Fig. 3.1A). This process creates an antigen design window that marches forward with time, placing an emphasis on newly emerging strains and eliminating contributions from older strains. The second COBRA consensus building scenario starts with the same 2.5-year back bone and incorporates secondary sequences from the most recent 6-months of influenza virus circulation. This scenario differs from the first, in that it retains the secondary sequences from the oldest influenza season and also adds in the secondary consensus sequences from the most recent 6-month time period

(Fig. 3.1B). This scenario places value on past sequences while also incorporating sequences from the most recent influenza virus season.

Multiple rounds of consensus assembly were layered in both scenarios to yield secondary, tertiary, and quaternary consensus sequences that were designed to represent different antigenic spaces that overlapped periods of time for which multiple wild-type vaccine strains were recommended for inclusion in seasonal vaccine formulations from 2009 to 2015. The antigens were deliberately designed up to 2015 so that these antigens could be tested as vaccines against future emerging H3N2 isolates. This process generated a combination of 27 COBRA antigen sequences from both scenarios of which 9 were unique. The final set of nine amino acid sequences were named the TJ-series. The nine H3 COBRA HA antigens, TJ-1 through TJ-9, were then synthesized and inserted into the pTR600 plasmid expression vector, as previously described and generated as VLPs [79]. The H3 next-generation HA antigens were designed to represent discrete time periods of recent A(H3N2) influenza virus circulation in humans. For example, as a proof of concept, constructs TJ-1 through TJ-4 were designed to represent past periods of time spanning 5 years, constituting the A(H3N2) influenza antigenic space from 2002 to 2007. This timeframe was chosen such that the antibodies elicited by these antigens could be tested against future A(H3N2) influenza isolates. In a similar manner TJ-5 through TJ-9 were generated using the two multi-consensus layering approaches to represent the time period of 2009 to 2015 (Fig. 3.1C).

Vaccine preparation

Mammalian 293T cells were transfected with each of three plasmids expressing either the influenza neuraminidase (A/mallard/Alberta/24/2001, H7N3), the HIV p55 Gag sequence, and one of the various influenza A(H3N2) wild-type HA or H3 COBRA HA expressing plasmids in

previously described mammalian expression vectors [80]. A(H3N2) wild-type influenza HA sequences were obtained from the GISAID EpiFlu database using MDCK passaged sequences which were inserted into the pTR600 expression vector [67]. This included the HA sequences for following H3 antigens: A/Fujian/411/2002 (EPI_ISL_11184) MDCK passage 1 (MDCKP1), A/Wisconsin/67/2005 (EPI_ISL_115646) MDCKP2, A/Brisbane/10/2007 (EPI_ISL_110723) MDCKP1, A/Perth/16/2009 (EPI_ISL_87516) MDCKP2, A/Victoria/361/2011 (EPI_ISL_121879) MDCKP2, A/Texas/50/2012 (EPI_ISL_170149) MDCKP1, A/Switzerland/9715293/2013 (EPI_ISL_166310) MDCKP2, A/Hong Kong/4801/2014 (EPI_ISL_198222) MDCKP2, A/Singapore/IFNIMH-16-0019/2016 (EPI_ISL_296168) MDCKP1. Additionally, the T8 and T11 COBRA HA sequences, which were generated using the traditional H3 COBRA methodology were inserted into the pTR600 expression vector and synthesized as VLP's to serve as comparators between the traditional methodology and the newly proposed next generation methodology. T8 was designed using H3 wild-type sequences from 1999-2012, and T11 using H3 sequences from 2011-2013[13]. Following 72 h of incubation at 37°C, supernatants from transiently transfected HEK 293-T cells were collected, centrifuged to remove cellular debris, and filtered through a 0.22μm pore membrane. Mammalian virus-like particles (VLPs) were purified and sedimented by ultracentrifugation on a 20% glycerol cushion at 135,000 x g for 4h at 4°C. VLPs were resuspended in phosphate buffered saline (PBS) and total protein concentration was assessed by conventional bicinchoninic acid assay (BCA) [19]. Hemagglutination activity of each preparation of VLPs was determined by adding equal volume of 0.75% guinea pig red blood cells (RBCs) to a V-bottom 96-well plate and incubating with serially diluted volumes of VLPs for a 60 min incubation at room temperature (RT). The highest dilution of VLP with full agglutination of RBCs was considered the endpoint HA titer.

Determination of HA content

A high-affinity, 96-well flat bottom ELISA plate was coated with 5-10μg of total protein of VLP and serial dilutions of a recombinant H3 antigen (3006_H3_Vc, Protein Sciences, Meriden, CT) in ELISA carbonate buffer (50mM carbonate buffer, pH 9.5) and the plate was incubated overnight at 4°C on a rocker. The next morning, plates were washed in PBS with 0.05% Tween-20 (PBST), then non-specific epitopes were blocked with 1% bovine serum albumin (BSA) in PBST solution for 1h at RT. Buffer was removed then stalk-specific Group 2 human antibody CR8020 (Sanofi Pasteur, Lyon, France) 1mg/mL, was added to the plate in blocking buffer at a working dilution of 1:4000, and incubated for 1 h at 37°C [81]. Plates were washed, then probed with goat anti-human IgG horseradish-peroxidase-conjugated secondary antibody (1mg/mL) diluted in blocking buffer at a working dilution of 1:4000 (2040-05, Southern Biotech, Birmingham, AL) for 1h at 37°C. Plates were washed then freshly prepared o-phenylenediamine dihydrochloride (OPD) (P8287, Sigma, City, State, USA) substrate in citrate buffer (P4922, Sigma) was added to wells for 3-5 minutes, followed by 1N H_2SO_4 stopping reagent. Plates were read at 492 nm absorbance using a microplate reader (Powerwave XS, Biotek, Winooski, VT) and background was subtracted from negative wells. Linear regression standard curve analysis was performed using the known concentrations of recombinant standard antigen to estimate HA content in VLP lots [19]. COBRA constructs were also analyzed for glycan content by searching for potential glycosylation motifs in the amino acid sequence. Using the sequence motif, N{P}[ST]{P}, to search for potential N-linked glycosylation sites using Geneious annotation software, it was determined that TJ5 through TJ9 all possess the same 12 potential glycosylation sites, and these sites are consistent with those found in wild-type HA's isolated in the last 10 years.

Phylogenetic comparison of next-generation COBRA H3 HA antigens.

A rooted (A/Nanchang/933/1995) phylogenetic tree was inferred from next-generation H3 HA and wild-type HA amino acid sequences derived from representative H3N2 viruses isolated from 1995-2016. Sequences were aligned with MUSCLE 3.8.425 software, and the alignment was refined by Gblocks0.91b software. Phylogeny was determined using a Jukes-Cantor genetic distance model and a neighbor-joining tree building method with Geneious bioinformatics software. Trees were rendered using Geneious tree builder software (Fig. 3.2).

Viruses and HA antigens

Influenza A(H3N2) viruses were obtained through the Influenza Reagents Resource (IRR), BEI Resources, the Centers for Disease Control (CDC), or provided by Virapur (San Diego, CA). Viruses were passaged once in the same growth conditions as they were received, in either embryonated chicken eggs or semi-confluent Madin-Darby canine kidney (MDCK) cell culture as per the instructions provided by the WHO [82]. Virus lots were titered with .75% guinea pig erythrocytes in the presence of 20nM Oseltamivir, and made into aliquots for single-use applications.

The A(H3N2) 1995-2019 WHO recommended historical influenza vaccine strain viral panel included the 16 following viral strains: A/Nanchang/933/1995 (Nan/95) egg passage 3 (EP3), A/Sydney/05/1997 (Syd/97) EP2, A/Panama/2007/1999 (Pan/99) EP4, A/Fujian/411/2002 (Fuj/02) MDCKP1, A/New York/55/2004 (NY/04) EP6, A/Wisconsin/67/2005 (Wisc/05) EP4, A/Brisbane/10/2007 (Bris/07) EP3, A/Perth/16/2009 (Per/09) EP4, A/Victoria/361/2011 (Vic/11) EP4, A/Texas/50/2012 (Tx/12) EP4, A/Switzerland/9715293/2013 (Switz/13) EP4, A/Hong Kong/4801/2014 (HK/14) EP11, and A/Singapore/IFNIMH-16-0019/2016 (Sing/16) EP3,

A/Kansas/14/2017 (Kan/17) EP1, A/Switzerland/8060/2017 (Switz/17) EP1, A/South Australia/34/2019 (SA/19) EP1.

The panel of 24 co-circulating H3N2 viral variants from the period of 2004-2016 included:, A/Florida/02/2006 (Fla/06) EP2, A/Santiago/7981/2006 (Santiago/06) EP1, A/Nepal/921/2006 (Nepal/06) EP1, A/Taiwan/760/2007 (Taiwan/07) MDCKP1, A/Texas/71/2007 (Texas/07) MDCKP1, A/Henan-Jinshui/147/2007 (Henan/07) EP1, A/Uruguay/716/2007 (Uruguay/07) EP2, A/Alabama/05/2010 (Ala/10) MDCKP2, A/Hessen/5/2010 (Hess/10) MDCKP3, A/Netherlands/009/2010 (Neth/10) MDCKP2, A/Norway/1330/2010 (Nor/10) MDCKP3, A/Madagascar/0648/2011 (Mad/11) MDCKP2, A/Norway/1186/2011 (Nor/11) MDCKP2, A/Utah/12/2011 (Utah/11) MDCKP2, A/Athens/112/2012 (Ath/12) MDCKP2, A/Jordan/30502/2012 (Jord/12) MDCKP2, A/Denmark/96/2013 (Den/13) MDCKP2, A/Hong Kong/12/2014 (HK/12/14) MDCKP2, A/Stockholm/28/2016 (Stock/16) MDCKP2.

When viruses could not be obtained, H3-A/Thailand/1/2004 N1-Gag VLPs were synthesized using codon optimized HA sequences. This included the following antigens for the 2004-2007 drift panel: A/Hong Kong/CUHK53726/2004 (HK/04) (EPI_ISL_14373) MDCKP1, A/Denmark/13/2006 (Denmark/06) (EPI_ISL_16064) MDCKP1, A/Malaysia/1674395/2006 (Malaysia/06) (EPI_ISL_120397) MDCKP1, A/Thailand/359/2007 (Thailand/07) (EPI_ISL_20528) MDCKP1, and A/Trieste/25/2007 (Trieste/07) (EPI_ISL_98951) MDCKP1.

Phylogenetic comparison of co-circulating variants (2004-2016)

Selection of the co-circulating variants was based upon multiple sequence alignments that were performed on extracted HA sequences; sequences were organized based on collection during the representative “Northern” or “Southern” Hemisphere influenza seasons from 2004-2016.

Phylogenetic tree models were assembled using a Jukes-Cantor genetic distance model, and a neighbor-joining tree building method in Geneious bioinformatics software. Branches were compared for sequence similarity to the panel of 24 drift viruses described above. The number of sequences that branched within 99% HA sequence identity of one of the 24 antigens was counted, and frequencies were calculated based on the total number of sequences available per season as described previously [65].

VLP Vaccination of mice

BALB/c mice (Mus musculus, female 6 to 8 weeks old) were purchased from the Jackson Laboratory (Bar Harbor, ME, USA), housed in microisolator units, and allowed free access to food and water. They were cared for under the University of Georgia Research Animal Resources guidelines for laboratory animals. All procedures were reviewed and approved by the Institutional Animal Care and Use Committee (IACUC). Mice (5 per group) were vaccinated with purified H3 VLPs (3.0mg HA/mouse/vaccination) based upon HA content from the ELISA quantification, and vaccines were delivered via intramuscular injection at week 0 (3ug) and then boosted with the same vaccine antigen and dose on weeks 4 (3ug) and 8 (3ug), as performed in previous studies [13]. Vaccines were formulated with an emulsified squalene-based oil-in-water emulsion adjuvant, Addavax (InvivoGen, San Diego, CA, USA). The final concentration after mixing 1:1 with VLPs is 2.5% squalene. Mice were vaccinated with either one COBRA H3 (TJ-1 through TJ-9) VLP vaccines or one wild-type (Fuj/02, Wisc/05, Bris/07, Perth/09, Vic/11, Tx/12, Switz/13, HK/14, Sing/16) H3 VLP vaccine with HA antigens representing selected vaccine strains isolated from 2002-2017. Fourteen days after each vaccination, blood samples were collected via the

submandibular vein and transferred to a microcentrifuge tube. The tubes were centrifuged at 10,000 rpm for 10 min, and serum samples were removed and frozen at -20°C ±5°C [13].

Hemagglutination-Inhibition (HAI) assay

The hemagglutination inhibition (HAI) assay was used to assess functional antibodies to the HA that are able to inhibit agglutination of guinea pig erythrocytes. The protocols were adapted from the WHO laboratory influenza surveillance manual [82]. Guinea pig red blood cells are frequently used to characterize contemporary A(H3N2) influenza strains that have developed a preferential binding to alpha (2,6) linked sialic acid receptors [83, 84]. To inactivate nonspecific inhibitors, sera samples were treated with receptor-destroying enzyme (RDE) (Denka Seiken, Co., Japan) prior to being tested. Briefly, three parts of RDE was added to one part of sera and incubated overnight at 37°C. RDE was inactivated by incubation at 56°C for 30 min. RDE-treated sera were diluted in a series of twofold serial dilutions in in v-bottom microtiter plates. An equal volume of each A(H3N2) virus, adjusted to approximately 8 hemagglutination units (HAU)/50µl in the presence of 20nM Oseltamivir carboxylate, was added to each well. The plates were covered and incubated at room temperature for 30 min, and then 0.75% guinea pig erythrocytes (Lampire Biologicals, Pipersville, PA, USA) in PBS were added. Red blood cells were washed with PBS, stored at 4°C, and used within 24 h of preparation. The plates were mixed by gentle agitation, covered, and the RBCs were allowed to settle for 1 h at room temperature. The HAI titer was determined by the reciprocal dilution of the last well that contained non-agglutinated RBCs. Positive and negative serum controls were included for each plate. All mice were negative (HAI ≤ 1:10) for pre-existing antibodies to currently circulating human influenza viruses prior to vaccination, and for this study sero-protection was defined as HAI titer >1:40 and seroconversion

as a 4-fold increase in titer compared to baseline, as per the WHO and European Committee for Medicinal Products to evaluate influenza vaccines [85]. Mice are naïve and seronegative at the time of vaccination, and thus seroconversion and sero-protection rates are interchangeable in this study.

Focus Reduction Assay (FRA)

The Focus Reduction Assay (FRA) used in this study was initially developed by the WHO collaborating Centre in London, U.K. and modified by U.S. Centers for Disease Control and Prevention (CDC) (Thomas Rowe, personal communication). MDCK-SIAT1 cells (Sigma, St. Louis, MO, USA) were plated at 2.5 – 3 x 10^5 cells/ml (100uL/well in 96-well plate) one day prior to use in the assay. Cells were cultured in Dulbecco's Modified Eagle Medium (DMEM) containing 5% heat-inactivated fetal bovine serum and antibiotics in 96-well flat bottom plates overnight to form a 95-100% confluent monolayer. The following day, the cell monolayers are rinsed with 0.01M phosphate-buffered saline pH 7.2 (PBS, Gibco, Waltham, MA, USA), followed by the addition of 2-fold serially diluted RDE treated serum (50uL per well) starting with a 1:20 dilution in virus growth medium containing TPCK-treated trypsin (1µg/ml), VGM-T, (DMEM containing 0.1% BSA, 1% Penicillin/Streptomycin (100 U/mL Penicillin, 100 ug/mL Streptomycin solution), and 1µg/ml TPCK-treated trypsin) (Sigma, St. Louis, MO, USA). 50uL of A(H3N2) influenza virus (1.2 x 10^4 focus forming units (FFU)/mL, which corresponds to 600 FFU/50µl) in VGM-T was added to the wells of each plate, or VGM-T only was added to cell control wells. Virus stocks were standardized by previous titration in the FRA [54, 55]. Following a 2 h incubation period at 37°C with 5% CO_2, the cells in each well were then overlaid with 100uL of equal volumes of 1.2% Avicel RC/CL (Type: RC581 NF; FMC Health and Nutrition,

Philadelphia, PA, USA) in 2X Modified Eagle Medium containing 1µg/ml TPCK-treated trypsin, 0.1% BSA and antibiotics [86]. Plates were incubated for 18-22 h at 37°C, 5% CO_2. The overlays were then removed from each well and the monolayer was washed once with PBS to remove any residual Avicel. The plates were then fixed with ice-cold 4% formalin in PBS for 30 min at 4°C, followed by a PBS wash and permeabilization using 0.5% Triton-X-100 in PBS/glycine at room temperature for 20 min. Plates were washed three times with wash buffer (PBS, 0.1% Tween-20; PBST) and then incubated for 1 h with a monoclonal antibody against the influenza A nucleoprotein [54, 87, 88] obtained from the Influenza Reagent Resource (IRR) (Manassas, VA, USA) (FR-1217) (1mg/mL), diluted 1:2000 in ELISA buffer (PBS,10% horse serum, 0.1% Tween-80). Following washing (3X PBST), the cells were incubated with goat anti-mouse peroxidase-labelled IgG (Sera Care, Inc., Milford, MA, USA) (KPL 474-1802) (1mg/mL), diluted 1:2000 in ELISA buffer for 1 hour at RT. Plates were washed again (3X PBST) and infectious foci were visualized using TrueBlue substrate (Sera Care, Inc., Milford, MA USA) containing 0.03% H_2O_2 incubated at room temperature (RT) for 10 min. The reaction was stopped by washing five times with dH_20. Plates were air dried and foci enumerated using a CTL BioSpot Analyser with ImmunoCapture 6.4.87 software (CTL, Shaker Heights, OH, USA). The FRA titer was reported as the reciprocal of the highest dilution of serum corresponding to 50% foci reduction compared to the virus control minus the cell control.

In order for a plate to pass quality control, both the average of the octuplet virus control wells (VC), as well as the average of the octuplet cell control wells (CC) must pass. The virus controls initially were between 150 to 650 foci and the cell controls must be less than 21 foci. The virus control wells were subsequently expanded to between 200 and 1600 foci. Additionally, the positive control virus, A(H3N2) historical influenza vaccine strain, was run in triplicate plates in

each individual assay and at least two out of three plates must pass VC and CC criteria and homologous ferret antisera, previously generated through infection with A(H3N2) influenza virus at 1e6 PFU/mL and collected 14 days post infection, must have the same titer across the plates [65]. Each assay plate (one virus per plate) contained a panel of ferret reference antisera, as well as a human influenza vaccine serum control to assess overall assay consistency [13]. The percentage of infected cells reported in the assay is calculated by averaging the foci count from the positive control (virus and cell only) wells, and dividing the number of foci in each experimental well by the average of the positive control.

Results

Phylogenetic characterization of H3 COBRA HAs

The next-generation COBRA multilayered consensus building approach was applied to 22,144 human A(H3N2) HA viral amino acid sequences collected from January 1, 2002 to December 31, 2015, that resulted in the generation of 9 unique Next Gen HA sequences. These Next Gen HA antigens were designed to cover influenza A(H3N2) viral isolates over multiple influenza seasons. All next-generation H3 HA amino acid sequences were unique and did not match the amino acid sequence of any HA in a wild-type A(H3N2) isolate. The four HA antigens named TJ-1 to TJ-4 were uniquely designed using input H3N2 HA sequences from 2002-2007 and TJ-5 to TJ-9 HA antigens were designed using HA sequences from 2008-2015 (Fig. 3.1C). The antigens were divided into 2 groups because an antigenic shift occurred in H3N2 viruses around 2008 with the emergence of the Perth/09 antigenic cluster [23].

Phylogenetic analysis was performed by constructing a phylogenetic tree model utilizing a neighbor-joining tree building method through Geneious Bioinformatics software. The tree was

rooted to the ancestral HA amino acid sequence of A/Nanchang/933/1995 A(H3N2) to determine the genetic distance between the designed Next Gen H3 HA proteins and wild-type H3 HA vaccine strains, as well as co-circulating variant HA antigens (Fig. 3.2).

The TJ-1 to TJ-4 HA amino acid sequences phylogenetically cluster around HA sequences from wild-type viruses isolated between 2002 – 2007. This was expected, as the HA sequence of TJ-1 is most similar to the sequence of the A/Fujian/411/2002 strain and they differ by only two amino acids, V239I and I377T respectively. The HA sequence for TJ-2 is most similar to A/New York/55/2004, with four amino acid differences, A154S, G202V, S235Y, and A546V. TJ-3 is most similar to A/Malaysia/1674395/2006, but carries two amino acid differences at N391D and R466K. TJ-4 is most similar to A/Fujian/411/2002 with four amino acid differences F175Y, N205S, V239I, and P243S (Fig. 3.2).

As expected, based on their input sequences the TJ-5, 6, 7, 8, and 9 HA sequences are closely aligned with HA sequences from viruses isolated between 2009-2014 (Fig. 3.2). TJ-5 is most similar to A/Madagascar/0648/2011 with five amino acid differences: L13R, I50V, T144A, K427R, and F550S respectively. TJ-6 is most similar to A/Victoria/361/2011, but with 2 amino acid differences at Y9H and S161N. TJ-7 is most similar to A/Hong Kong/12/2014 with 4 amino acid differences, Q49R, Y110H, S328N, and D505N. TJ-8 is most similar to A/Perth/16/2009 with 4 amino acid differences, N160K, H199L, I230S, and S328N. TJ-9 is most similar to A/Athens/112/2012 with 4 amino acid differences, I4V, S70R, N161S, and D503N (Fig. 3.2). The two traditional COBRA antigens fall in areas of the phylogenetic tree that are similar to the sequences used to design each antigen, with T8 clustering near wild-type viruses from 2009-2011, and T11 falling near wild-type viruses from 2010-2012 (Fig 3.2).

Antigenic characterization of TJ-1 to TJ-4 H3 COBRA HA proteins

In order to assess the immunogenicity of the next-generation H3 COBRA vaccine antigens, BALB/c mice were vaccinated in a prime, boost, boost regimen with VLPs expressing the first set of next-generation H3 HA proteins, TJ-1 to TJ-4, that were designed for the 2002-2007 era, or VLPs expressing the wild-type H3 HA proteins representing historical vaccine strains from 2002-2007. Antisera was collected 14 days after the third vaccination and then tested against a panel of viruses representing A(H3N2) vaccine strains from 1995-2016 for HAI activity. Serum from mice vaccinated with TJ-1 VLPs elicited antibodies with HAI titers $\geq$1:40 against 3/12 H3N2 viruses in the panel (the 1997, 1995, and 2002 viruses) (Table 3.1). TJ-2 and TJ-3 VLP vaccines also elicited antibodies with HAI activity against 3/12 strains (the 2004, 2005, and 2007 viruses). Mice vaccinated with VLPs expressing the TJ-4 or Fuj/02 HA protein had antibodies with HAI activity against the 1999 and 2002 viruses, and vaccination with Wisc/05 or Bris/07 VLPs only elicited antibodies with HAI activity against the homologous virus. The mock vaccinated animals did not have antibodies with HAI activity against any of the strains in the panel (Table 3.1). The COBRA antigens TJ-2 and TJ-3 that were designed for the 2002-2007 era elicited HAI titers $\geq$40 against multiple A(H3N2) vaccine strains from the same era that they were designed for while the wild-type H3 vaccines from this era, Wisc/05 and Bris/07, only elicited HAI antibodies $\geq$40 against the homologous vaccine strains. Of note, the TJ-2 and TJ-3 vaccines elicited HAI antibodies against the historical influenza vaccine strains from 2005 and 2007 at titers higher than the homologous matched wild-type vaccine strains.

Sera collected from vaccinated mice were then tested for HAI activity against a panel of viruses representing co-circulating H3N2 influenza strains isolated between 2004-2007 (Table 3.2). Surprisingly, TJ-1 and TJ-4 VLPs were unable to elicit antibodies with HAI activity ($\geq$1:40)

against any of the viruses in the panel (Table 3.2). In contrast, mice vaccinated with TJ-3 VLPs had antibodies with HAI activity against 10 of the 12 strains in the panel and mice vaccinated with TJ-2 VLPs had antibodies with HAI activity against all 13 drift variant viruses (Table 3.2). This was superior to any of the wild-type vaccines tested from this era, of which the best ones, Wisc/05 and Bris/07, elicited HAI antibodies against at most 3/12 strains in the panel at a titer $\geq$40. In contrast, the Fuj/02 VLP vaccines were unable to generate antibodies with HAI activity against any of the strains in the panel (Table 3.2). Mice vaccinated with Wisc/05 VLPs elicited antibodies with seroprotective HAI titers against 3 out of 12 viruses (Malaysia/06, Thailand/07, and Trieste/07). Bris/07 VLPs also elicited seroprotective HAI antibody titers against the Thailand/07 and Trieste/07 strains. Mock vaccinated animals did not have detectable HAI activity against any of the strains in the 2004-2007 co-circulating strains panel (Table 3.2).

Antigenic characterization of TJ 5-9 H3 COBRA HAs

The next-generation COBRA design methodology was then used to create a second round of H3 next-generation HA antigens designed to focus on the 2009-2015 time-frame. These constructs, TJ-5 to TJ-9, were compared to previously designed H3 COBRA VLPs and wild-type H3 VLPs that represented vaccine strains from 2009-2016 against a panel of historical A(H3N2) influenza virus vaccine strains from 1995-2019 for their ability to induce protective levels of HAI reactive antibodies (Table 3.3). Mice vaccinated with TJ-5 possessed serum with antibodies with HAI activity $\geq$40, seroconversion, against all 11 historical vaccine strains isolated from 2005-2019 at levels as high or higher than homologous wild-type VLP vaccines (Table 3.3). Additionally, TJ-5 was the only vaccine to induce seroconversion against the Kan/17 virus, although titers $\geq$40 were only achieved by 2 of the 5 animals in the group (data not shown). Vaccination of naïve

mice with TJ-6, TJ-7, TJ-8, or Tx/12 induced seroconversion against 8 of the 16 strains in the panel including strains from 2005, 2009-2016, and 2019. TJ-6 also elicited seroprotective antibodies against the Switz/17 strain. TJ-9 and Vic/11 VLP vaccines generated antibodies with seroprotective HAI activity against all of the viruses from 2009-2016, and the SA/19 isolate. Mice vaccinate with T8 COBRA VLP's generated sero-protective antibodies against H3N2 vaccine strains from 2004-2012, and mice vaccinated with T11 seroconverted against H3N2 vaccine strains from 2004-2014 (Table 3.3). The Perth/09 wild-type VLP vaccine caused the mice to seroconvert to the vaccine strains from 2009-2016 with the exception of the Switz/13 vaccine strain. Mice vaccinated with Switz/13 VLPs only produced antibodies with HAI activity against viruses from 2011-2013, while mice vaccinated with HK/14 seroconverted against the vaccine isolates from 2013-2016 and the SA/19 virus. The Sing/16 VLP vaccines elicited sero-protective antibodies against all of the strains from 2009-2019 with the exception of the Switz/13 and Kan/17 vaccine isolates, both of which belong to the co-circulating clade 3c.3a. Mock vaccinated animals did not have HAI activity $\geq$40 against any of the strains in the panel (Table 3.3).

Sera collected from the vaccinated mice was then evaluated against a panel of co-circulating H3N2 strains representing 2010-2016 (Table 3.4). Mice vaccinated with Perth/09 possessed HAI activity against all of the strains in the panel isolated from 2010-2014. All of the next-generation H3 COBRAs, TJ-5 to TJ-9, VLP vaccines elicited similar HAI responses to Vic/11, Tx/12, Switz/13, and HK/14 generating HAI titers $\geq$1:40 against all of the strains in the panel from 2010-2016. However, mice vaccinated with TJ-5 had exceptional antibody titers that were as high or higher than the best wild-type vaccines across the panel of co-circulating strains. Mice vaccinated with Sing/16 VLPs or mock vaccines were unable to elicit antibodies with HAI activity $\geq$1:40 against any of the strains in the panel (Table 3.4).

H3N2 Neutralization Assessment

The ability of vaccine elicited antibodies to neutralize live virus infection was evaluated using a focal reduction assay (FRA) (Fig. 3.3). Mice vaccinated with TJ-2 or TJ-3 VLPs had the highest antibody neutralization titers amongst all of the next generation COBRA H3 vaccines against the Bris/07 virus, with a FRA_{50} of 10.38 and 11.06 respectively. Mice vaccinated with TJ-5, TJ-6, or TJ-8 VLP vaccines also elicited a FRA_{50} against Bris/07 albeit at lower titers of 7.71, which was lower than sera from Bris/07 VLP vaccinated mice. Sera from mice vaccinated with TJ-7 and TJ-9 were unable to elicit antibodies that inhibited Bris/07 infection at a level $\geq$50% (Fig 3.3A). However, most of the VLP vaccines expressing wild-type HA antigens were also unable to elicit antibodies with neutralization titers against Bris/07, except for the homologous Bris/07 VLP (10.66 FRA_{50} titer) and the Tx/12 VLP (7.79 FRA_{50} titer) (Fig 3.3B). Due to their lack of HAI breadth, serum from mice vaccinated with TJ-1 and TJ-4 were not tested in the FRA for their ability to neutralize future emerging strains.

Serum samples collected from mice vaccinated with TJ-2 and TJ-3 VLPs had moderate neutralizing titers against Tx/12 virus, with a FRA_{50} of 6.82 and 7.84 respectively. In general, all of the other COBRA HA VLP vaccines, TJ-5 – TJ-9, had antibodies that neutralized the Tx/12 virus at levels greater than 80% in all of the serum dilutions tested (Fig. 3.3C). The wild-type VLP vaccines Switz/13, HK/14, and Sing/16 all elicited antibodies with moderate capacity to neutralize the Tx/12 virus, while Perth/09, Vic/11, and Tx/12 VLP elicited antibodies that were highly effective at neutralizing the Tx/12 challenge virus. The Bris/07 VLP and mock vaccinated animals did not have antibodies that could prevent Tx/12 infections of the host cells (Fig. 3.3D).

TJ-5, TJ-7, TJ-8, and TJ-9, vaccines were effective at generating antibodies that inhibit Switz/13 infections with a FRA_{50} of ~11.0. Of the Next Gen H3 vaccines, serum collected from

mice vaccinated with TJ-6 VLPs were most effective at neutralizing the Switz/13 virus. In contrast, TJ-2 and TJ-3 VLPs failed to neutralize Switz/13 viral infections (Fig. 3.3E). In general, mice vaccinated with either Vic/11, Tx/12, Switz/13, or HK/14 VLPs were most effective at neutralizing the Switz/13. All of these vaccines neutralized more than 50% of the viral infections at almost all of the dilutions tested, with the homologously matched Switz/13 VLP vaccine eliciting antibodies with the greatest capacity to neutralize the challenge virus. The wild-type vaccines, Bris/07, Perth/09, Sing/16, as well as mock vaccinated animals were much less effective at neutralizing Switz/13 than the other wild-type strains (Fig. 3.3F).

Mice vaccinated with TJ-2 or TJ-3 VLPs were unable to elicit antibodies that could neutralize the HK/14 virus. However, five COBRA vaccine antigens (TJ-5 to TJ-9) elicited levels of antibodies that were broadly neutralizing across the 2012-2016 timeframe, whereas the wild-type seasonal vaccine antigens from that timeframe elicited antibodies that were more strain specific and less cross reactive (Fig. 3.3G). Of the wild-type vaccines, Perth/09, Vic/11, Tx/12, HK/14, and Sing/16 VLPs all elicited antibodies that could neutralize the HK/14 with a FRA_{50} greater than 10. The Switz/13 VLP vaccines elicited neutralizing with a FRA_{50} of 8.37, while the Bris/07 VLP and mock vaccines were unable to prevent any virus infections (Fig. 3.3H).

TJ-5 to TJ-9 VLP vaccines elicited antibodies had a FRA_{50} titer of 10.6 or higher against Sing/16 virus at any serum dilution tested. However, mice vaccinated with either TJ-2 or TJ-3 were unable to neutralize the Sing/16 virus (Fig. 3.3I). In general, mice vaccinated with wild-type vaccines from 2009-2014 had antibodies that prevented more than 50% of the viral infections caused by the Sing/16 virus with an FRA_{50} of 9.88. In contrast, the homologously matched Sing/16 VLPs neutralized more than 50% of the infections at all dilutions tested. Switz/13 and

Bris/07 VLPs, as well as the mock vaccinated animals, did not elicit antibodies capable of neutralizing Sing/16 virus (Fig. 3.3J).

Overall, the next-generation H3 COBRA HA vaccine antigens designed for the 2009-2015 era elicited high levels of neutralizing antibody titers across a timeframe, 2012-2016, where 4 different wild-type A(H3N2) vaccine strains were chosen to be included in the seasonal influenza vaccine. Additionally, the TJ-5 – TJ-9 VLP vaccines elicited antibodies that neutralized infections against the future drifted Sing/16 virus at titers two-fold higher than any wild-type vaccine other than the homologous Sing/16 vaccine.

Discussion

The overall objective of the next-generation COBRA methodology is to apply the usefulness of the in-silico vaccine antigen design process to a more commercial vaccine manufacturing-type setting where vaccines are produced in real-time in response to current antigenic and genetic viral variations. Although vaccines against the influenza virus were developed as early as the 1940's, the use of inactivated wild-type viruses as vaccines are still the best method of inducing protection in the human population [89]. Current seasonal wild-type A(H3N2) influenza vaccines are typically strain specific and sometimes induce a narrow range of antigenic breadth against co-circulating viral variants [11, 75]. However, there are some eras of H3N2 influenza virus circulation where the wild-type vaccines elicit highly cross-reactive antibodies. In this study, the wild-type vaccines that were isolated from 2009-2016 elicited cross-reactive antibodies against the strains of this era. This is in contrast to isolates collected prior to this time period that do not elicit cross-reactive antibodies and were often antigenically strain specific [13]. The relatively continuous genetic and antigenic drift of influenza A(H3N2) viruses

requires the WHO to perform extensive genetic and antigenic surveillance on circulating isolates, as well as accurately predicting the protective efficacy of candidate vaccine viruses each season [11]. The selection of mismatched strains by the WHO can also lead to greatly reduced vaccine effectiveness, as observed during the 2014-2015 influenza season, where a poor match between the A(H3N2) vaccine strain and those viruses in circulation reduced the vaccine effectiveness to ~19% in the U.S. [77].

There is a need for more broad immune protection against co-circulating A(H3N2) influenza viruses, and improvements need to be made to both vaccine candidate selection and deployment against emerging viral strains [76]. From the moment that vaccine manufacturers receive the strain recommendation from the WHO in late February, there are ~6 months to produce and purify enough vaccine to make hundreds of millions of doses [11]. . Speed of production is critical and there would be less pressure if vaccine manufacturers could produce a vaccine that elicits long-lived protective immune responses [89, 90]. In 2018, the U.S. government was tasked with expanding the capacity for more agile and rapid vaccine production methods to advance the development of broadly reactive vaccine candidates [75]. The accelerated pace of generating and selecting up to date next-generation COBRA-based antigens would be highly advantageous over traditional methods of selecting wild-type vaccine candidate viruses. Since these COBRA vaccine antigens are designed using the year-round influenza virus surveillance data, a candidate vaccine could be generated in real time, antigenically tested, and selected long before traditional strain recommendations. Therefore, broadly reactive vaccine candidates could be rolled out at any time to combat the antigenic diversity of co-circulating A(H3N2) viral strains.

As a result of a combination of rapid viral mutation, reassortment, natural selection in hosts, and epidemiology, A(H3N2) influenza viruses are evolving in humans faster than any other

subtype of influenza virus. As a result, the WHO has recommended to change the A(H3N2) influenza strain in the commercial seasonal vaccines 11 times for Northern hemisphere since the 1998-1999 season [76]. The high level of diversity of the surface epitopes present on A(H3N2) influenza viruses are challenging for both immune recognition and traditional vaccine effectiveness. However, the next-generation COBRA HA design approach presented in this report resulted in unique HA sequences that incorporated the antigenic epitopes from numerous co-circulating strains of A(H3N2) influenza viruses transmitting during the most recent influenza virus seasons. This next-generation process reduces potential biases in input sequences by weighting isolates based on sequence identity and time of isolation, thereby allowing the COBRA HA antigens to retain highly immunogenic and cross-reactive epitopes [91].

Antibodies directed against conserved regions in the HA protein can provide broad protection against many different influenza viruses [92]. It is likely that the next-generation H3 COBRA antigens elicited broadly reactive antibodies in a similar manner to traditional COBRA HA vaccine antigens, by driving diverse B cell responses and targeting conserved HA epitopes that are maintained in future A(H3N2) influenza drift variants. Unlike many other broadly reactive influenza virus vaccine candidates, that direct antibodies to the conserved regions of the HA stem, COBRA HA antigens preferentially direct antibodies against conserved structures of the HA globular head, such as the receptor binding site that remains relatively similar in structure to allow for sialic acid binding functions [91]. This is advantageous since antibodies directed against the HA globular head are induced at higher titers and with greater potency than those directed against the stalk [92, 93]. However, whether or not these broadly reactive antibody responses are the result of synergistic polyclonal antibodies targeting multiple conserved epitopes, or are the product of a highly specific monoclonal antibody response targeting one epitope remains unclear. COBRA HA

based vaccines elicit a broader set of monoclonal antibodies (mAbs) than wild-type HA antigens [91]. Therefore, understanding the mechanism(s) that COBRA HA proteins use to elicit broadly-reactive antibodies is important for the design and improvement of broadly reactive antigens and will be the goal of future investigations.

The methodology presented herein differs from the approach used to generate previous COBRA HA antigens. The next generation strategy places an emphasis on current and recently circulating viruses rather than on historical influenza isolates, antigenic eras, or past outbreak groups. The previously published COBRA methodology is good for producing antigens that are broadly reactive for shorter periods of time, i.e., 5 to 10 year periods, but as wild-type viruses evolve and change, modifications to the broadly reactive vaccine candidate must be made to keep the vaccines up to date. The overall goal of this study was to develop a methodology that would allow manufacturers the ability to keep their broadly reactive vaccine candidates up to date in the event that their current vaccine begins to elicit suboptimal antibody breadth against the viruses in circulation.

Two next-generation COBRA design scenarios were tested in this study for their ability to produce broadly reactive vaccine antigens that elicit antibodies against influenza strains from within and across multiple influenza virus seasons. However, neither scenario proved to be advantageous over the other. In fact, for many of the seasons modeled in this study, both scenarios produced identical antigens (data not shown) further emphasizing that both design scenarios are capable of producing broadly reactive antigens. However, both design approaches also produced antigens, TJ-1 and TJ-4, that were not very broadly reactive. This is likely because the HA sequences of TJ-1 and TJ-4 are most similar to the A/Fujian/411/2002 virus, which belongs to a different antigenic era than the H3N2 influenza viruses in circulation between 2004-2007 [13, 94].

Both TJ-1 and TJ-4 possess a lysine at HA site 161, which is located in antigenic site B, and a valine at site 242 in antigenic site D, which is identical to the amino acids in those positions for A/Fujian/411/2002. Contrastingly, TJ-2 and TJ-3 possess an asparagine at site 161 and an isoleucine at site 242 which is also carried by the A/Wisconsin/67/2005 strain. Together, these amino acid changes are likely responsible for the observed differences in HAI activity between TJ-1/TJ-4 and TJ-2/TJ-3, especially the differences at site 161 as mutations in antigenic site B are often immunodominant and responsible for antigenic drift [95]. Future studies will focus on deconvoluting the differences between the quality of antigens produced by each of the design scenarios, and their ability to induce antibody breadth against both dominant and co-circulating influenza virus strains within and across multiple influenza seasons.

Overall, the H3 COBRA HA antigens designed using both of the next-generation methodologies were able to broadly elicit both HAI reactive and neutralizing antibodies against historical, co-circulating, and future drifted strains of A(H3N2) influenza viruses at a level that was equivalent or greater than wild-type antigens from the same era. Two of the vaccine candidates in particular, TJ-2 and TJ-5, elicited the strongest anti-influenza antibody responses against the era for which they were designed, as well as against future A(H3N2) influenza virus strains. Subsequent studies will focus on further characterizing the immune responses generated by these two vaccine candidates in various animal models.

Despite the value of testing potential vaccine candidates in immunologically influenza-naïve animal models, these systems only provide information about how these antigens will stimulate a de novo immune response, but most human adults have previously been exposed to influenza viruses either through infection or vaccination and possess immunological memory that will differentially drive immune responses to subsequent vaccinations [96]. Future investigations will

aim to determine if the breadth of response generated by these next-generation H3 COBRA vaccines are the result of the stimulation of a larger number of pre-existing memory B cells leading to a more diverse antibody repertoire than those stimulated by wild-type vaccines. Therefore, evaluation of these vaccine candidates in animals with pre-existing immunity elicited by previous exposure(s) to influenza viruses will provide information on how an individual's immune history plays a role in generating effective antibody responses following vaccination.

In summary, this next-generation antigen design methodology is an effective and novel approach for designing broadly reactive subtype-specific seasonal A(H3N2) influenza virus antigens in real time. This process allows the natural evolution of influenza viruses to dictate the antigen design process, and places an emphasis on currently drifted strains rather than historical strains or making predictions on emerging strains that may or may not become dominant in circulation. Designing custom influenza HA antigens through this next-generation process is likely to reduce the need for frequently updating vaccine components and increase protection within a season. This would be highly advantageous for commercial vaccine manufacturers since it would decrease the risk of including a mismatched strain in the vaccine, while increasing vaccine effectiveness, and allow year-round vaccine production. This next generation methodology provides a way to update broadly reactive influenza vaccine candidates with the use of in-silico designs and real time surveillance information, rather than relying on annual predictions, which is a necessary step forward in the fight to protect humans against the ever-changing landscape of co-circulating H3N2 influenza viruses.

	Log (2) GMT												
	Nan/95	Syd/97	Pan/99	Fuj/02	NY/04	Wis/05	Bris/07	Perth/09	Vic/11	Tx/12	Swz/13	HK/14	Sing/16
TJ1	3.72	5.52	8.32	6.52	3.32	3.32	3.52	3.32	3.32	3.32	3.32	3.32	3.32
TJ2	3.32	3.72	4.32	4.32	7.92	8.12	8.52	3.32	3.52	3.32	3.32	3.32	3.32
TJ3	3.32	3.32	3.32	3.32	5.92	8.32	7.92	3.92	3.32	3.32	3.32	3.32	3.32
TJ4	3.52	4.92	8.32	7.12	3.32	3.32	3.32	3.32	3.32	3.32	3.32	3.32	3.32
Fuj/02	3.32	3.32	5.92	5.32	3.52	3.92	3.92	3.32	3.32	3.32	3.32	3.32	3.32
Wisc/05	3.32	3.32	3.32	3.32	3.92	5.52	4.92	3.32	3.32	3.32	3.32	3.32	3.32
Bris/07	3.32	3.52	3.32	3.32	3.32	3.32	6.12	3.32	3.32	3.32	3.32	3.32	3.32
Mock	3.32	3.32	3.32	3.32	3.32	3.32	3.32	3.32	3.32	3.32	3.32	3.32	3.32

Table 3.1. Historical influenza virus D77 HAI panel. HAI assays were performed against a panel of historical influenza virus vaccine strains isolated from 1995 – 2016 with day 77 serum from vaccinated mice. The average $\log_2$ geometric mean HAI serum antibody titers (GMTs) were determined for each group of mice (n=5) and are presented in a heat map form. Colored cells represent groups that achieved a GMT ≥5.32, which correlates to an average antibody titer ≥ 1:40. Values closest to 5.32 are colored yellow and become a darker shade of green as the GMT value increases. Cells with no color represent groups that did not achieve a GMT ≥5.32.

	Log (2) GMT											
	HK/04	Fla/06	Santiago/06	Denmark/06	Malaysia/06	Nepal/06	Taiwan/07	Texas/07	Henan/07	Thailand/07	Uruguay/07	Trieste/07
TJ1	4.32	3.32	3.32	3.32	4.12	3.32	3.32	3.32	3.32	2.92	3.32	4.12
TJ2	7.92	7.72	7.32	6.72	7.52	6.92	8.12	7.12	7.12	6.32	7.52	8.32
TJ3	5.32	7.52	7.12	4.32	6.32	7.32	7.52	6.32	6.32	5.12	7.32	6.92
TJ4	3.32	3.32	3.32	3.32	3.92	3.32	3.32	3.32	3.32	2.32	3.32	3.72
Fuj/02	3.72	3.52	3.52	3.52	3.52	3.72	3.32	3.32	3.32	2.72	3.52	3.72
Wisc/05	3.52	3.92	3.92	3.32	6.32	3.32	4.32	3.52	3.72	5.72	4.12	6.52
Bris/07	3.32	3.32	4.52	3.32	3.32	3.32	3.32	3.32	4.52	5.72	5.12	5.52
Mock	3.32	3.32	3.32	3.32	3.32	3.32	3.32	3.32	3.32	2.32	3.32	3.32

Table 3.2. 2004-2007 Co-circulating influenza virus HAI panel. HAI assays were performed against a panel of co-circulating influenza strains isolated from 2004-2007 with day 77 serum from vaccinated mice. The average $\log_2$ geometric mean HAI serum antibody titers (GMTs) were determined for each group of mice (n=5) and are presented in a heat map form. Colored cells represent groups that achieved a GMT ≥5.32, which correlates to an average antibody titer ≥ 1:40. Values closest to 5.32 are colored yellow and become a darker shade of green as the GMT value increases. Cells with no color represent groups that did not achieve a GMT ≥5.32.

	Log(2) GMT												
	Nan/95	Syd/97	Pan/99	Fuj/02	NY/04	Wisc/05	Bris/07	Perth/09	Vic/11	Tx/12	Switz/13	HK/14	Sing/16
TJ-5	2.32	2.32	2.32	2.32	2.32	6.92	5.72	9.12	10.12	10.32	7.52	9.12	10.32
TJ-6	2.32	2.32	2.32	2.32	2.32	5.72	5.12	9.12	9.72	9.92	8.72	8.72	8.52
TJ-7	2.32	2.32	2.32	2.32	2.32	5.32	4.12	9.32	9.72	9.92	8.12	7.92	7.52
TJ-8	2.32	2.32	2.32	2.32	2.32	6.12	3.92	8.52	8.92	9.32	7.32	8.12	7.32
TJ-9	2.32	2.32	2.32	2.32	2.32	4.72	3.52	8.72	9.72	9.72	7.92	8.12	8.72
Perth/09	2.32	2.32	2.32	2.32	2.32	2.52	2.52	6.72	7.12	8.32	4.72	7.32	8.92
Vic/11	2.32	2.32	2.32	2.32	2.32	4.52	3.32	7.52	9.92	10.32	6.32	6.92	7.32
Tx/12	2.32	2.32	2.32	2.32	3.52	6.12	4.12	8.12	9.72	10.12	7.72	7.52	8.12
Sz/13	2.32	2.32	2.32	2.32	2.32	2.32	3.12	4.32	6.32	6.32	8.72	4.92	4.12
Hk/14	2.32	2.32	2.32	2.32	2.52	2.72	3.92	3.72	4.92	4.92	6.72	6.32	5.92
Sing/16	2.32	2.32	2.32	2.32	2.32	3.12	5.72	8.52	5.52	8.52	5.12	10.52	10.32
Mock	2.32	2.32	2.32	2.32	2.32	2.32	2.32	2.32	2.32	2.32	2.32	2.32	2.32

Table 3.3. Historical influenza virus D77 HAI panel. HAI assays were performed against a panel of historical influenza virus vaccine strains isolated from 1995 – 2019 with day 77 serum from vaccinated mice. The average $\log_2$ geometric mean HAI serum antibody titers (GMTs) were determined for each group of mice (n=5) and are presented in a heat map form. Colored cells represent groups that achieved a GMT ≥5.32, which correlates to an average antibody titer ≥ 1:40. Values closest to 5.32 are colored yellow and become a darker shade of green as the GMT value increases. Cells with no color represent groups that did not achieve a GMT ≥5.32.

	Log(2) GMT											
	Ala/10	Hess/10	Neth/10	Nor/10	Mad/11	Nor/11	Utah/11	Ath/12	Jord/12	Den/13	HK/12/14	Stock/16
TJ-5	11.32	11.32	11.32	12.32	11.32	12.32	10.32	11.32	12.32	10.32	10.32	6.32
TJ-6	9.32	10.32	10.32	10.32	10.32	11.32	10.32	10.32	11.32	10.32	9.32	6.32
TJ-7	8.32	9.32	10.32	10.32	9.32	9.32	10.32	9.32	10.32	9.32	8.32	6.32
TJ-8	9.32	9.32	10.32	10.32	9.32	9.32	10.32	9.32	10.32	9.32	8.32	5.32
TJ-9	9.32	9.32	10.32	11.32	10.32	10.32	10.32	10.32	10.32	10.32	8.32	5.32
Perth/09	9.32	8.32	9.32	8.32	10.32	10.32	9.32	8.32	9.32	8.32	8.32	2.32
Vic/11	11.32	9.32	11.32	10.32	11.32	12.32	10.32	10.32	10.32	9.32	10.32	6.32
Tx/12	10.32	10.32	10.32	10.32	10.32	10.32	10.32	10.32	10.32	9.32	10.32	6.32
Sz/13	6.32	7.32	7.32	7.32	8.32	7.32	8.32	7.32	7.32	7.32	8.32	6.32
Hk/14	6.32	6.32	7.32	7.32	7.32	6.32	8.32	8.32	6.32	8.32	8.32	7.32
Sing/16	3.32	2.32	2.32	2.32	2.32	2.32	2.32	2.32	3.32	2.32	3.32	2.32
Mock	2.32	2.32	2.32	2.32	2.32	2.32	2.32	2.32	2.32	2.32	2.32	2.32

Table 3.4. 2010-2016 Co-circulating influenza virus D77 HAI panel. HAI assays were performed against a panel of co-circulating influenza strains isolated from 2010-2016 with day 77 serum from vaccinated mice. The average $\log_2$ geometric mean HAI serum antibody titers (GMTs) were determined for each group of mice (n=5) and are presented in a heat map form. Colored cells represent groups that achieved a GMT ≥5.32, which correlates to an average antibody titer ≥ 1:40. Values closest to 5.32 are colored yellow and become a darker shade of green as the GMT value increases. Cells with no color represent groups that did not achieve a GMT ≥5.32.

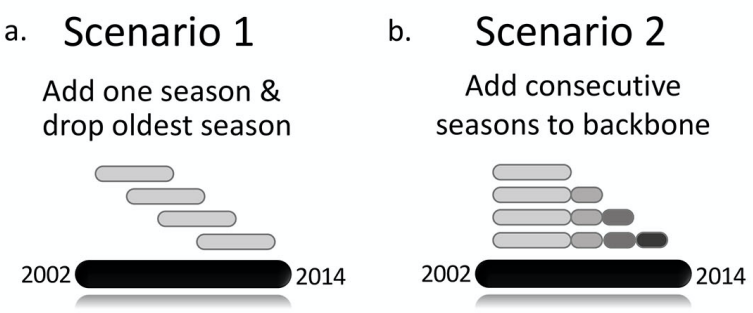

c.

H3 COBRA Antigen	Design Era	Layering Approach	H3 COBRA Antigen	Design Era	Layering Approach
TJ-1	2002-2004	Scenario 2	TJ-5	2008-2012	Scenario 2
TJ-2	2002-2005	Scenario 1	TJ-6	2009-2014	Scenario 2
TJ-3	2003-2005	Scenario 2	TJ-7	2009-2015	Scenario 2
TJ-4	2004-2007	Scenario 1	TJ-8	2009-2012	Scenario 1
			TJ-9	2011-2014	Scenario 1

Figure 3.1. Next-generation H3 COBRA HA multi-consensus sequence layering approach scenarios and final antigen designs. Secondary layer consensus sequences derived from influenza isolates spanning a 2.5-year period are used to generate a "backbone" consensus sequence (light grey bar). (a) Scenario 1. Secondary consensus sequences produced from the most recent 6-months of influenza circulation are added into the backbone sequences, and secondary sequences from the oldest 6-month season of the 3-year period are dropped off. This process is repeated for each 6-month period of the design era. (b) Scenario 2. Secondary sequences produced from the most recent 6-months of influenza circulation are added to the "backbone" sequence and the oldest sequences from the design era are retained. This process is repeated for each 6-month period of the design era. (c) Description of the next-generation COBRA H3 HA vaccine antigens and their design eras. TJ1-4 were designed utilizing wild-type influenza virus HA sequences from 2002-2007, and TJ5-9 were generated from HA input sequences that were in circulation from 2008-2015.

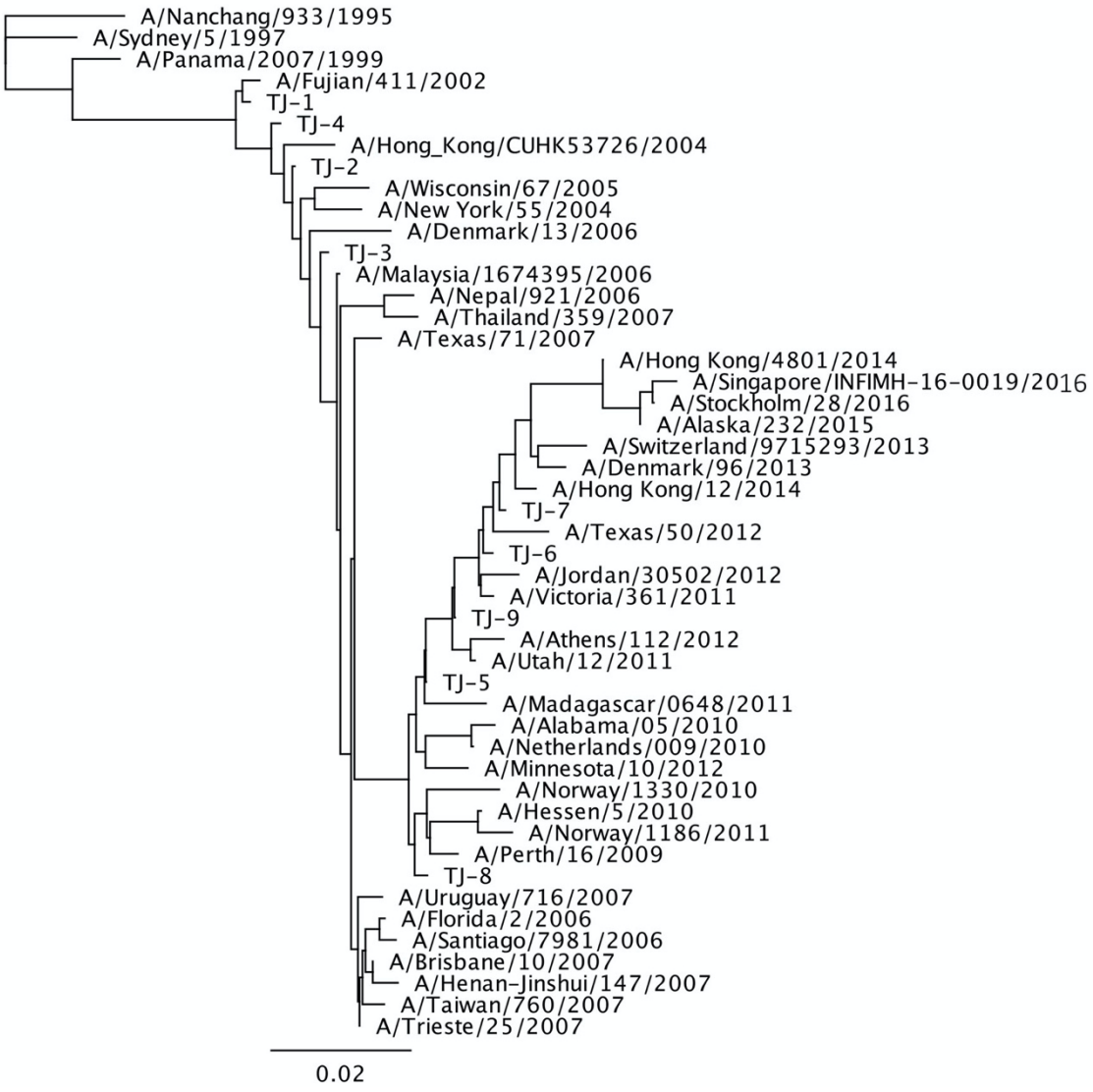

Figure 3.2. Phylogenetic tree of next-generation COBRA and wild-type H3 HA antigens. The rooted (A/Nanchang/933/1995) phylogenetic tree was inferred from next-generation H3 HA and wild-type HA amino acid sequences derived from representative H3N2 viruses isolated from 1995-2016 using the maximum-likelihood method. Sequences were aligned with MUSCLE 3.7 software, and the alignment was refined by Gblocks0.91b software. Phylogeny was determined using the maximum-likelihood method with PhyML software. Trees were rendered using TreeDyn 198.3 software.

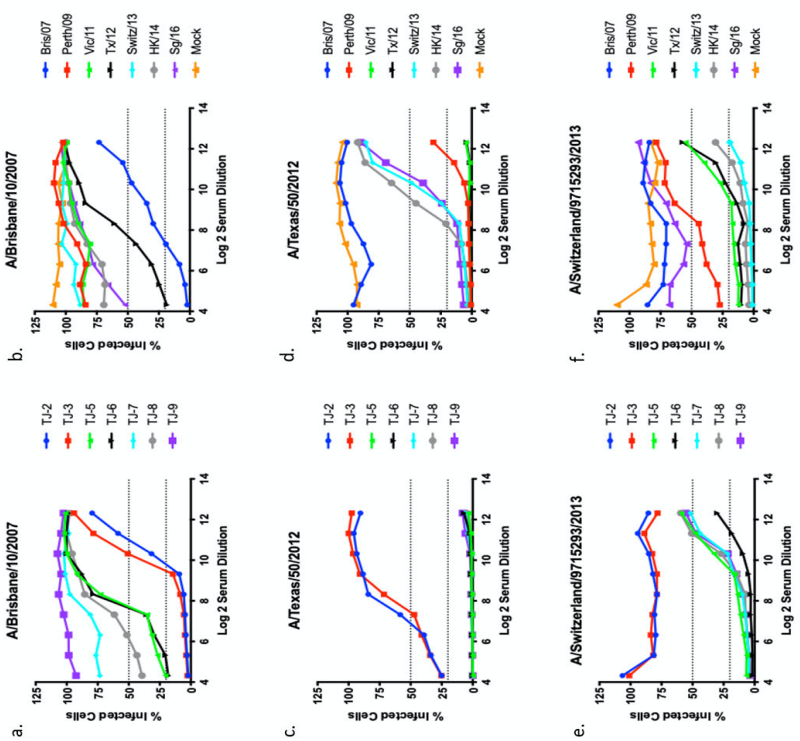
a.
A/Brisbane/10/2007
b.
A/Brisbane/10/2007
c.
A/Texas/50/2012
d.
A/Texas/50/2012
e.
A/Switzerland/9715293/2013
f.
A/Switzerland/9715293/2013
g.
A/Hong Kong/4801/2014
h.
A/Hong Kong/4801/2014
i.
A/Singapore/IFNIMH-16-0019/2016
j.
A/Singapore/IFNIMH-16-0019/2016
% Infected Cells
Log 2 Serum Dilution
TJ-2
TJ-3
TJ-5
TJ-6
TJ-7
TJ-8
TJ-9
Bris/07
Perth/09
Vic/11
Tx/12
Switz/13
HK/14
Sg/16
Mock

Figure 3.3 H3N2 Focal Reduction Assay. FRA neutralizing antibody titers were determined using pooled sera for each group of naïve mice vaccinated 3 times with one of 7 next-generation COBRA H3 HA antigens (TJ-2, TJ-3, or TJ5-9) or H3 VLP vaccines expressing wild-type HA proteins (Bris/07, Perth/09, Vic/11, Tx/12, Switz/13, HK/14, or Sg/16) from historical influenza virus isolates at day 77. (a, b) Average Log_2 neutralizing antibody titers against the A/Brisbane/10/2007 H3N2 virus. (c, d) Average Log_2 neutralizing antibody titers against the A/Texas/50/2012 H3N2 virus. (e, f) Average Log_2 neutralizing antibody titers against the A/Switzerland/9715293/2013 H3N2 virus. (g, h) Average Log_2 neutralizing antibody titers against the A/Hong Kong/4801/2014 H3N2 virus. (i, j) Average Log_2 neutralizing antibody titers against the A/Singapore/IFNIMH-16-2016 H3N2 virus. For each virus, the virus concentration was standardized to $1.2x10^4$ PFU/mL. The dotted lines represent the 50% and 80% inhibition of viral infection by antisera compared to virus only control wells.

CHAPTER 4

EVALUATION OF NEXT-GENERATION H3 INFLUENZA VACCINES IN FERRETS PRE-IMMUNE TO HISTORICAL H3N2 VIRUSES[1]

[1]Allen, James D., and Ted M. Ross. *Evaluation of Next-generation H3 Influenza Vaccines in Ferrets Pre-immune to Historical H3N2 Viruses*. Frontiers in Immunology, **12** (2021). Reprinted here with permission from Frontiers in Immunology. This is an Accepted Manuscript of an article published in Frontiers in Immunology on August 2021, available online: doi: 10.3389/fimmu.2021.707339.

Abstract

Each person has a unique immune history to past influenza virus infections. Exposure to influenza viruses early in life establishes memory B cell populations that influence future immune responses to influenza vaccination. Current influenza vaccines elicit antibodies that are typically strain specific and do not offer broad protection against antigenically drifted influenza strains in all age groups of people. This is particularly true for vaccine antigens of the A(H3N2) influenza virus subtype, where continual antigenic drift necessitates frequent vaccine reformulation. Broadly-reactive influenza virus vaccine antigens offer a solution to combat antigenic drift, but they also need to be equally effective in all populations, regardless of prior influenza virus exposure history. This study examined the role that pre-existing immunity plays on influenza virus vaccination. Ferrets were infected with historical A(H3N2) influenza viruses isolated from either the 1970's, 1980's, or 1990's and then vaccinated with computationally optimized broadly reactive antigens (COBRA) or wild-type (WT) influenza virus like particles (VLPs) expressing hemagglutinin (HA) vaccine antigens to examine the expansion of immune breadth. Vaccines with the H3 COBRA HA antigens had more cross-reactive antibodies following a single vaccination in all three pre-immune regimens than vaccines with WT H3 HA antigens against historical, contemporary, and future drifted A(H3N2) influenza viruses. The H3 COBRA HA vaccines also induced antibodies capable of neutralizing live virus infections against modern drifted A(H3N2) strains at higher titers than the WT H3 HA vaccine comparators.

Introduction

Influenza viruses induce a major respiratory disease that causes ~3-5 million cases of severe illness and 290,000 – 600,000 deaths globally every year [5, 56, 57, 97, 98]. Currently, vaccines are the most effective measure at preventing influenza virus infections. However, viral infections in vaccinated individuals are still common with antigenically distinct viral strains and subtypes[5, 61, 99]. Most commercial influenza virus vaccines elicit antibodies against the major surface proteins, hemagglutinin (HA) and neuraminidase (NA)[5, 100-102]. These surface proteins continuously acquire antigenically relevant HA and NA substitutions through the process of antigenic drift, requiring frequent updates to the seasonal influenza vaccine formulations[5, 73, 103]. Recently, this rapid evolution has been most evident in viruses belonging to the A(H3N2) subtype. A(H3N2) influenza viruses were first introduced to the human population in 1968 and since then they have undergone substantial antigenic drift leading to numerous seasonal epidemics [10]. In the last 20 years, the A(H3N2) component of the Northern Hemisphere vaccine has been changed 13 times, nearly twice as often the A(H1N1) component [12]. This rapid evolution makes annual A(H3N2) vaccine strain selection difficult and can lead to the inclusion of mismatched strains in seasonal influenza virus vaccines [9, 10, 58]. In the 2018-2019 influenza season, a mismatch between the selected vaccine strain and circulating A(H3N2) viruses led to a vaccine efficacy of ~9%, compared to ~44% for A(H1N1)[12, 60, 104].

The effectiveness of influenza virus vaccines is known to fluctuate from season to season and from person to person based on age and vaccination history[47, 102, 105]. In 1960, Francis introduced the concept of "original antigenic sin" (OAS), to describe patterns of antibody responses following vaccination, whereby antibody responses to influenza viruses encountered early in life are preferentially recalled upon exposure to antigenically distinct influenza viral

strains[105-108]. OAS is a crucial factor that helps shape the immune responses in an individual within and between subtypes of influenza [106]. Most humans are infected with influenza viruses by 3-4 years of age and are either infected and or vaccinated with antigenically distinct viral strains later in life resulting in extensive immune memory to historical influenza viruses [5, 97, 99, 100]. Human antibody responses are often biased toward the HA epitopes present on the viral strains that were first encountered in childhood, but as people grow older, antibodies to additional families of viruses are acquired [5, 107]. Therefore, birth year can have a considerable impact on a person's future immune responses against drifted stains of influenza virus. This can result in age-specific susceptibility to modern isolates of A(H3N2) viruses based on a particular immune history [106, 109].

Current inactivated influenza vaccines (IIV) primarily induce strain-specific antibodies, but typically do not provide protection against antigenically drifted and shifted strains of influenza[56, 75, 110]. Thus, a cross-protective vaccine that can provide immediate protection against antigenically drifted influenza isolates is urgently needed [110]. Universal influenza vaccine candidates are currently being designed to overcome the problems associated with strain-specific seasonal influenza vaccines by eliciting broad immune responses against antigenically diverse viral strains in individuals with complex immune histories[5, 101]. Previously, our group has reported on the development a next-generation algorithm for generating computationally optimized broadly reactive antigens (COBRA) [111] that can be used as influenza HA vaccines for H1, H2, H3, and H5 subtypes [13, 62, 65-71, 111]. These broadly reactive vaccines elicit antibodies capable of blocking HA-specific receptor binding, inhibiting infection, and limiting virus induced pathogenesis in immunologically naïve mice and ferrets against a range of seasonal and pandemic influenza strains [65, 72-74].

Since most humans have extensive immune histories induced by previous influenza virus infections, this study explored how previous exposure to historical A(H3N2) influenza isolates impacted the COBRA HA elicited immune responses against modern A(H3N2) isolates. Ferrets were first infected with A(H3N2) viruses isolated from different eras (the 1970's, 1980's, or 1990's) to model the immune histories of individuals primed with viruses from these decades. Then, these pre-immune ferrets were vaccinated with next generation H3 COBRA HA vaccines or WT H3 HA antigens expressed on the surface of VLPs. Collected sera was evaluated for the ability to neutralize drifted and future isolates of A(H3N2) influenza viruses[111]. Vaccinations in all pre-immune animals increased the breadth of anti-influenza virus neutralizing antibodies. Following a single vaccination with COBRA HA antigens, the collected sera had HAI and neutralizing antibodies that recognized a broader number of A(H3N2) vaccine strains and drifted influenza virus isolates than WT vaccine antigens; demonstrating that the COBRA methodology would be highly advantageous for vaccine manufacturers who want their products to generate potent cross-reactive antibody responses following a single dose of vaccine. However, differences in the vaccine-induced antibody breadth and titer were observed between groups based on their initial exposure to A(H3N2) virus, indicating that an individual's immune history plays a large role in their response to vaccination. In general, animals primed with viruses that were more genetically related to the vaccine antigens had more cross-reactive antibody breadth following vaccination compared to unprimed ferrets.

Materials and Methods

Vaccine Preparation

Mammalian HEK 293-T cells were transfected with three individual plasmids expressing either the influenza N3 neuraminidase (A/mallard/Alberta/24/2001, H7N3), the HIV p55 Gag sequence, to serve as the outer membrane of the particle, and one of the various influenza A(H3N2) wild-type HA or H3 COBRA HA expressing plasmids in previously described mammalian expression vectors [80]. A mismatched N3 neuraminidase was included to enable budding of the VLPs from the host cell membrane, while at the same time eliminating any potential protection offered by N2, NA antibodies that could be observed in assays using H3N2 viruses. A(H3N2) wild-type influenza HA sequences were obtained from the Global Initiative on Sharing Avian Influenza Data (GISAID) EpiFlu database using MDCK passaged sequences which were inserted into the pTR600 expression vector [67]. This included the H3 HA sequences for A/Wisconsin/67/2005 (EPI_ISL_115646) MDCKP2, A/Texas/50/2012 (EPI_ISL_170149) MDCKP1. Additionally, the TJ-2 and TJ-5 COBRA H3 HA sequences, which were generated using the next generation COBRA methodology[111] were inserted into the pTR600 expression vector and synthesized as virus like particles (VLP's). TJ-2 was designed using H3N2 wild-type HA sequences from 2002-2005, and TJ-5 using H3N2 sequences from 2008-2012 [111]. Following transfection, cells were allowed to incubate at 37°C, 5% CO_2 for 72 hours, at which point supernatants from transiently transfected HEK 293-T cells were collected, centrifuged at 2500 rpm to remove cellular debris, and sterile filtered through a 0.22µm pore membrane. Mammalian VLPs were purified and sedimented by ultracentrifugation on a 20% glycerol cushion at 135,000 x g for 4h at 4°C. VLPs were resuspended in sterile phosphate buffered saline (PBS) and total protein concentration was assessed by conventional bicinchoninic acid assay (BCA) [13].

Hemagglutination activity of each preparation of VLPs was determined by adding equal volume of 0.75% guinea pig red blood cells (RBCs) in the presence of 20nM Oseltamivir, to a V-bottom 96-well plate and incubating with serially diluted volumes of VLP's for 60 minutes at room temperature (RT). The highest dilution of VLP with full agglutination of RBCs was considered the endpoint HA titer.

Determination of HA content

A high-affinity, 96-well flat bottom ELISA plate (Immulon 4 HBK, Thermo Fisher, Waltham, MA, USA) was coated with 5-10µg of total protein of VLP and serial dilutions of a recombinant H3 antigen (3006_H3_Vc, Protein Sciences, Meriden, CT, USA) in ELISA carbonate buffer (50mM carbonate buffer, pH 9.5), and the plate was incubated overnight at 4°C on a plate rocker. The next morning, coated plates were washed in PBS with 0.05% Tween-20 (PBST), then non-specific epitopes were blocked with 1% bovine serum albumin (BSA) in PBST solution for 1h at room temperature. Then, the buffer was removed and stalk-specific Group 2 human antibody CR8020 (Sanofi Pasteur, Lyon, France) 1mg/mL, was added to the plate in blocking buffer at a working dilution of 1:4000, and incubated for 1 h at 37°C [81]. Plates were then washed, and probed with goat-anti-human IgG horseradish-peroxidase-conjugated secondary antibody (1mg/mL) diluted in blocking buffer at a working dilution of 1:4000 (2040-05, Southern Biotech, Birmingham, AL, USA) for 1h at 37°C. Plates were washed, and then freshly prepared o-phenylenediamine dihydrochloride (OPD) (P8287, Sigma-Aldrich, St. Louis, MO, USA) substrate in citrate buffer (P4922, Sigma-Aldrich, St. Louis, MO, USA) was added to wells for 3-5 minutes, followed by the addition of 3M H_2SO_4 stopping reagent. Plates were then read at 492 nm absorbance using a microplate reader (Powerwave XS, Biotek, Winooski, VT, USA) and

background was subtracted from negative wells. Linear regression standard curve analysis was performed using the known concentrations of recombinant standard antigen to estimate HA content in VLP lots [19].

Viruses and HA antigens

Influenza A(H3N2) viruses were obtained through either the Influenza Reagents Resource (IRR), BEI Resources, the Centers for Disease Control (CDC), or provided by Virapur (San Diego, CA, USA). Viruses were passaged once in the same growth conditions as they were received, in either embryonated chicken eggs or semi-confluent Madin-Darby canine kidney (MDCK) cell cultures as per the instructions provided by the WHO [82]. Virus lots were titered with 0.75% guinea pig erythrocytes in the presence of 20nM Oseltamivir, and made into aliquots for single-use applications.

The A(H3N2) 1968-2019 historical influenza vaccine strain viral panel for HAI analysis included the 25 following viral strains: A/Hong Kong/8/1968 (HK/68) egg passage 3 (EP3), A/Port Chalmers/1/1973 (PC/73) EP1, A/Texas/1/1977 (Tx/77) EP2, A/Bangkok/1/1979 (Bgk/79) EP1, A/Mississippi/1/1985 (Miss/85) EP2, A/Sichuan/2/1987 (Sich/87) EP1, A/Shandong/9/1993 (Shan/93) EP1, A/Nanchang/933/1995 (Nan/95) EP3, A/Sydney/05/1997 (Syd/97) EP2, A/Panama/2007/1999 (Pan/99) EP4, A/Fujian/411/2002 (Fuj/02) MDCKP1, A/New York/55/2004 (NY/04) EP6, A/Wisconsin/67/2005 (Wisc/05) EP4, A/Brisbane/10/2007 (Bris/07) EP3, A/Uruguay/716/2007 (Uru/07) EP2, A/Perth/16/2009 (Per/09) EP4, A/Victoria/361/2011 (Vic/11) EP4, A/Texas/50/2012 (Tx/12) EP4, A/Switzerland/9715293/2013 (Switz/13) EP4, A/Hong Kong/4801/2014 (HK/14) EP11, and A/Singapore/IFNIMH-16-0019/2016 (Sing/16)

EP3, A/Kansas/14/2017 (Kan/17) EP1, A/Switzerland/8060/2017 (Switz/17) EP1, A/South Australia/34/2019 (SA/19) EP1, A/Hong Kong/2671/2019 (HK/19) EP1.

The panel of 13 co-circulating H3N2 viral variants from the period of 2009-2016 included:, A/Victoria/210/2009 (Vic/09) MDCKP3, A/Alabama/05/2010 (Ala/10) MDCKP2, A/Hessen/5/2010 (Hess/10) MDCKP3, A/Netherlands/009/2010 (Neth/10) MDCKP2, A/Norway/1330/2010 (Nor/10) MDCKP3, A/Madagascar/0648/2011 (Mad/11) MDCKP2, A/Norway/1186/2011 (Nor/11) MDCKP2, A/Stockholm/18/2011 (Stock/11) MDCKP3 A/Athens/112/2012 (Ath/12) MDCKP2, A/Jordan/30502/2012 (Jord/12) MDCKP2, A/Denmark/96/2013 (Den/13) MDCKP2, A/Hong Kong/12/2014 (HK/12/14) MDCKP2, A/Stockholm/28/2016 (Stock/16) MDCKP2.

When viruses could not be obtained, H3N1-Gag VLPs were synthesized using codon optimized wild-type H3 HA sequences obtained from GISAID. A mismatched N1 neuraminidase, from A/Thailand/1/2004, was included to enable budding of the viruses from the host cell membranes, while at the same time eliminating any potential protection offered by N2, NA antibodies that could be observed in assays using H3N2 viruses. This included the following 9 antigens for the 2016-2019 co-circulating strains panel: A/Fiji/110/2016 (Fiji/2016) EPI_ISL_289834, A/Georgia/12/2018 (Geo/18) EPI_ISL_329856, A/Nevada/37/2016 (Nev/16) EPI_ISL_237356, A/Moscow/41/2017 (Mos/17) EPI_ISL_276910, A/Washington/50/2017 (Wash/17) EPI_ISL_286341, A/Sao Paulo/690385/2018 (SP/18) EPI_ISL_299888, A/Abu Dhabi/240/2018 (Abu/18) EPI_ISL_338293, A/Colombia/0082/2019 (Col/19) EPI_ISL_356289, and A/Louisiana/39/2019 (LA/19) EPI_ISL_398579.

Selection of co-circulating H3N2 variants (2009-2019)

Selection of the co-circulating variants was based upon multiple sequence alignments that were performed on HA sequences downloaded from the GISAID database that were aligned and clustered using Geneious bioinformatics software (Biomatters, Ltd. Auckland, New Zealand). Sequences downloaded from 2009-2019 were organized based on collection during representative "Northern" or "Southern" Hemisphere influenza "seasons". In this approach, the downloaded sequences were separated into periods of time representing the "Northern" and "Southern" Hemisphere influenza seasons spanning from 2009-2019. The "Southern Hemisphere" season was defined to include sequences from all over the globe isolated from 5/1/XX – 9/30/XX of a given year, and each "Northern Hemisphere" season was defined to include sequences from around the world that were isolated from 10/1/XX - 4/30/XY of the following year. For example, sequences included in the 2009 "Southern Hemisphere" collection timeframe included those isolated between 5/1/2009 – 9/30/2009, and the isolates included in the 2009-2010 "Northern Hemisphere" collection contains sequences that were isolated between 10/1/2009 – 4/30/2010, regardless of where the sequences were isolated geographically. Phylogenetic tree models were assembled using a Jukes-Cantor genetic distance model, and a neighbor-joining tree building method in Geneious bioinformatics software. Branches were compared for sequence similarity to the panel of 22 co-circulating viruses. The sequences that branched within 95% HA sequence identity of one of the antigens was counted as a cluster, and frequencies of these clusters in each "influenza season" were calculated based on the total number of sequences available per season as described previously (Fig. 4.5) [65].

Viral infection and COBRA VLP vaccination of ferrets.

Fitch ferrets (Mustela putorius furo, female, 6 to 8 months of age), negative for antibodies to circulating influenza A (H1N1, H3N2) and influenza B viruses, were de-scented and purchased from Triple F Farms (Sayre, PA, USA). Ferrets were pair housed in stainless steel cages (Shor-line, Kansas City, KS, USA) containing Sani-Chips laboratory animal bedding (P.J. Murphy Forest Products, Montville, NJ, USA). Ferrets were provided with Teklad Global Ferret Diet (Harlan Teklad, Madison, WI, USA) and fresh water ad libitum. Ferrets (n = 4/group) were pre-infected with one of three seasonal H3N2 influenza viruses (1×10^6 PFU) intranasally with 1mL of inoculum diluted in phosphate-buffered saline (PBS, Corning, Tewksbury, MA, USA). One group of ferrets (N=20) was infected with seasonal H3N2 isolate A/Panama/2007/1999 (EP1), another (N=20) with A/Sichuan/2/1987 (EP1) H3N2, and a third (N=20) with A/Port Chalmers/1/1973 (EP1) H3N2 virus. A fourth group (N=20) was mock infected with 1mL of PBS (Fig. 4.1). Animals were monitored daily during the infection for adverse events, including weight loss, labored breathing, loss of activity, nasal discharge, sneezing, and diarrhea and allowed to recover for 84 days. Ferrets did not lose more than 5% body weight from any of the pre-infections and serum collected 14 days after the infection was tested in the HAI assay to confirm that animals had seroconverted to the strain used for infection (Fig. 4.2). 84 days after the pre-infection, ferrets were vaccinated with 15ug of either one of 2 H3N3 COBRA VLP vaccines (TJ2 or TJ5), one of the wild-type Wisc/05 or Tx/12 H3N3 VLP vaccines, or phosphate-buffered saline alone as a mock vaccination. All the vaccines, (TJ-2, TJ-5, Tx/12, Wisc/05, Mock), were formulated with an emulsified squalene-based oil-in-water emulsion adjuvant, Addavax (InvivoGen, San Diego, CA, USA). The final concentration after mixing 1:1 with VLPs is 2.5% squalene. Ferrets were boosted with an additional 15ug of homologous VLP 84 days after initial vaccination (Day 168). Blood

was harvested from all anesthetized ferrets via the anterior vena cava at days 14, 84, 98, 168, and 182. Serum was transferred to a centrifuge tube and centrifuged at 2500 rpm for 10 minutes, to separate the serum from the whole blood. Clarified serum was removed and frozen at −20 ± 5°C.

Hemagglutination-Inhibition (HAI) assay

The hemagglutination inhibition (HAI) assay was used to assess functional antibodies to the HA that are able to inhibit agglutination of guinea pig erythrocytes. The protocols were adapted from the WHO laboratory influenza surveillance manual [82]. Guinea pig red blood cells are frequently used to characterize contemporary A(H3N2) influenza strains that have developed a preferential binding to alpha (2,6) linked sialic acid receptors [83, 84]. To inactivate nonspecific inhibitors, sera samples were treated with receptor-destroying enzyme (RDE) (Denka Seiken, Co., Japan) prior to being tested. Briefly, three parts of RDE was added to one part of sera and incubated overnight at 37°C. RDE was inactivated by incubation at 56°C for 30 min. RDE-treated sera were diluted in a series of two-fold serial dilutions in v-bottom microtiter plates. An equal volume of each A(H3N2) virus, adjusted to approximately 8 hemagglutination units (HAU)/50µl in the presence of 20nM Oseltamivir carboxylate, was added to each well. The plates were covered and incubated at room temperature for 30 min, and then 0.75% guinea pig erythrocytes (Lampire Biologicals, Pipersville, PA, USA) in PBS were added. Red blood cells were washed twice with PBS, stored at 4°C, and used within 24 h of preparation. The plates were mixed by gentle agitation, covered, and the RBCs were allowed to settle for 1 h at room temperature. The HAI titer was determined by the reciprocal dilution of the last well that contained non-agglutinated RBCs. Positive and negative serum controls were included for each plate. All ferrets were negative (HAI ≤ 10) for pre-existing antibodies to human influenza viruses prior to vaccination, and for this study

sero-protection was defined as HAI titer >40 and seroconversion as a 4-fold increase in titer compared to baseline, as per the WHO and European Committee for Medicinal Products to evaluate influenza vaccines [85]. The ferrets were naïve and seronegative at the time of vaccination, and thus seroconversion and sero-protection rates are interchangeable in this study.

Focus Reduction Assay (FRA)

The Focus Reduction Assay (FRA) used in this study was initially developed by the WHO collaborating Centre in London, U.K. and modified by U.S. Centers for Disease Control and Prevention (CDC) (Thomas Rowe, personal communication). MDCK-SIAT1 cells (Sigma, St. Louis, MO, USA) were plated at 2.5 – 3 x 10^5 cells/ml (100uL/well in 96-well plate) one day prior to use in the assay. Cells were cultured in Dulbecco's Modified Eagle Medium (DMEM) containing 5% heat-inactivated fetal bovine serum and antibiotics in 96-well flat bottom plates overnight to form a 95-100% confluent monolayer. The following day, the cell monolayers are rinsed with 0.01M phosphate-buffered saline pH 7.2 (PBS, Gibco, Waltham, MA, USA), followed by the addition of 2-fold serially diluted RDE treated serum (50uL per well) starting with a 1:20 dilution in virus growth medium containing TPCK-treated trypsin (1µg/ml), VGM-T, (DMEM containing 0.1% BSA, 1% Penicillin/Streptomycin (100 U/mL Penicillin, 100 ug/mL Streptomycin solution), and 1µg/ml TPCK-treated trypsin) (Sigma, St. Louis, MO, USA). 50uL of A(H3N2) influenza virus (1.2 x 10^4 focus forming units (FFU)/mL, which corresponds to 600 FFU/50µl) in VGM-T was added to the wells of each plate, or VGM-T only was added to cell control wells. Virus stocks were standardized by previous titration in the FRA [54, 55]. Following a 2 h incubation period at 37°C with 5% CO_2, the cells in each well were then overlaid with 100uL of equal volumes of 1.2% Avicel RC/CL (Type: RC581 NF; FMC Health and Nutrition,

Philadelphia, PA, USA) in 2X Modified Eagle Medium containing 1µg/ml TPCK-treated trypsin, 0.1% BSA and antibiotics [86]. Plates were incubated for 18-22 h at 37°C, 5% CO_2. The overlays were then removed from each well and the monolayer was washed once with PBS to remove any residual Avicel. The plates were then fixed with ice-cold 4% formalin in PBS for 30 min at 4°C, followed by a PBS wash and permeabilization using 0.5% Triton-X-100 in PBS/glycine at room temperature for 20 min. Plates were washed three times with wash buffer (PBS, 0.1% Tween-20; PBST) and then incubated for 1 h with a monoclonal antibody against the influenza A nucleoprotein [54, 87, 88] obtained from the Influenza Reagent Resource (IRR) (Manassas, VA, USA) (FR-1217) (1mg/mL), diluted 1:2000 in ELISA buffer (PBS,10% horse serum, 0.1% Tween-80). Following washing (3X PBST), the cells were incubated with goat anti-mouse peroxidase-labelled IgG (Sera Care, Inc., Milford, MA, USA) (KPL 474-1802) (1mg/mL), diluted 1:2000 in ELISA buffer for 1 hour at RT. Plates were washed again (3X PBST) and infectious foci were visualized using TrueBlue substrate (Sera Care, Inc., Milford, MA USA) containing 0.03% H_2O_2 incubated at room temperature (RT) for 10 min. The reaction was stopped by washing five times with dH_20. Plates were air dried and foci enumerated using a CTL BioSpot Analyser with ImmunoCapture 6.4.87 software (CTL, Shaker Heights, OH, USA). The FRA titer was reported as the reciprocal of the highest dilution of serum corresponding to 50% foci reduction compared to the virus control minus the cell control.

In order for a plate to pass quality control, both the average of the octuplet virus control wells (VC), as well as the average of the octuplet cell control wells (CC) must pass. The virus controls initially were between 150 to 650 foci and the cell controls must be free of foci. The virus control wells were subsequently expanded to between 200 and 1600 foci. Additionally, the positive control virus, A(H3N2) historical influenza vaccine strain, was run in triplicate plates in

each individual assay and at least two out of three plates must pass VC and CC criteria and homologous ferret antisera, previously generated through infection with A(H3N2) influenza virus at 1e6 FFU/mL and collected 14 days post infection, must have the same titer across the plates [65]. Each assay plate (one virus per plate) contained a panel of ferret reference antisera, as well as a human influenza vaccine serum control to assess overall assay consistency [13]. The percentage of infected cells reported in the assay is calculated by averaging the foci count from the positive control (virus and cell only) wells, and dividing the number of foci in each experimental well by the average of the positive control.

Results

Historical HAI Landscape of VLP Vaccinated Pre-immune Ferrets

Previously, nine distinct H3 COBRA antigens, TJ-1 – TJ-9 were designed and tested in immunologically naïve mice to determine the breadth of antibody reactivity induced by these universal vaccine candidates against both historical and co-circulating H3N2 influenza strains [111]. The results of this investigation led to the selection of two lead candidate COBRA HA immunogens, TJ-2 (designed from WT H3N2 sequences in circulation during 2002-2008) and TJ-5 (designed from WT H3N2 sequences in circulation during 2008-2012), that needed to be tested further in the ferret, a more clinically relevant animal model, to assess their performance in populations with prior influenza immune history. In this study the two next-generation H3 COBRA HA vaccine antigens were compared to two WT historical H3 vaccine antigens, Wisc/05 for comparison to TJ-2, and Tx/12 for comparison to TJ-5, in order to assess their abilities to elicit cross-reactive antibodies in ferrets that are pre-immune to H3N2 viruses representing different historical eras. Ferrets (n=20/group) were infected with a representative virus isolated from the

1973, 1987, or 1999 (Fig. 4.1). Sera collected from ferrets at 14 days post-infection had HAI activity against the infecting strain, as well as a few other antigenically related viruses (Fig. 4.2). Ferrets infected with the 1990's representative virus, Pan/99, had antibodies with HAI activity against both Syd/97 and Pan/99. The ferrets infected with the 1980's representative virus, Sich/87, had antibodies with HAI activity against Miss/85 and Sich/87 with a few serum samples recognizing the HK68 virus and Shan/93. Ferrets infected with the 1970's representative virus, PC/73, had sera with HAI activity against PC/73 and HK/68. The mock infected influenza naïve ferrets had no HAI activity against any of the 25 H3N2 influenza viruses in the panel (Fig. 4.2). Overall, the viruses used to establish pre-immunity elicited the highest antibody titers against the homologous infecting strain with some reactivity to 1 or 2 other viruses in the panel.

At 84 days post infection, ferrets were divided into groups (4 animals/group) and then were vaccinated with VLPs expressing either TJ-2, TJ-5, Tx/12, or Wisc/05 H3 HA mixed with Addavax oil-in-water emulsion adjuvant. A mock group was also vaccinated with phosphate buffered saline (PBS) mixed with adjuvant. At day 98 post infection (14 days following vaccination), antisera were collected from the animals and analyzed for HAI activity against a panel of 25 historical H3N2 vaccine strain isolates from 1968-2019 (Fig. 4.3). Ferrets pre-immune to Pan/99 and vaccinated with VLPs expressing TJ-2 HA had antibodies with HAI activity against 11/25 (44%) of the strains in the panel including all of the strains from 1995-2007, 2011, 2012, and 2014 (Fig 4.3A). Ferrets pre-immune to Pan/99 and vaccinated with VLPs expressing TJ-5 HA had HAI activity to 17/25 (68%) of the strains comprising all of the isolates from 1995-2019 with the exception of HK/19 (Fig. 4.3A). The animals pre-immunized with Pan/99 and vaccinated with VLPs expressing Tx/12 HA HAI activity to 14/25 (56%) of strains comprising strains from 1997-2019, excluding Uru/07, Sing/16, and HK/19 (Fig. 4.3A). Similar to the animals vaccinated

with VLPs expressing TJ-2 HA, the ferrets pre-immune to Pan/99 and vaccinated with VLPs expressing Wisc/05 HA had HAI against 11/25 (44%) of the strains, including all of the strains from 1995-2014 excluding Uru/07 and Switz/13 (Fig. 4.3A). The animals infected with Pan/99 and given a mock vaccination seroconverted to the same strains induced by the infection at day 14, Syd/97 and Pan/99, albeit at slightly lower titers than at day 14 post infection (Fig. 4.3A).

Animals pre-immunized with Sich/87 and vaccinated with VLPs expressing TJ-2 HA had antibodies against 7/25 (28%) of the strains. These animals retained the antibodies from the infection with HAI activity against Miss/85 and Sich/87 that were present at day 14, while adding HAI activity against viruses isolated from 2002-2007 (Fig. 4.3B). The ferrets infected with Sich/87 and vaccinated with VLPs expressing TJ-5 HA had antibodies with the broadest HAI activity compared to any vaccinated group at day 98, and recognized 20/25 (80%) of the viruses in the panel. These animals seroconverted to PC/73 and all of the strains from 1985-2019 excluding Uru/07 and HK/19 (Fig. 4.3B). Ferrets pre-immune to Sich/87 and vaccinated with VLPs expressing Tx/12 HA had HAI activity against 12/25 (48%) of the strains in the panel, including isolates from 1985-1995, Fuj/02, and the strains from isolated between 2009-2019, excluding Sing/16 and HK/19 (Fig. 4.3B). Ferrets pre-immune to Sich/87 and vaccinated with VLPs expressing Wisc/05 HA had HAI activity against only 4/25 (16%) of the strains isolated between 1985-1993 and the homologously matched Wisc/05 strain (Fig. 4.3B). Ferrets that were only infected with Sich/87 and then mock vaccinated retained their antibody titers to Miss/85 and Sich/87, but did not seroconvert to any of the other strains in the panel (Fig. 4.3B). Overall, VLPs with COBRA H3 HA antigens elicited antibodies that recognized more H3N2 influenza strains than VLPs expressing WT H3 HA proteins in the animals that were primed with the Sich/87 virus.

The ferrets infected with PC/73 and vaccinated with VLPs expressing TJ-2 HA had HAI activity against 5/25 (20%) of the H3N2 strains, the two strains from the initial infection, HK/68 and PC/73, as well as the strains from 2002-2005 (Fig. 4.3C). Ferrets pre-immune to PC/73 and vaccinated with VLPs expressing TJ-5 HA antisera with HAI activity against 4/25 (16%) of the strains, including the strains from 1968-1973 and 2011-2012 (Fig. 4.3C). Animals pre-immune to PC/73 and vaccinated with VLPs expressing WT Tx/12 HA had HAI activity against 5/25 (20%) of the strains, the strains from 1968-1973 and 2009-2012 (Fig. 4.3C). Animals pre-immune to PC/73 and vaccinated with VLPs expressing Wisc/05 HA had HAI activity against 3/25 (12%) of the strains in the panel, consisting of viruses isolated from 1968-1973 and the homologously matched Wisc/05 strain (Fig. 4.3C). Ferrets that were pre-immunized with PC/73 and administered a mock vaccination retained their antibody HAI activity against HK/68 and PC/73, but did not seroconvert to any of the other strains in the panel (Fig. 4.3C). In general, the animals primed with PC/73 had antisera with the least cross-reactive HAI breadth of the three pre-immune regimens. No animals that were mock infected had any HAI seroconversion against any of the strains in the panel following a single VLP vaccination, regardless of the vaccine antigen (Fig. 4.3D). The mock pre-immune animals vaccinated with Wisc/05 and Tx/12 do have HAI titers against the homologous virus, however these titers are not high enough to yield an average HAI titer of 40 or higher for the group (log2 GMT of 4.07 and 3.82 respectively). This is not overly surprising as our group has published on this phenomenon before, where in influenza naïve ferrets more than one vaccination is often required to induce seroconversion to the homologously matched virus [65].

In order to determine if the cross-reactive breadth elicited by the COBRA vaccine antigens could increase the sero-conversion against more historical H3N2 isolates through repeated

vaccination, all ferrets were boosted with a second dose of vaccine at 168 days post infection, and antisera was collected 14 days later, at day 182 (Fig. 4.4). Ferrets pre-immune to Pan/99 and vaccinated twice with VLPs expressing TJ-2 HA had HAI activity to 17/25 (68%) of the strains in the panel including of all the strains from 1995-2019 with the exception of Ks/17 (Fig. 4.4A). The animals pre-immune to Pan/99 and vaccinated two times with VLPs expressing TJ-5 HA had HAI activity against 17/25 (68%) of the strains, including all of the strains isolated from 1997-2019 (Fig. 4.4A). Ferrets pre-immunized with Pan/99 and boosted with VLPs expressing Tx/12 HA had HAI activity against 17/25 (68%) of the H3N2 strains, recognizing the same isolates (1997-2019) as ferrets vaccinated with VLPs expressing TJ-5 HA (Fig. 4.4A). Animals pre-immune to Pan/99 and boosted with VLPs expressing Wisc/05 HA seroconverted to 17/25 (68%) of the strains, including all the strains isolated from 1995-2019 with the exception of Ks/17 (Fig. 4.4A). The ferrets that were infected with Pan/99 and boosted with mock vaccines retained their HAI activity against Syd/97 and Pan/99, but did not seroconvert against any other strains in the panel (Fig. 4.4A).

Animals pre-immunized with Sich/87 and boosted with VLPs expressing TJ-2 HA had antisera with HAI activity against 11/25 (44%) of the strains in the panel, including Sich/87, Shan/93, and all of the isolates from 2002-2013 (Fig. 4.4B). The ferrets pre-immune to Sich/87 and boosted with VLPs expressing TJ-5 HA had antisera with HAI activity against 18/25 (72%) of the strains, including all the strains isolated from 1985-1993 and 2002-2019 (Fig. 4.4B). Ferrets infected with Sich/87 and boosted with VLPs expressing Tx/12 HA also had antisera with HAI activity against 18/25 (72%) of the strains in the panel, including viruses isolated from 1987-1995 and 2002-2019 (Fig. 4.4B). Animals pre-immune to Sich/87 and boosted with VLPs expressing Wisc/05 HA had antisera with HAI activity against 9/25 (36%) of the strains in the panel including

isolates from 1987-1993, 2002-2007, and 2011-2013 (Fig. 4.4B). Ferrets that were only infected with Sich/87 and given two mock vaccinations retained their antibody HAI activity against Sich/87 and gained HAI activity against Shan/93, but did not seroconvert to any of the other strains in the panel (Fig. 4.4B).

Ferrets infected with PC/73 and boosted with VLPs expressing TJ-2 HA had HAI activity against 11/25 (44%) of the H3N2 strains, including HK/68 and PC/73, as well as the isolates from 2002-2013 (Fig. 4.4C). The animals pre-immune to PC/73 and boosted with VLPs expressing TJ-5 HA had HAI activity against 18/25 (72%) of the strains in the panel including the viruses isolated between 1968-1977, Shan/93, and all of the isolates from 2004-2019 (Fig. 4.4C). Ferrets infected with PC/73 and then boosted with VLPs expressing Tx/12 HA had HAI activity against 15/25 (60%) of the viruses including strains isolated from 1968-1977, Shan/93, and all of the viruses from 2005-2019, excluding Uru/07 and Ks/17 (Fig. 4.4C). Ferrets pre-immune to PC/73 were boosted with VLPs expressing Wisc/05 HA had HAI activity against 10/25 (40%) of the strains, including the viruses isolated from 1968-1973 and all of the strains from 2002-2013, excluding Perth/09 (Fig. 4.4C). Ferrets that were pre-immunized with PC/73 and mock vaccination retained their HAI activity against HK/68 and PC/73, but had no HA activity against any other strains. in the panel (Fig. 4.4C).

Mock infected/naïve ferrets that were vaccinated twice with TJ-5 HA had HAI activity against 5/25 (20%) strains in the panel, including the isolates from 2011-2016, excluding Switz/13 and the SA/19 virus (Fig. 4.4D). All mock infected/naïve ferrets that were vaccinated with VLPs expressing either TJ-2, Tx/12, or Wisc/05 HA had HAI activity against only 1/25 (4%) of the strains in the panel, either Tx/12 or Wisc/05 virus (Fig. 4.4D). As expected, the mock infected and mock vaccinated ferrets had no HAI activity against any of the strains in the panel (Fig. 4.4D).

In general, the second vaccination increased the cross-reactive antibody HAI breadth for all of the pre-immune animals, while the naïve animals had limited HAI activity against the panel after the second vaccination.

Co-Circulating Strain (2009-2019) HAI Landscape of VLP Vaccinated Pre-immune Ferrets

Antisera collected from vaccinated ferrets 98 days post-infection was also analyzed in HAI assays across a panel of 15 co-circulating H3N2 influenza drift variants isolated from 2016-2019, as well as 7 H3 drift variants from 2009-2016 which were previously identified [65] (Fig. 4.5). Ferrets pre-immune to Pan/99 and vaccinated with VLPs expressing either TJ-2, TJ-5, Tx/12, or Wisc/05 HA proteins all had HAI activity against 13/22 (59.09%) of the co-circulating strains (Fig. 4.6A). All ferrets had HAI activity against strains isolated from 2009-2016 excluding Fiji/16, and Nev/16, regardless of which HA vaccine was used for vaccination. None of the vaccines elicited HAI activity against the strains isolated from 2017-2019 following a single vaccination (Fig. 4.6A). Ferrets infected with Pan/99 infected, but only mock vaccinated, had HAI activity against 6/22 (27.27%) of the co-circulating strains, including Nor/10, Nor/11, Mad/11, Ath/12, Den/13, and HK/12/14 (Fig. 4.6A).

The ferrets pre-immune to Sich/87 and vaccinated with VLPs expressing TJ-2 HA had HAI activity against 10/22 (45.45%) of the co-circulating strains in the panel, which were all isolated from 2009-2014 with the exception of the Hess/10 and Neth/10 viruses (Fig. 4.6B). Animals pre-immune to Sich/87 and vaccinated with VLPs expressing either TJ-5 or Tx/12 HA had HAI activity against the same 13/22 (59.09%) viruses in the panel, which included the strains isolated from 2009-2016, excluding Fiji/16, and Nev/16 (Fig. 4.6B). Ferrets pre-immune to Sich/87 and vaccinated with VLPs expressing Wisc/05 HA had HAI activity against 10/22 (45.45%) of the co-

circulating strains that were all isolated from 2010-2014 with the exception of the Neth/10 virus (Fig. 4.6B). The mock vaccinated Sich/87 pre-immune animals had HAI activity against 5/22 (22.72%) of the co-circulating viruses in the panel, including Nor/10, Mad/11, Ath/12, Den/13, and HK/12/14 (Fig. 4.6B).

Animals infected with PC/73 and then vaccinated with VLPs expressing TJ-2 HA had HAI activity against 10/22 (45.45%) of the co-circulating strains, comprising all of the strains from 2010-2014, but excluding Stock/11 (Fig. 4.6C). Ferrets pre-immune to PC/73 and vaccinated with VLPs expressing either TJ-5 or Tx/12 HA had had HAI activity against the same 12/22 (54.54%) viruses in the panel, which included all of the strains isolated from 2009-2014 (Fig. 4.6C). The ferrets pre-immune to PC/73 and vaccinated with VLPs expressing Wisc/05 HA had HAI activity against 10/22 (45.45%) of the co-circulating strains in the panel, consisting of all the isolates from 2009-2014, but excluding Neth/10 and Stock/11 (Fig. 4.6C). The animals that were infected with PC/73 and were only mock vaccinated had HAI activity against 3/22 (13.64%) of the strains that included the Nor/10, Mad/11, and Den/13 viruses (Fig. 4.6C). Interestingly the antibodies generated though COBRA vaccination with TJ-5 in animals preimmune to PC/73 were cross-reactive against the co-circulating variants (Fig. 4.6C), but not the historical vaccine strains (Fig. 4.3C) isolated from 2010-2014.

Overall, the ferrets that were mock infected and then vaccinated with VLPs expressing TJ-2 HA had HAI activity against 4/22 (18.18%) of the viruses in the panel, including the Nor/10, Mad/11, Den/13, and HK/12/14 strains (Fig. 4.6D). Ferrets vaccinated with TJ-5 HA had HAI activity against 5/22 (22.72%) of the strains in the panel, including the Nor/10, Mad/11, Ath/12, Jord/12, and Den/13 viruses (Fig. 4.6D). Ferrets vaccinated with VLPs expressing either Wisc/05 or Tx/12 HA antigens, or mock vaccinated did not have HAI activity against any of the strains in

the panel (Fig. 4.6D). Overall, after single vaccination, the pre-immune animals had HAI activity against most of the drift variants isolated from 2009-2014, while the immunologically naïve animals had limited HAI activity against across the panel.

At 182 days post-infection (14 days post-boost), additional antisera were collected from vaccinated ferrets. In general, after two vaccinations, the Pan/99 pre-immune ferrets had the most cross-reactive HAI activity with the highest magnitude of antibody titers compared to the other pre-immune regimens across the panel (Fig. 4.7A). The animals pre-immune to Pan/99 and vaccinated with VLPs expressing either TJ-5 or Tx/12 HA had HAI activity against all 22 strains in the panel from 2009-2019 and those vaccinated with VLPs expressing Wisc/05 HA had HAI activity against all of the strains in the panel, except LA/19 (Fig. 4.7A). The TJ-2 HA VLP vaccinated ferrets had slightly less cross-reactive breadth, but still had HAI activity against all of the strains from 2009-2016, as well as the SP/18 strain (Fig. 4.7A). The mock vaccinated animals only had HAI activity against 5/22 (22.72%) of the strains in the panel (Fig. 4.7A).

Ferrets pre-immune to Sich/87 and then vaccinated twice with VLPs expressing either TJ-5 or Tx/12 HA had HAI activity against all the drift variants from 2009-2019, but at slightly lower titers than the same groups that were made pre-immune to Pan/99 (Fig. 4.7B). The groups pre-immune to Sich/87 and vaccinated with VLPs expressing either TJ-2 or Wisc/05 HA had similar patterns of HAI reactivity against the panel of viruses, with HAI activity against 12/22 (54.54%) and 13/22 (59.09%) of the viruses respectively. The Wisc/05 HA VLP vaccines elicited HAI activity against the Hess/10 virus that VLPs expressing TJ-2 HA did not (Fig. 4.7B). The mock vaccinated Sich/87 pre-immune animals had HAI activity against 3/22 (13.64%) of the viruses in the panel (Fig. 4.7B).

Ferrets that were pre-immune to PC/73, two vaccinations with VLPs expressing either TJ-5 or Tx/12 HA was again sufficient to elicit antibodies with HAI activity against all 22 strains in the panel (Fig. 4.7C). However, once again, the overall magnitude of the HAI titer was reduced compared to ferrets that were pre-immune to Pan/99 or Sich/87 (Fig. 4.7C). Ferrets pre-immune to PC/73 and vaccinated with VLPs expressing TJ-2 HA had HAI activity against 14/22 (63.64%) of the strains and performed slightly better than ferrets vaccinated with VLPs expressing Wisc/05 HA that had HAI activity to 11/22 (50%) strains (Fig. 4.7C). Ferrets pre-immune to PC/73 and then mock vaccinated had HAI activity against 3/22 (13.64%) of the strains in the panel (Fig. 4.7C).

Overall, naïve ferrets that were not infected, but vaccinated with VLPs expressing HA vaccines, had antibodies with HAI activity that recognized few viruses in the panel than ferrets pre-immunized with a historical H3N2 viruses (Fig. 4.7D). Naive ferrets vaccinated twice with VLPs expressing TJ-2 HA had HAI activity against 4/22 (18.18%) of the viruses in the panel (Fig. 4.7D). Naïve ferrets vaccinated with VLPs expressing TJ-5 HA had the most cross-reactivity HAI antibodies compared to other naïve vaccinated ferrets with HAI activity against 11/22 (50%) of the drift variants in the panel (Fig. 4.7D). Vaccination of naïve ferrets with VLPs expressing the Tx/12 HA had HAI activity against 5/22 (22.72%) of the viruses, while VLPs expressing the Wisc/05 HA and mock vaccinations did not generate seroprotective HAI antibody titers against any of the strains in the panel (Fig. 4.7D). In naïve animals, the COBRA HA VLP vaccinations induced more cross-reactive antibody breadth than the era matched WT HA VLP comparators.

H3N2 Neutralization Assays

Influenza focal reduction assays (FRAs) were used to determine the ability of vaccine elicited antibodies to neutralize live virus infections against a panel of 7 historical influenza A(H3N2) vaccine strain isolates from 2012-2019 at day 98 post infection (Fig. 4.8). All of the ferrets pre-immune to Pan/99 and vaccinated one time, regardless of vaccine, had Log_2 50% neutralization ($Neut_{50}$) titers that were superior to mock vaccinated animals across all of the viruses in the panel (Fig. 4.8A). In general, for the Pan/99 pre-immune animals, TJ-5 produced the highest magnitude $Neut_{50}$ titers against every virus in the panel compared to the other vaccine antigens (Fig. 4.8A). The lowest $Neut_{50}$ titers from this pre-immune regimen were produced against the Ks/17 virus, against which none of the vaccines produced a $Neut_{50}$ titer greater than 1:40 (Fig. 4.8A). An antibody titer of 1:40 in this assay does not correlate with a sero-protective titer, but it is a correlate for sero-protection for the HAI assay, so we used this as a baseline to make comparisons between responses.

Ferrets pre-immune to Sich/87 and vaccinated with VLP antigens also consistently produced higher $Neut_{50}$ titers than those that received mock vaccine (Fig. 4.8B). Again, TJ-5 produced higher $Neut_{50}$ titers across the panel of H3N2 viruses than any other vaccine, with the exception of Tx/12 against HK/19 where it slightly outperformed TJ-5 with a Log_2 $Neut_{50}$ titer of 6.04 compared to 5.89 (Fig. 4.8B). Much like the Pan/99 groups, the Sich/87 pre-immune groups also had trouble generating neutralizing antibody titers greater than 1:40 against the Ks/17 virus, and additionally against the SA/19 virus where only TJ-5 and Tx/12 vaccines generated $Neut_{50}$ titers greater than 1:40 (Fig. 4.8B).

Much like the Pan/99 and Sich87 pre-immune ferrets the PC/73 pre-immune animals vaccinated with any of the H3 VLP antigens generated a strong neutralizing antibody response

against the viruses from 2012-2016 (Fig. 4.8C). The TJ-5 and Tx/12 antigens generated the highest antibody responses across the panel, and those antigens also possessed $Neut_{50}$ titers greater than 40 against both SA/19 and HK/19 (Fig. 4.8C). None of the vaccine antigens produced $Neut_{50}$ titers greater than 1:40 against the Ks/17 isolate in the PC/73 pre-immune animals (Fig. 4.8C). All four of the vaccines induced high neutralization titers against the Tx/12 and Sing/16 viruses in the influenza naïve mock pre-immune groups (Fig. 4.8D). In this group TJ-5 induced the most breadth and produced the highest neutralization antibody titers across the panel of viruses, with its highest response being against the Sing/16 virus (Fig. 4.8D). Mock pre-immune animals vaccinated with TJ-2 produced $Neut_{50}$ titers greater than 1:40 against 3 of the viruses in the panel while Tx/12 and Wisc/05 only achieved this feat against 2 of the viruses, Tx/12 and Sing/16 (Fig. 4.8D).

Discussion

OAS to influenza viruses is a phenomenon that was first recognized in the 1960's and has been observed in many different clinical studies and animal models under controlled conditions [112]. However, recapitulating the human immune response in relevant influenza virus animal models, like the ferret, is difficult. Multiple studies have demonstrated that ferrets and humans have different antibody responses to influenza virus infection, primarily because humans have extensive immune histories with the virus through natural infections and vaccinations [104]. The influenza virus strains that a person encounters within the first few years of life can leave lasting impacts that effect how an individual responds to antigenically distinct viral strains later in life [113, 114]. The study presented herein aimed to investigate the effects of historical A(H3N2) influenza virus imprinting on the elicitation of antibodies that recognize a broad number H3N2 viruses following subsequent vaccination with VLP vaccines expressing either COBRA or wild-

type H3 HA antigens. Ferrets were initially primed using live A(H3N2) influenza virus infection using representative viruses isolated from the 1970's, 1980's, and 1990's to model a person's first infection with the virus during these eras. VLPs expressing the COBRA or WT HA vaccine antigens were then evaluated in this animal model to determine their elicitation of antibodies against drifted strains of influenza virus, since ideal vaccine candidates should induce robust immune responses in all individuals, regardless of their specific immune history.

Differences in COBRA and WT HA VLP vaccine performances were observed between groups of ferrets depending on their specific immune histories to A(H3N2) influenza viruses. In general, VLPs expressing H3 HA vaccine antigens that were more genetically similar to the specific priming virus induced the highest level of HAI breadth across the panel of historical A(H3N2) influenza vaccine strains (Fig. 4.3). VLPs expressing the TJ-5 and Tx/12 HA antigens induced the most breadth of HAI responses in ferrets primed with the Pan/99 or Sich/87 viruses. The HA proteins of these vaccines share ~91% genetic similarity to both of the priming strains (Pan/99 and Sich/87). After one vaccination, these vaccines elicited seroconversion to 56-80% viruses in the panel. However, ferrets pre-immune to the PC/73 virus and then administered these same vaccines elicited antibodies with HAI activity against only 16-20% of the viruses in the panel. The PC/73 HA is ~87% similar to the two vaccine strains. In this study it appears that when the genetic distance between priming strain and vaccine antigen is greater ~87%, the ability of the HA vaccine antigens to elicit broadly-reactive antibodies against the panel drops significantly. This is potentially a result of the number of shared antigenic epitopes between the priming strain and the vaccine antigen. Genetic similarity between the two could possibly present the immune system with more shared antigenic epitopes that can be recalled by vaccination, leading to a more robust antibody response [102].

However, in this study it appears that this genetic distance bias can be overcome through repeated vaccination with the same H3 antigen. After boosting the PC/73 primed ferrets with a homologous vaccination of VLPs expressing TJ-5 or Tx/12 HA, the seroconversion rates across the panel of historical vaccine isolates rose from 16-20% to 60-72% (Fig. 4.4). A similar phenomenon also occurred in the 2009-2019 co-circulating A(H3N2) strains panel (Fig. 4.6). After one vaccination with VLPs expressing either TJ-5 or Tx/12 HA, the ferrets seroconverted to 45-59% of the strains regardless of the priming virus, but none of the animals had seroprotective titers against any of the strains isolated from 2017-2019 (Fig. 4.6). Although seroconversion rates against this panel were similar amongst all of the pre-immune ferrets, ferrets primed with the genetically distant PC/73 virus had a drop in HAI titers compared to the ferret's pre-immune to either Sich/87 or Pan/99. After the second vaccination with VLPs expressing the TJ-5 or Tx/12 HA, all of the pre-immune ferrets seroconverted to all of the strains in the panel, regardless of the priming virus (Fig. 4.7). This was in stark contrast to the immunologically naïve animals that seroconverted to at most 50% of the co-circulating A(H3N2) strains after two vaccinations with VLPs expressing TJ-5 HA. Overall, it appears that the H3 vaccine candidates induced more seroconversion in animals that possess an immunological history with A(H3N2) influenza strains and the differences in immunological reactivity driven by that history can be overcome with repeated vaccination. This is likely due to the generation of new memory B cell populations elicited by the first vaccination, which can then be recalled upon subsequent vaccination with the same antigen [115]. However, current limitations in ferret B cell immunology and the availability of ferret immunoassay reagents prevent us from investigating these questions within our current study, therefore future experiments will be aimed at answering these types of questions.

All of the A(H3N2) pre-immune ferrets that received vaccines, COBRA or WT HA, also had a high level of neutralizing antibody activity across the panel of A(H3N2) historical vaccine viruses from 2012-2019, with the exception of the Ks/17 virus (Fig. 4.8). The Ks/17 virus is slightly different from most of the other viruses in the panel as it, as well as Switz/13 belong to clade 3c3.a. Other viruses in the panel either belong to clade 3c2 or its subclades 3c2.a and 3c2.a1. 3c3.a viruses elicit antibody responses in ferrets that are biased toward antigenic site B [104]. 3c3.a viruses possess a K160 in site B, while 3c.2a viruses possess a T160 that results in the addition of an N-linked glycosylation at site 158 [104]. This glycosylation present on the HA of 3c2.a viruses may cover up antigenic epitopes that are necessary to generate strong neutralizing antibody responses to 3c3.a viruses [113]. Switz/13 and Ks/17 differ by 4 amino acids (AA) in antigenic site B, N160K, G202V, D206N, and F209S, which may also drive the observed differences in their neutralization titers, but neither possess the glycosylation motif at site 158 that is present in the 3c2.a viruses. The neutralization assays performed in this study also take into account the contributions of non-HA reactive antibodies, such as antibodies directed against the viral NA, obtained from the virus priming, that may play a role in the observed differences in neutralization titers across the panel. This may play a significant role as animals that did not possess immunologic memory to the NA of the A(H3N2) priming viruses did not acquire high neutralization titers after repeated vaccinations with H3N3 VLP vaccines. Additionally, differences were observed in the antibody reactivity between the HAI and FRA assays. The HAI assay predominately detects antibodies directed towards the head region of the HA molecule that prevent binding of the HA with the host sialic acid. Antibodies directed towards the stem of the HA protein typically will not show up in this analysis as they can still allow this interaction between the HA head and the host sialic acid to take place. These antibodies still possess the

ability to prevent viral replication, but typically this is done by preventing the conformational changes that take place in the endosome once the virus has entered into the host cell preventing membrane fusion or cleavage of the HA0 into HA1 and HA2 fragments [116]. In contrast to the HAI, the FRA detects all antibodies that possess the ability to prevent viral infection. It is likely that the differences in HAI and FRA titer are being driven by HA stem reactive antibodies that do not play a role in HAI based protection. However, HAI specific antibodies are typically immunodominant over stalk-specific antibodies, and also tend to generate more effective neutralizing immune responses, lower IC50; therefore, antigen design methodologies such as COBRA which drive HA head-based antibody responses could be highly advantageous for generating potent, cross-reactive immune responses [73, 91-93].

The ferrets vaccinated with antigens representing the early 2010's, VLPs expressing TJ-5 and Tx/12 HA, possessed the most cross-reactive HAI antibodies in all three pre-immune regimens, centered around A(H3N2) viruses isolated from 2002-2019. These two antigens are quite similar, as they differ by only 9AA (1 AA in antigenic site A, 2 in site B, and none in the other antigenic sites C-E). Both possess 12 potential glycosylation site motifs, including the glycosylation motif at site 158, generate similar patterns of HAI cross-reactivity, and display similar live virus neutralizing ability across the panels. The similar HAI antibody profiles elicited by these two vaccines could in part be attributed to the cross-reactivity of the A(H3N2) vaccine strains isolated from 2009-2016 [13]. The majority of these viral isolates belong to clade 3c2 or its subclades 3c2.a and 3c2.a1 that tend to elicit HAI cross-reactive antibodies to one another [111]. What differentiates these two vaccines are the magnitude of antibody titer that is generated after one vaccination in the pre-immune model. In most cases, for both the Pan/99 and Sich/87 pre-immune ferrets, TJ-5 HA consistently produces higher HAI antibody titers than Tx/12 HA across

the panel after just one vaccination (Fig. 4.3); while VLPs expressing Tx/12 HA appear to require 2 vaccinations to achieve antibody titers that are similar to those elicited by VLPs expressing TJ-5 HA (Fig. 4.4). A similar trend was observed with the two vaccine candidates representing the 2002-2005 era, TJ-2 and Wisc/05 HA proteins. These are also similar antigens to one another as they differ by only 8AA (2 differences in antigenic site A, 2 in site B, and none in the other antigenic sites C-E). Much like VLPs expressing TJ-5 HA, TJ-2 HA was more cross-reactive in the HAI assay, in the pre-immune ferrets, than Wisc/05 HA after one vaccination (Fig. 4.3). After 2 vaccinations with VLPs expressing Wisc/05 or TJ-2 HA, antibody titers across the historical vaccine strain panel increased to similar levels for both vaccine antigens (Fig. 4.4). The HAI reaction for TJ-2 does decrease against 2 of the viruses from day 98 to day 182. This decrease is not great in magnitude, but it is enough to cause the animals to fall below the 1:40 seroconversion cutoff. This drop in titer is likely the result of B cells undergoing affinity maturation toward epitopes present in the vaccine antigen, and making the animal's immune responses more tailored to targeting vaccine-based epitopes rather than ones present on the Sich/87 priming strain. After one vaccination the animals possess memory cells to both the priming strain and vaccine strain that can be preferentially recalled by the second vaccination. The number of strains that the vaccinated animals seroconvert to also increases from day 98 to 182, and at the later timepoint future drifted strains from 2016-2018 that were not seroconverted against after one vaccination are now being picked up. This phenomenon could also be explained by B cell affinity maturation; whereby epitopes present on the vaccine that are not shared with the Sich/87 priming strain are driving the immune response towards recalling new epitopes that are shared between the vaccine and future drifted strains that may not be present on past viruses.

In this study, it appears that the VLPs expressing COBRA HA vaccine antigens are superior at eliciting cross-reactive HAI antibody breadth after one vaccination than VLPs expressing the WT HA vaccine antigens. Additionally, VLPs expressing the WT HA vaccines require a boost to elicit similar levels of breadth as VLPs expressing the COBRA HA antigens. This is particularly evident in the Sich/87 pre-immune groups (Fig. 4.3B). Animals vaccinated with TJ-2 induced seroconversion against 7/25 strains in the panel, while the WT comparator, Wisc/05, only induced seroconversion against 4/25 strains. Furthermore, animals vaccinated with TJ-5 induced seroconversion against 20/25 strains in the panel, while its WT comparator Tx/12 only induced seroconversion against 12/25 strains. The COBRA vaccines also do as good, or better than the WT comparators in the Pan/99 pre-immune group after one vaccination. TJ-2 induces seroconversion to the same number of strains as Wisc/05, and TJ-5 induces seroconversion to 3 more strains than Tx/12. Additionally, TJ-5 induces higher magnitude HAI titers than Tx/12 (Fig 4.3A), in 11 of the 14 viruses that they both induce seroconversion against. These cross-reactive responses and high magnitude antibody titers generated by the COBRA antigens after just one vaccination are highly advantageous, as most commercial influenza vaccines are delivered as single dose vaccines; whereas the WT vaccine antigens used as comparators in this study required two doses in order to achieve a similar immune response to those elicited by the COBRA vaccines.

In some cases, WT antigens such as Tx/12 can produce more cross-reactive antibodies than other WT strains, and this is evidenced by recent seasons where H3 WT vaccine efficacy is much lower in humans than in the previous season [12, 60, 104]. For comparison, the Wisc/05 vaccine in this study is much less cross-reactive than Tx/12 in all 3 pre-immune settings (Fig 4.3). This phenomenon is likely dependent on the number of shared antigenic epitopes between the chosen vaccine strain and those present in circulating viruses. The COBRA methodology aims to decrease

the chances of having a mismatched vaccine strain by producing an optimized antigen that contains multiple antigenic epitopes from a number of different recently circulating viruses, in order to maximize the cross-reactive potential of the induced antibody pool.

Similar to other broadly reactive influenza vaccine candidates, COBRA HA vaccines likely generate B cell responses that target conserved epitopes on the HA molecule that are present on both historical and modern isolates of A(H3N2) influenza [75]. Studies utilizing monoclonal antibodies generated from COBRA HA antigens have shown a preference for binding conserved epitopes on the HA globular head, such as the receptor binding site, while others are directed at the stem region of COBRA HA [91]. This is advantageous, as antibodies that bind conserved regions of the HA protein can provide protection against multiple influenza viruses [92]. Additionally, antibodies directed against the HA globular head induce higher titers and have more neutralizing potency than those directed against the HA stalk region [73, 92, 93]. However, it is still unknown whether the cross-reactivity of COBRA HA generated antibody responses are the result of polyclonal antibodies working together to target multiple conserved epitopes or specific monoclonal responses targeting a single epitope [91]. Future studies will focus on determining the COBRA HA mechanisms of action that elicit broadly reactive antibodies, as this will provide valuable information on improved vaccine design.

There are some limitations to the pre-immune ferret model presented in this study. First, this model only used one influenza A(H3N2) infection to establish pre-immunity. Most people have a much more extensive immune history from influenza virus infections, stemming from multiple infections and vaccinations with multiple subtypes of influenza throughout the course of their lives [101]. Using a more diverse regimen of infections and vaccinations that include A(H1N1) and influenza B antigens to establish pre-immunity in ferrets may represent the immune

state of an adult human more accurately. Additionally, all of the ferrets used in this study were the same gender and approximately the same age. Influenza vaccine effectiveness is known to vary depending on vaccination history, age, sex, and high-risk condition [115]. Differences in immunological memory and responses to vaccination may exist between genders and age groups and should be investigated in future studies. Also, this model is set up to represent individuals who were first exposed to A(H3N2) influenza during the early part of their lives, but it does not accurately depict the differential immune state of individuals born in the 1970's, 1980's and 1990's. Older individuals first exposed in the 1970's should have more extensive immune histories with influenza than an individual born in the 1980's and 1990's [109]. Also, the effects of immunosenescence that may be present in older individuals are not accounted for in this study, as all of the ferrets were the same age at the time of infection and vaccination [117]. The use of VLP vaccines in this study may also generate different immune responses in pre-immune animals than more conventional vaccine antigens like live attenuated (LAIV), split inactivated (IIV), or subunit influenza vaccines. Live influenza virus vaccines, for example, induce superior immune responses because they are administered via the natural route of infection, intranasally, and drive diverse adaptive immune responses including secretory IgA, serum IgG, and cell mediated responses; while inactivated vaccines tend to primarily induce a serum anti-HA IgG antibody response [101, 109].

Future studies will be aimed at investigating the effects of pre-immunity with heterologous subtypes of influenza viruses on vaccination with monovalent formulations or cocktails of universal H1 and H3 COBRA HA vaccine candidates. It is currently unknown how universal vaccine candidates will perform in a population that has a diverse pre-existing immune history to A(H1N1), A(H3N2), and influenza B subtypes. The impact of whether an individual's first

exposure to an A(H1N1) or A(H3N2) influenza virus can have a large influence on future immune responses [114, 118]. Imprinting with one subtype of influenza may make it more difficult to generate antibodies to other heterologous subtypes later in life [109, 114]. Additionally, most influenza virus vaccines are administered as cocktails containing antigens from multiple subtypes of influenza A, H1N1 and H3N2, and influenza B [6, 7]. Therefore, priming with one subtype of influenza may bias an individual to generating antibodies against that particular subtype upon subsequent vaccination, as immunodominance of one subtype over another may also play a role in the elicited immune responses. This is an important aspect to understand, since antigens from HA group 1 (e.g. H1, H5) appear to induce narrower immune responses and less cross-group protection than HA group 2 antigens (e.g. H3, H7) [114]. Studies designed to more accurately recapitulate the complex immune histories of humans are greatly needed and will provide valuable information that can be used to design universal vaccine candidates, such that they are effective in all populations, regardless of an individual's unique pre-existing immune history to influenza virus.

A.

Day 0	Day 14	Day 84	Day 98	Day 168	Day 182
Preimmune Infection	Bleed	Vaccination	Bleed	Vaccination	Bleed
A/Panama/2007/1999		TJ-2		TJ-2	
		Wisc/05		Wisc/05	
		TJ-5		TJ-5	
		Tx/12		Tx/12	
		Mock		Mock	

B.

A/Sichuan/2/1987		TJ-2		TJ-2	
		Wisc/05		Wisc/05	
		TJ-5		TJ-5	
		Tx/12		Tx/12	
		Mock		Mock	

C.

A/Port Chalmers/1/1973		TJ-2		TJ-2	
		Wisc/05		Wisc/05	
		TJ-5		TJ-5	
		Tx/12		Tx/12	
		Mock		Mock	

D.

Mock		TJ-2		TJ-2	
		Wisc/05		Wisc/05	
		TJ-5		TJ-5	
		Tx/12		Tx/12	
		Mock		Mock	

Figure 4.1. Experimental Design. Ferrets were infected intranasally at day 0 with $1x10^6$ PFU/mL of influenza A(H3N2) virus: A/Panama/2007/1999 (A), A/Sichuan/1/1987 (B), A/Port Chalmers/1/1973 (C), or 1mL of PBS (Mock) (D). At 14 days post infection blood was collected from all animals. After 84 days animals were divided into groups (n=4 ferrets/group) and vaccinated intramuscularly with 15ug of either TJ-2, TJ-5, Tx/12, or Wisc/05 H3N3 VLP's, or PBS (Mock) mixed 1:1 with adjuvant. At 98 days post infection blood was collected from all animals. At day 168 all animals were boosted with a homologous vaccine to that administered on day 84. A final blood draw was collected at day 182 post infection.

A.

Preimmunity	Vaccine	Historical H3N2 Vaccine Strain Panel Average Log(2) GMT																								
		HK/68	PC/73	TX/77	Bgk/79	Miss/85	Sich/87	Shan/93	Nan/95	Syd/97	Pan/99	Fuj/02	NY/2004	Wisc/05	Bris/07	Uru/07	Perth/09	Vic/11	Tx/12	Switz/13	HK/14	Sing/16	Ks/17	Switz/17	SA/19	HK/19
Pan/99	TJ-2	2.32	2.32	2.32	2.32	2.32	2.32	2.32	4.07	6.07	7.57	4.57	3.57	3.82	4.07	2.32	2.32	2.32	2.57	2.32	3.07	2.32	2.57	2.57	2.57	2.57
	Wisc/05	2.32	2.32	2.32	2.32	2.32	2.57	2.32	3.57	5.57	7.07	3.32	3.07	3.32	3.32	2.32	2.32	2.32	2.32	2.32	3.07	2.32	2.82	2.82	2.82	2.82
	TJ-5	2.32	2.32	2.32	2.32	2.32	2.32	2.32	3.32	5.32	7.57	4.07	3.57	3.57	3.32	2.32	2.57	2.32	3.07	2.32	2.82	3.07	2.57	2.57	2.57	3.07
	Tx/12	2.32	2.32	2.32	2.32	2.32	2.57	2.32	3.57	5.82	7.57	3.07	2.32	3.82	3.57	2.32	2.32	2.32	2.32	2.32	3.07	2.32	2.82	2.32	2.32	2.32
	Mock	2.32	2.32	2.32	2.32	2.32	2.32	2.82	4.07	5.82	7.82	4.57	3.32	3.57	3.32	2.32	2.32	2.32	2.82	2.32	3.07	2.32	2.82	2.82	3.07	3.32

B.

Sich/87	TJ-2	5.32	2.32	2.32	2.32	6.82	7.82	4.82	3.57	2.32	2.32	2.32	2.32	2.82	2.32	2.32	2.32	2.32	2.32	2.32	2.32	2.32	2.32	2.32	2.32	2.32
	Wisc/05	5.07	2.32	2.32	2.57	6.82	8.32	5.82	3.57	2.32	2.32	2.32	2.32	2.32	2.32	2.32	2.32	2.32	2.32	2.32	3.32	2.32	2.32	3.07	3.32	3.57
	TJ-5	5.32	2.32	2.32	2.32	6.82	8.57	5.07	3.32	3.07	2.82	2.57	2.32	2.32	2.32	2.32	2.32	2.32	2.32	2.32	2.32	2.32	2.32	2.32	2.32	2.32
	Tx/12	6.32	2.32	2.32	2.32	6.82	8.07	4.82	4.07	2.32	2.32	2.32	2.32	2.32	2.32	2.32	2.32	2.32	2.32	2.32	2.32	2.32	2.32	2.32	2.32	2.32
	Mock	4.57	2.32	2.32	2.82	6.57	7.82	4.32	3.57	2.32	2.32	2.32	2.32	2.32	2.32	2.32	2.32	2.32	2.32	2.32	2.57	2.32	2.32	2.32	2.32	2.32

C.

PC/73	TJ-2	5.82	8.57	2.82	3.32	2.32	2.32	2.32	2.32	2.32	2.32	2.32	2.32	2.32	2.32	2.32	2.32	2.32	2.32	2.32	2.32	2.32	2.32	2.32	2.32	2.32
	Wisc/05	7.07	9.07	2.82	3.32	3.07	2.57	2.32	2.57	2.32	2.32	2.32	2.32	2.32	2.32	2.32	2.32	2.32	2.32	2.32	2.32	2.32	2.32	2.32	2.32	2.32
	TJ-5	6.57	8.57	3.32	3.82	3.07	2.32	2.32	2.32	2.32	2.32	2.32	2.32	2.32	2.32	2.32	2.32	2.32	2.32	2.32	2.32	2.32	2.32	2.32	2.32	2.32
	Tx/12	6.32	8.57	2.82	2.32	2.82	2.82	2.32	2.32	2.32	2.32	2.32	2.32	2.32	2.32	2.32	2.32	2.32	2.32	2.32	2.32	2.32	2.32	2.32	2.32	2.32
	Mock	7.32	8.99	3.32	2.66	2.32	2.66	2.32	2.32	2.32	2.32	2.32	2.32	2.32	2.32	2.32	2.32	2.32	2.32	2.32	3.32	2.32	2.32	2.32	2.32	2.32

D.

Mock	TJ-2	2.32	2.32	2.32	2.32	2.32	2.32	2.32	2.32	2.32	2.32	2.32	2.32	2.32	2.32	2.32	2.32	2.32	2.32	2.32	2.32	2.32	2.32	2.32	2.32	2.32
	Wisc/05	2.32	2.32	2.32	2.32	2.32	2.32	2.32	2.32	2.32	2.32	2.32	2.32	2.32	2.32	2.32	2.32	2.32	2.32	2.32	2.32	2.32	2.32	2.32	2.32	2.32
	TJ-5	2.32	2.32	2.32	2.32	2.32	2.32	2.32	2.32	2.32	2.32	2.32	2.32	2.32	2.32	2.32	2.32	2.32	2.32	2.32	2.32	2.32	2.32	2.32	2.32	2.32
	Tx/12	2.32	2.32	2.32	2.32	2.32	2.32	2.32	2.32	2.32	2.32	2.32	2.32	2.32	2.32	2.32	2.32	2.32	2.32	2.32	2.32	2.32	2.32	2.32	2.32	2.32
	Mock	2.32	2.32	2.32	2.32	2.32	2.32	2.32	2.32	2.32	2.32	2.32	2.32	2.32	2.32	2.32	2.32	2.32	2.32	2.32	2.32	2.32	2.32	2.32	2.32	2.32

Figure 4.2. Day 14 H3N2 Historical Vaccine Strain HAI Panel. Serum collected from animals 14 days post infection was analyzed for HAI activity against a panel of historical H3N2 influenza vaccine strains spanning 1968-2019. Table is divided into sections based on the virus each animal received to establish preimmunity: A/Panama/2007/1999 (A), A/Sichuan/1/1987 (B), A/Port Chalmers/1/1973 (C), or PBS (Mock) (D). Cells in table are color coded as a heat map based upon Log (2) HAI geometric mean titer (GMT) for each group of ferrets (N=4). The heat map colors cells yellow at a Log (2) GMT of 5.32 which correspond to an HAI titer of 1:40, and cells become a darker shade of green as the average antibody titer of the group increases. Cells with no color correspond to groups that did not achieve a GMT ≥5.32.

A.

Preimmunity	Vaccine	Historical H3N2 Vaccine Strain Panel Average Log(2) GMT																									
		HK/68	PC/73	TX/77	Bgk/79	Miss/85	Sich/87	Shan/93	Nan/95	Syd/97	Pan/99	Fuj/02	NY/04	Wisc/05	Bris/07	Uru/07	Perth/09	Vic/11	Tx/12	Switz/13	HK/14	Sing/16	Ks/17	Switz/17	SA/19	HK/19
Pan/99	TJ-2	2.32	2.32	3.32	4.07	2.82	4.07	2.32	6.07	9.57	9.07	10.07	9.32	9.07	8.07	5.32	5.07	8.57	7.82	4.07	7.07	2.82	4.82	3.07	2.82	2.32
	Wisc/05	2.82	2.32	4.32	4.57	3.82	4.82	2.57	6.57	8.07	9.82	9.32	8.57	9.07	8.32	4.82	5.57	9.57	8.57	4.82	8.07	4.07	5.07	3.57	4.32	3.32
	TJ-5	2.32	2.32	2.32	3.32	3.82	3.07	2.82	5.57	8.82	9.32	9.32	9.07	9.32	8.32	5.32	7.32	10.07	9.07	5.32	8.57	5.32	6.32	5.32	6.82	3.57
	Tx/12	2.32	2.32	2.82	3.32	2.82	3.57	2.32	5.07	7.57	8.82	8.57	7.57	8.07	6.32	3.57	5.57	9.07	8.07	5.82	7.57	4.57	5.82	5.57	5.57	2.32
	Mock	2.32	2.32	2.57	2.32	2.32	2.32	2.32	3.82	5.32	6.32	5.07	2.32	3.82	3.32	2.32	2.32	2.57	2.57	2.32	2.82	2.82	3.07	2.32	2.32	2.32

B.

Sich/87	TJ-2	2.82	2.32	2.82	3.07	5.82	6.32	5.07	4.82	3.57	4.57	6.32	6.82	6.82	5.57	5.32	2.32	4.07	3.32	2.32	3.32	2.32	3.07	2.32	2.32	2.32
	Wisc/05	2.32	3.82	3.57	4.07	5.57	9.57	5.32	4.57	2.82	3.82	3.57	3.07	6.07	4.32	3.32	2.32	4.32	4.82	3.07	3.57	2.32	3.82	2.32	2.32	2.32
	TJ-5	3.32	5.32	4.07	4.32	6.32	10.07	5.82	5.32	5.32	6.07	5.32	5.32	6.57	5.57	5.07	5.57	6.82	7.07	5.32	6.57	5.82	6.07	5.32	5.82	2.57
	Tx/12	4.07	3.07	4.57	3.32	5.57	8.07	5.32	5.32	2.32	2.57	6.57	3.07	5.07	4.32	2.82	5.57	7.82	7.82	5.57	5.32	4.57	5.32	3.07	7.07	3.32
	Mock	2.32	2.32	2.82	2.82	5.32	8.57	4.57	4.57	2.32	2.32	2.32	2.32	2.32	2.32	2.32	2.32	2.32	2.32	2.32	2.32	2.32	4.82	2.32	2.32	2.32

C.

PC/73	TJ-2	6.57	9.07	4.32	3.57	3.57	3.07	2.57	3.07	2.82	2.32	5.57	7.07	5.32	4.32	3.57	2.57	2.32	3.32	2.32	2.57	2.32	2.32	2.32	2.32	2.32
	Wisc/05	6.07	8.32	4.57	3.07	3.57	3.07	2.57	3.07	2.32	2.32	2.57	3.07	5.57	4.57	2.82	2.82	3.82	4.07	2.57	2.32	2.32	3.82	2.57	2.32	2.32
	TJ-5	6.32	8.32	4.57	3.07	2.82	4.82	2.32	2.82	2.32	2.32	2.32	2.32	3.57	3.57	2.32	4.82	6.07	6.32	2.32	4.82	3.82	2.57	2.57	3.32	2.32
	Tx/12	6.57	8.82	5.07	4.07	3.82	3.82	2.57	3.32	2.82	2.32	2.32	2.32	4.32	3.82	2.32	5.32	7.07	7.07	4.57	3.82	3.32	3.07	2.32	3.82	2.32
	Mock	5.99	8.99	4.32	3.32	2.99	2.32	2.32	2.32	2.32	2.32	2.32	2.32	2.32	2.32	2.32	2.32	2.32	2.32	2.32	2.32	2.32	3.21	2.32	2.32	2.32

D.

Mock	TJ-2	2.32	3.82	2.82	2.32	2.32	2.32	2.32	2.32	2.32	2.32	2.32	4.82	2.32	2.32	2.32	2.32	2.32	2.32	2.32	2.32	2.32	3.32	2.32	2.57	2.32
	Wisc/05	2.32	2.32	2.32	2.32	2.32	2.32	2.32	2.32	2.32	2.32	2.82	2.32	4.07	2.82	2.32	2.32	2.32	2.32	2.32	2.32	2.32	2.32	2.32	2.32	2.32
	TJ-5	2.32	2.32	2.32	2.32	2.32	2.32	2.32	2.32	2.32	2.32	2.32	2.32	2.32	2.32	2.32	2.57	3.82	4.32	2.32	2.32	2.32	2.57	2.32	2.57	2.32
	Tx/12	2.32	2.32	2.32	2.32	2.32	2.32	2.32	2.32	2.32	2.32	2.32	2.32	2.32	2.32	2.32	2.32	3.82	3.82	2.32	2.32	2.32	2.32	2.32	2.32	2.32
	Mock	2.32	2.32	2.32	2.32	2.32	2.32	2.32	2.32	2.32	2.32	2.32	2.32	2.32	2.32	2.32	2.32	2.32	2.32	2.32	2.32	2.32	2.32	2.32	2.32	2.32

Figure 4.3. Day 98 H3N2 Historical Vaccine Strain HAI Panel. Serum collected from animals 98 days post infection (14 days after first vaccination) was analyzed for HAI activity against a panel of historical H3N2 influenza vaccine strains spanning 1968-2019. Table is divided into sections based on the virus each animal received to establish preimmunity: A/Panama/2007/1999 (A), A/Sichuan/1/1987 (B), A/Port Chalmers/1/1973 (C), or PBS (Mock) (D). Cells in table are color coded as a heat map based upon Log (2) HAI geometric mean titer (GMT) for each group of ferrets (N=4). The heat map colors cells yellow at a Log (2) GMT of 5.32 which correspond to an HAI titer of 1:40, and cells become a darker shade of green as the average antibody titer of the group increases. Cells with no color correspond to groups that did not achieve a GMT ≥5.32.

A.

Preimmunity	Vaccine	Historical Vaccine Strain Panel Average Log2 GMT																								
		HK/68	PC/73	TX/77	Bgk/79	Miss/85	Sich/87	Shan/93	Nan/95	Syd/97	Pan/99	Fuj/02	NY/04	Wisc/05	Bris/07	Uru/07	Perth/09	Vic/11	Tx/12	Switz/13	HK/14	Sing/16	Ks/17	Switz/17	SA/19	HK/19
Pan/99	TJ-2	2.32	2.32	3.07	2.82	2.32	2.32	2.32	5.32	7.82	7.82	9.32	7.82	7.32	6.07	5.82	5.57	6.57	6.82	5.57	5.57	5.57	4.32	5.32	5.57	5.57
	Wisc/05	2.32	2.32	2.82	3.57	2.82	4.32	3.32	5.82	6.32	6.82	9.07	8.32	9.57	8.07	7.07	7.07	9.07	9.07	8.07	7.32	7.32	4.32	5.57	5.82	5.57
	TJ-5	2.32	3.32	3.82	3.32	2.32	3.57	2.82	5.07	7.82	8.07	9.32	8.32	9.32	8.07	7.32	8.07	9.82	10.07	7.32	9.40	7.82	7.32	7.82	8.57	6.82
	Tx/12	2.32	2.32	3.07	2.57	2.32	2.32	3.32	4.82	6.82	7.32	9.07	7.07	8.07	6.07	6.07	8.57	9.57	10.07	7.82	8.82	7.82	6.07	7.82	8.57	6.32
	Mock	2.32	2.32	3.32	3.07	2.32	2.32	2.57	4.57	5.57	6.82	4.57	3.57	3.82	2.82	2.82	2.32	2.32	3.32	3.32	2.32	2.82	2.32	3.82	2.32	2.32

B.

Sich/87	TJ-2	2.32	2.32	3.57	4.32	4.32	5.82	5.32	4.32	3.07	3.07	7.32	7.32	7.32	6.57	6.57	6.07	6.82	6.82	5.82	2.32	3.32	3.57	2.82	2.82	2.32
	Wisc/05	2.32	3.32	3.82	4.82	5.07	6.82	5.82	4.82	3.57	2.32	6.32	7.07	8.82	6.57	2.32	4.32	6.82	6.32	5.32	3.82	4.07	3.57	3.82	5.07	3.32
	TJ-5	3.32	3.57	4.32	5.07	5.32	6.57	5.82	5.07	4.07	4.07	6.57	5.82	7.82	7.32	7.07	8.82	9.32	9.82	7.07	8.57	8.57	7.07	6.57	7.32	6.57
	Tx/12	4.32	3.32	4.57	5.07	3.32	6.82	5.82	5.82	4.57	4.57	6.49	7.07	9.07	7.32	5.57	8.32	9.82	10.07	8.82	8.57	8.32	5.57	7.07	8.32	6.57
	Mock	2.32	3.32	4.32	4.57	3.32	5.82	5.57	4.82	2.32	2.32	4.07	2.32	2.32	2.32	3.07	2.32	2.32	2.32	2.82	2.32	2.82	2.57	2.82	2.32	2.32

C.

PC/73	TJ-2	6.57	8.57	5.07	4.07	2.32	3.32	5.07	3.07	2.32	2.32	6.07	5.82	6.07	6.32	6.32	5.57	6.82	6.82	6.57	4.32	3.82	4.07	4.57	4.32	2.32
	Wisc/05	6.57	8.57	4.82	4.57	3.57	3.82	4.32	3.32	2.32	2.32	5.57	6.07	8.82	6.07	5.82	5.07	7.82	7.82	6.57	4.82	4.82	4.07	3.82	4.82	2.82
	TJ-5	6.82	8.32	5.57	3.82	2.32	2.32	5.57	2.32	2.32	2.32	4.57	5.32	7.82	6.57	6.82	7.57	9.07	9.57	6.57	8.32	8.32	7.57	6.32	7.32	5.82
	Tx/12	7.07	8.82	5.32	5.07	3.82	3.57	5.32	2.82	2.32	2.32	3.57	4.82	8.07	5.57	5.07	8.07	9.32	10.07	9.07	7.57	7.82	4.32	6.57	9.07	7.32
	Mock	6.66	8.66	4.66	4.32	2.66	2.32	2.32	2.66	2.32	2.32	2.99	2.32	2.32	2.32	2.66	2.32	2.32	4.32	3.66	2.32	2.99	3.66	3.66	3.32	2.32

D.

Mock	TJ-2	2.32	3.32	2.32	2.57	2.32	2.32	2.32	2.32	2.32	2.32	3.82	2.32	5.57	2.32	3.32	2.32	2.32	3.82	3.32	2.32	3.57	3.32	2.82	2.32	2.32
	Wisc/05	2.32	2.32	2.32	2.32	2.32	2.32	2.32	2.32	2.32	2.32	2.82	2.32	5.32	2.82	2.32	2.32	2.32	2.32	2.32	2.32	2.32	2.32	2.32	2.32	2.32
	TJ-5	2.32	2.82	3.32	3.07	2.32	2.32	2.32	2.32	2.32	2.32	3.57	4.32	4.57	3.57	3.57	4.57	6.07	6.57	5.07	5.82	6.57	4.07	4.32	5.57	3.32
	Tx/12	2.32	2.32	2.32	2.32	2.32	2.32	2.32	4.32	2.57	2.32	2.32	2.32	2.32	2.32	2.32	3.82	4.32	5.32	4.32	4.07	4.57	2.82	4.32	4.82	3.82
	Mock	2.32	2.32	2.32	2.32	2.32	2.32	2.32	2.32	2.32	2.32	2.32	2.32	2.32	2.32	2.32	2.32	2.32	2.32	2.32	2.32	2.32	2.32	2.32	2.32	2.32

Figure 4.4. Day 182 H3N2 Historical Vaccine Strain HAI Panel. Serum collected from animals 182 days post infection (14 days after second vaccination) was analyzed for HAI activity against a panel of historical H3N2 influenza vaccine strains spanning 1968-2019. Table is divided into sections based on the virus each animal received to establish preimmunity: A/Panama/2007/1999 (A), A/Sichuan/1/1987 (B), A/Port Chalmers/1/1973 (C), or PBS (Mock) (D). Cells in table are color coded as a heat map based upon Log (2) HAI geometric mean titer (GMT) for each group of ferrets (N=4). The heat map colors cells yellow at a Log (2) GMT of 5.32 which correspond to an HAI titer of 1:40, and cells become a darker shade of green as the average antibody titer of the group increases. Cells with no color correspond to groups that did not achieve a GMT ≥5.32.

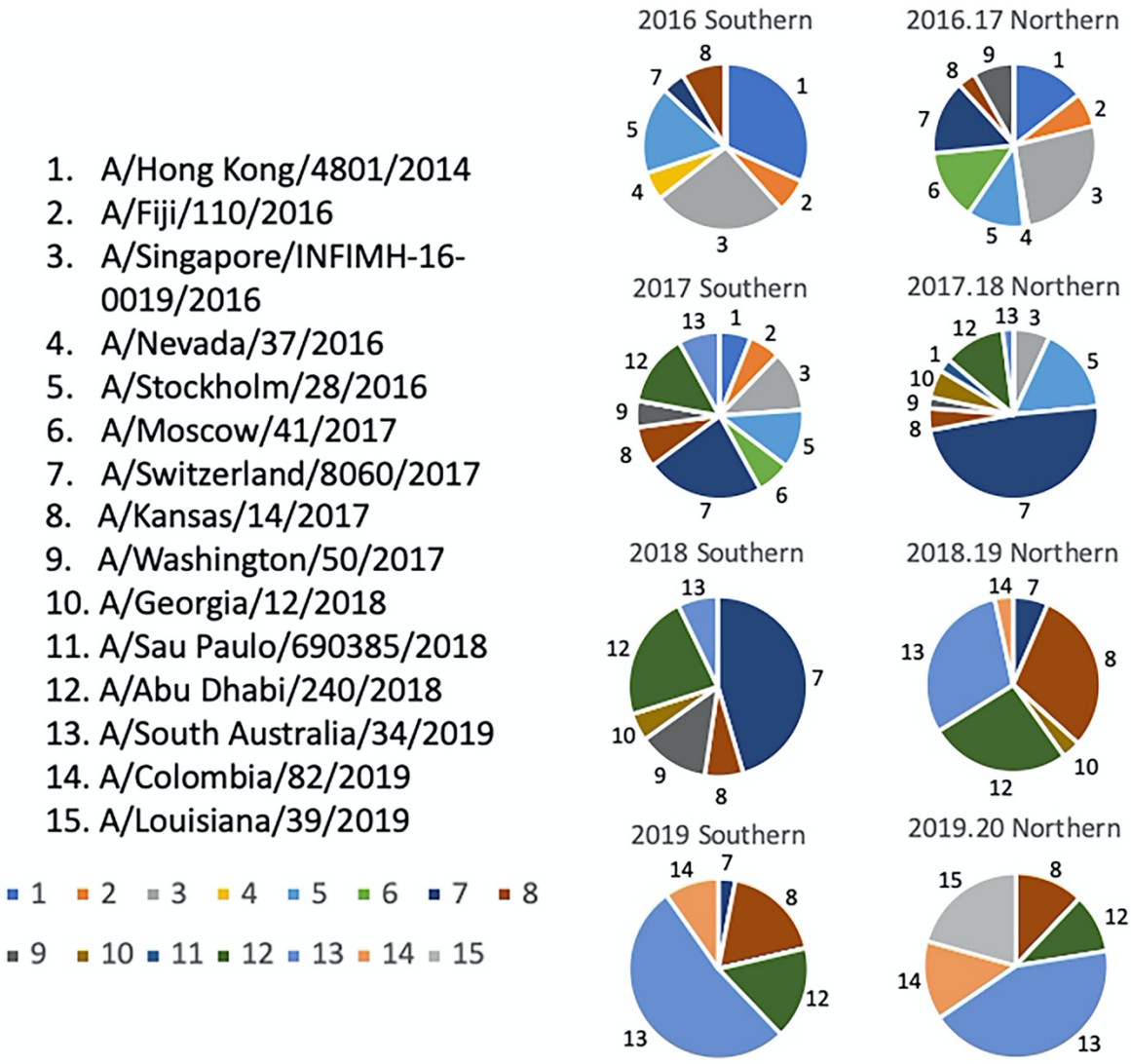

Figure 4.5. Determination of Co-circulating H3N2 Strains 2016-2020. Relative frequencies of influenza HA clusters from co-circulating H3N2 strains in consecutive seasons from 2016-2020. Influenza HA sequences were obtained from the GISAID database, aligned, and clustered into families for each representative Northern and Southern Hemisphere influenza season timeframe. The HA sequences from each season were then divided into clusters based on a 95% sequence similarity cutoff, and are depicted by a different color and slice of each pie chart. A representative strain from each cluster was chosen and assigned a number 1-15. Colors assigned to each number match the color in the pie charts.

A.

Preimmunity	Vaccination	2009-2019 H3N2 Co-circulating Strain Panel																					
		Vic/09	Ala/10	Hess/10	Neth/10	Nor/10	Mad/11	Nor/11	Stock/11	Ath/12	Jord/12	Den/13	HK/12/14	Stock/16	Fiji/2016	Nev/16	Mos/17	Wash/17	Abu/18	Geo/18	SP/18	Col/19	LA/19
Pan/99	TJ-2	8.07	8.57	7.57	8.07	7.57	10.07	7.32	6.32	9.07	8.32	7.32	7.82	6.57	4.82	4.82	3.82	3.82	2.82	4.07	4.57	3.07	2.57
	Wisc/05	8.32	8.57	7.57	9.57	7.07	9.82	7.57	6.57	8.82	9.32	6.57	8.07	7.07	4.82	4.82	4.07	4.07	2.82	3.57	4.82	3.57	3.07
	TJ-5	9.07	9.32	8.32	9.57	8.82	9.82	8.82	6.32	9.07	10.07	7.82	9.32	7.82	2.82	4.82	4.32	4.07	3.82	3.82	4.32	3.82	3.57
	Tx/12	8.07	8.32	7.57	8.82	8.57	10.07	7.32	6.32	9.07	8.57	8.07	8.32	6.07	4.07	3.57	4.57	2.82	2.82	3.82	4.57	3.32	3.32
	Mock	3.32	4.82	5.07	4.07	7.32	7.57	5.32	4.82	7.57	4.57	5.82	5.32	3.32	2.32	2.32	2.32	2.32	2.32	2.32	2.32	2.32	2.32

B.

Sich/87	TJ-2	5.32	5.32	5.07	5.07	8.57	7.57	5.82	5.32	7.32	6.07	6.32	5.57	4.82	3.07	3.82	3.07	3.07	2.32	3.32	5.07	3.07	2.57
	Wisc/05	4.57	5.32	5.57	4.57	7.57	7.57	5.82	5.32	6.32	5.82	5.57	5.32	4.57	2.32	2.32	2.82	2.32	2.32	2.32	4.07	2.32	2.32
	TJ-5	7.57	7.57	7.32	7.82	8.32	9.32	7.57	6.57	8.57	8.07	7.57	7.32	5.57	4.82	3.32	4.07	2.82	2.57	4.32	4.07	3.07	2.82
	Tx/12	7.57	7.32	7.32	7.57	9.07	9.57	7.57	7.32	8.57	7.82	8.32	7.82	5.82	3.07	4.07	4.32	2.82	2.32	4.57	4.57	4.07	3.57
	Mock	2.82	3.57	2.82	2.82	8.32	7.32	2.57	4.07	6.07	3.32	5.32	6.07	3.32	3.07	2.32	2.32	2.32	2.32	2.32	2.32	2.32	2.32

C.

PC/73	TJ-2	5.07	6.07	5.82	5.57	7.32	8.82	6.07	5.07	7.57	6.32	6.32	5.57	4.82	3.07	2.57	3.07	2.32	2.57	2.57	3.57	2.32	2.32
	Wisc/05	6.07	6.07	6.32	5.07	7.57	8.57	6.82	4.07	7.32	5.57	6.07	5.82	4.07	2.32	3.07	3.32	2.32	2.57	2.82	3.82	2.32	2.57
	TJ-5	7.32	6.57	7.32	7.32	8.07	9.32	7.07	5.82	7.32	7.82	6.82	6.82	5.07	3.32	2.82	2.57	2.32	2.32	2.82	4.82	2.57	2.82
	Tx/12	7.32	6.82	7.32	7.57	8.32	9.32	7.32	5.82	9.32	7.32	7.32	7.07	5.07	3.57	3.32	3.57	2.32	2.32	3.57	4.57	2.57	2.57
	Mock	3.99	4.66	4.66	4.66	6.21	7.99	4.32	4.66	4.66	4.66	7.32	4.66	3.99	2.32	2.32	2.32	2.32	2.32	2.32	2.66	2.32	2.32

D.

Mock	TJ-2	3.82	2.82	4.57	4.07	7.32	7.82	3.57	4.57	4.82	4.07	7.57	5.32	4.07	2.32	2.32	2.32	2.32	2.32	2.57	3.57	2.82	2.32
	Wisc/05	2.32	3.07	2.32	2.32	2.57	4.07	2.32	2.32	3.82	2.57	3.32	2.32	2.32	2.32	2.32	2.32	2.32	2.32	2.32	2.32	2.32	2.32
	TJ-5	4.82	3.57	5.07	4.57	7.32	7.57	4.82	4.07	6.32	5.32	7.57	4.57	3.32	2.32	2.32	2.32	2.32	2.32	2.32	2.32	2.32	2.32
	Tx/12	2.32	3.32	3.57	2.32	3.82	5.07	3.57	2.57	4.82	4.82	4.57	4.57	2.32	2.32	2.32	2.32	2.32	2.32	2.32	2.32	2.32	2.32
	Mock	2.32	2.32	2.32	2.32	2.32	2.32	2.32	2.32	2.32	2.32	2.32	2.32	2.32	2.32	2.32	2.32	2.32	2.32	2.32	2.32	2.32	2.32

Figure 4.6. Day 98 H3N2 Co-Circulating Strain HAI Panel. Serum collected from animals 98 days post infection (14 days after first vaccination) was analyzed for HAI activity against a panel of co-circulating H3N2 influenza strains spanning 2009-2019. Table is divided into sections based on the virus each animal received to establish preimmunity: A/Panama/2007/1999 (A), A/Sichuan/1/1987 (B), A/Port Chalmers/1/1973 (C), or PBS (Mock) (D). Cells in table are color coded as a heat map based upon Log (2) HAI geometric mean titer (GMT) for each group of ferrets (N=4). The heat map colors cells yellow at a Log (2) GMT of 5.32 which correspond to an HAI titer of 1:40, and cells become a darker shade of green as the average antibody titer of the group increases. Cells with no color correspond to groups that did not achieve a GMT ≥5.32.

A.

Preimmunity	Vaccination	2009-2019 H3N2 Co-circulating Strain Panel																				
		Vic/09	Ala/10	Hess/10	Neth/10	Nor/10	Mad/11	Nor/11	Stock/11	Ath/12	Jord/12	Den/13	HK/12/14	Stock/16	Fiji/2016	Nev/16	Mos/17	Wash/17	Abu/18	Geo/18	SP/18	Col/19	LA/19
Pan/99	TJ-2	7.57	8.07	7.32	7.57	7.07	9.57	7.07	5.82	8.32	7.57	6.82	7.32	6.07	5.82	5.82	5.07	4.82	4.32	5.07	6.32	4.32	3.82
	Wisc/05	7.57	8.07	7.32	8.82	6.57	9.32	7.07	5.82	8.57	8.57	6.32	7.57	6.32	6.57	6.32	5.57	5.32	5.57	5.82	6.82	6.32	5.07
	TJ-5	8.57	8.82	8.07	9.32	8.57	9.82	8.57	7.07	9.57	10.07	8.32	9.82	8.07	7.57	7.57	7.82	6.32	6.32	7.32	7.57	7.07	6.32
	Tx/12	8.07	8.07	7.32	8.82	8.32	10.07	7.32	7.07	9.57	9.07	8.32	8.82	7.32	7.57	6.82	6.82	6.32	5.82	6.82	7.07	6.82	6.82
	Mock	3.32	4.57	4.82	3.82	6.32	7.32	5.32	4.07	7.07	4.07	5.32	4.57	3.07	2.32	2.32	2.82	4.07	3.32	2.32	4.07	2.82	2.32

B.

Sich/87	TJ-2	4.57	5.32	4.57	4.82	8.07	7.32	5.57	5.32	6.57	5.57	6.07	5.07	4.57	7.57	4.32	3.07	6.07	5.82	3.82	6.07	4.82	3.32
	Wisc/05	4.32	5.32	5.32	4.32	7.57	7.57	5.57	5.32	6.07	5.32	5.32	5.07	4.57	6.57	4.82	4.07	5.32	5.57	4.82	6.07	4.32	4.07
	TJ-5	7.32	7.32	7.07	7.57	8.32	9.32	7.82	7.07	9.32	8.57	8.07	7.82	6.32	6.57	6.57	6.32	5.32	5.57	6.57	7.07	6.32	6.07
	Tx/12	7.32	7.32	7.07	7.32	8.82	9.57	7.82	7.57	9.32	8.07	8.32	8.07	6.32	7.57	7.57	7.57	6.07	5.82	7.07	7.32	6.57	6.82
	Mock	2.82	4.32	2.82	2.82	7.07	6.57	2.57	3.57	5.32	3.07	4.57	4.57	3.07	3.32	2.32	2.32	3.32	3.32	2.32	2.32	2.32	2.32

C.

PC/73	TJ-2	4.82	5.82	5.57	5.32	7.07	8.32	5.82	4.82	7.07	6.07	6.32	5.32	4.57	2.32	5.32	5.57	2.32	2.32	5.32	5.82	4.57	4.32
	Wisc/05	5.57	5.82	5.82	4.82	7.32	8.32	6.32	4.57	7.07	5.07	6.07	5.57	3.82	4.07	4.82	5.07	2.32	2.57	5.32	5.57	4.57	4.32
	TJ-5	6.82	6.57	6.82	7.07	7.82	9.07	7.32	6.32	8.07	8.32	6.82	7.32	5.82	5.57	5.57	5.57	5.32	5.57	5.82	6.82	5.57	5.82
	Tx/12	6.82	6.57	6.82	7.32	8.07	9.07	7.57	6.32	9.32	7.82	7.32	7.57	5.82	6.57	6.82	6.82	5.32	5.57	6.82	6.82	6.32	5.82
	Mock	3.57	4.32	4.57	4.32	6.07	7.07	4.07	3.32	4.32	4.07	7.32	4.32	3.32	2.32	2.66	2.32	3.07	2.32	2.99	4.32	2.66	2.32

D.

Mock	TJ-2	3.57	2.82	4.32	3.82	6.82	7.07	3.32	4.07	4.57	3.57	7.57	5.32	3.82	2.32	2.57	3.07	2.32	2.32	3.32	2.82	2.32	2.57
	Wisc/05	2.32	3.07	3.07	2.32	3.57	4.57	3.57	2.57	4.07	3.57	3.32	4.82	3.07	4.07	4.07	2.82	3.57	2.57	3.82	2.82	3.57	2.57
	TJ-5	4.32	3.82	5.07	4.32	7.07	7.57	5.32	4.57	7.07	5.82	7.57	5.82	4.57	6.32	4.57	4.57	6.32	6.07	4.57	5.32	4.32	3.57
	Tx/12	2.32	3.57	3.07	2.32	3.82	5.82	4.32	3.57	4.57	3.57	4.57	5.57	4.32	6.32	4.57	3.57	6.32	6.07	4.32	4.57	4.32	3.57
	Mock	2.32	2.32	2.32	2.32	2.32	2.32	2.32	2.32	2.32	2.32	2.32	2.32	2.32	2.32	2.32	2.32	2.32	2.32	2.32	2.32	2.32	2.32

Figure 4.7. Day 182 H3N2 Co-Circulating Strain HAI Panel. Serum collected from animals 182 days post infection (14 days after second vaccination) was analyzed for HAI activity against a panel of co-circulating H3N2 influenza strains spanning 2009-2019. Table is divided into sections based on the virus each animal received to establish preimmunity: A/Panama/2007/1999 (A), A/Sichuan/1/1987 (B), A/Port Chalmers/1/1973 (C), or PBS (Mock) (D). Cells in table are color coded as a heat map based upon Log (2) HAI geometric mean titer (GMT) for each group of ferrets (N=4). The heat map colors cells yellow at a Log (2) GMT of 5.32 which correspond to an HAI titer of 1:40, and cells become a darker shade of green as the average antibody titer of the group increases. Cells with no color correspond to groups that did not achieve a GMT ≥5.32.

			H3N2 Log(2) Virus Neutralization(50%) Antibody Titers						
			Tx/12	Switz/13	HK/14	Sing/16	Ks/17	SA/19	HK/19
	PreImmunity	Vaccine	Neut 50	Neut 50	Neut 50	Neut 50	Neut 50	Neut 50	Neut 50
A.	Pan/99	TJ-2	10.32	8.32	7.97	9.26	4.32	5.63	5.88
		Wisc/05	11.32	8.39	8.34	9.21	4.32	6.12	6.16
		TJ-5	12.35	9.27	8.71	9.63	5.21	7.54	7.36
		Tx/12	11.34	8.72	8.01	9.12	4.64	7.11	6.37
		Mock	6.15	7.28	6.88	7.38	2.32	2.32	5.36
B.	Sich/87	TJ-2	7.06	7.75	7.51	8.59	2.32	4.32	5.72
		Wisc/05	6.97	6.72	6.89	8.24	2.32	4.32	5.35
		TJ-5	9.81	8.37	8.08	9.42	4.98	6.69	5.89
		Tx/12	9.69	8.16	7.83	9.18	4.92	6.56	6.04
		Mock	5.43	6.36	6.39	7.73	2.32	2.32	5.13
C.	PC/73	TJ-2	7.31	7.96	6.51	8.93	4.32	4.49	5.71
		Wisc/05	8.13	7.57	6.03	8.23	4.51	4.76	5.3
		TJ-5	10.01	8.44	7.47	9.18	5.14	6.01	5.87
		Tx/12	10.16	8.01	6.95	9.08	5.14	6.04	6.03
		Mock	5.44	6.42	5.68	7.27	2.32	2.32	4.88
D.	Mock	TJ-2	5.46	5.39	4.54	7.7	2.32	2.32	2.32
		Wisc/05	5.84	2.32	2.32	5.32	2.32	2.32	2.32
		TJ-5	6.7	6.68	5.36	9.08	4.89	5.18	5.56
		Tx/12	6.71	2.32	4.85	5.82	4.44	5.18	4.95
		Mock	2.32	2.32	2.32	2.32	2.32	2.32	2.32

Figure 4.8. Day 98 H3N2 Focal Reduction Assay. Serum collected from animals 98 days post infection (14 days after first vaccination) was analyzed for neutralizing antibody activity against a panel of historical H3N2 influenza vaccine strains spanning 2012-2019 using a focal reduction assay. Table is divided into sections based on the virus each animal received to establish preimmunity: A/Panama/2007/1999 (A), A/Sichuan/1/1987 (B), A/Port Chalmers/1/1973 (C), or PBS (Mock) (D). Cells in table are color coded as a heat map based upon Log (2) geometric mean titer (GMT) where 50% virus neutralization ($Neut_{50}$) was observed for each group of ferrets (N=4). The heat map colors cells yellow at a Log (2) GMT of 5.32 which correspond to an antibody titer of 1:40, and cells become a darker shade of green as the average antibody titer of the group increases. Cells with no color correspond to groups that did not achieve a $Neut_{50}$ GMT ≥5.32. The lowest serum dilution analyzed was 1:20, if no $Neut_{50}$ titer was observed at this dilution a $Neut_{50}$ GMT value of 2.32, which corresponds to an antibody titer of 1:5 was assigned to the group.

CHAPTER 5

BIVALENT H1+H3 COBRA rHA VACCINES ELICIT SERO-PROTECTIVE ANTIBODIES AGAINST H1N1 AND H3N2 INFLUENZA VIRUSES FROM 2009-2019[1]

A version of this chapter was submitted to *The Journal of Virology* on September 22, 2021.

[1]Allen, James D and Ross, Ted M. *Bivalent H1+H3 COBRA rHA Vaccines Elicit Sero-protective Antibodies Against H1N1 and H3N2 Influenza Viruses from 2009-2019*.

Abstract

Human influenza viruses cause ~3-5 million cases of severe illness and more than 500,000 deaths globally every year. Vaccines are currently the most effective means of preventing influenza virus infections, but many commercially available vaccines often elicit strain specific immune responses and have difficulties preventing illness against antigenically drifted viral strains, especially for the influenza A(H3N2) subtype. In the last 20 years, the H3N2 component of the annual vaccine has been updated nearly twice as often as the H1N1 component, and in 2019, a mismatch between the wild-type H3N2 vaccine strain and circulating H3N2 influenza strains led to vaccine efficacy of ~9%. Modern methods of developing Computationally Optimized Broadly Reactive Antigens (COBRAs) for H3N2 influenza viruses offer a solution to this problem by utilizing current viral surveillance information to design more broadly-reactive vaccine antigens. In this study, 7 new recombinant hemagglutinin (rHA) H3 COBRA antigens were developed and evaluated in influenza immunologically naïve mice. Subsequently, two H3 COBRA rHA candidates, J4 and NG2, were selected for further testing in influenza pre-immune mice based on their ability to elicit broadly reactive antibodies against antigenically drifted H3N2 viral isolates. In the pre-immune model, monovalent formulations of J4 and NG2 were also superior to H3 WT vaccine antigens at eliciting antibodies against recently circulating H3N2 influenza viruses from 2019. Bivalent formulations of COBRA H1 and H3 HA candidates were then tested in pre-immune mice for their ability to elicit broadly reactive antibodies against panels of H1N1 and H3N2 influenza viruses. Bivalent mixtures of COBRA H1+H3 rHA, Y2+J4, and Y2+NG2, outperformed multiple WT H1+H3 bivalent rHA mixtures by eliciting sero-protective HAI antibody titers against H1N1 and H3N2 vaccine strain isolates from 2009-2019. They also elicited higher antibody titers capable of neutralizing more virus infections with H1N1 and H3N2 isolates than any bivalent mixture of WT rHA antigens in neutralization assays. The bivalent COBRA

rHA antigens also elicited antibodies that protected vaccinated mice from H3N2 influenza virus challenge and these animals had no detectable virus in their lungs at day 3 post infection. Overall, the newly generated H3 COBRA HA antigens, Y2, J4, and NG2, had the ability to induce broadly reactive antibodies in influenza naïve and pre-immune animals in both monovalent and bivalent formulations and these antigens outperformed H1 and H3 WT rHA vaccine antigens by eliciting sero-protective antibodies against panels of antigenically drifted historical H1N1 and H3N2 vaccine strains from 2009-2019.

Introduction

Influenza A viruses (IAVs) cause acute respiratory diseases in humans that are responsible for an estimated 290,000-650,000 deaths worldwide every year, with the highest mortality occurring in young children and elderly individuals [5, 57, 97, 98, 102]. Currently, vaccination is the most effective approach for preventing influenza virus induced disease, but reinfections with antigenically distinct viruses are common [97, 99, 115, 119]. Most seasonal influenza virus vaccines attempt to generate antibodies that target the hemagglutinin (HA) or neuraminidase (NA) proteins on the surface of the virus [5, 101]. However, influenza is an antigenically variable virus that undergoes continual antigenic drift, whereby mutations in immunodominant epitopes in the HA and NA proteins are generated in response to immunological pressure, allowing the virus to escape population herd immunity [5, 73, 97, 102, 103]. As a result, there is considerable variation in vaccine efficacy from season to season depending on the antigenic match between the chosen wild-type (WT) vaccine strain and those in circulation [101, 103, 119]. This is particularly true for influenza A(H3N2) viruses, which evolve slightly faster than influenza A(H1N1) viruses, and can quickly escape pre-existing immune memory [5, 114, 120]. In the last 20 years, the World Health Organization (WHO) has recommended 13 different WT strains to serve as the H3N2 component of the Northern hemisphere influenza virus annual vaccine; nearly twice as many as the H1N1 component over that same timeframe [12]. During the 2018-2019 influenza virus season, a mismatch between circulating strains and the WHO selected H3N2 vaccine strain led to a vaccine efficacy of ~9% compared to 41% for the H1N1 component [12, 60, 104]. The WHO strain selection committee convenes twice per year to recommend WT vaccine strains for upcoming influenza seasons in the Northern and Southern hemispheres, but these decisions are decided more than six months prior to the onset of the influenza season to allow sufficient time for

manufacturing of the vaccines [5, 102, 110, 121]. Typically, these components are selected based on predictions of predominant or emerging viral clades that are derived from global surveillance information, but this predictive method can lead to the selection of mismatched strains that may only provide limited protection against currently circulating viruses [12, 56, 122]. Despite these efforts, selecting a mismatched vaccine strain may be unavoidable and, as a result, vaccine efficacy typically ranges between 10% to 65% annually [5, 112]. Thus, a vaccine that can provide immediate protection against antigenically drifted influenza virus strains is urgently needed [5, 102, 110].

Designing an influenza virus vaccine that induces broadly reactive antibodies across multiple antigenic clusters and possesses the ability to neutralize viruses over multiple influenza seasons is a pivotal challenge [64]. Current standard of care inactivated influenza (IIV) vaccines primarily induces strain-specific antibodies and do not provide protection against antigenically drifted strains of influenza [56, 75, 110]. Previously, our group reported on the development of a next-generation methodology for generating Computationally Optimized Broadly Reactive Antigens (COBRA) for influenza, focusing on the viral HA protein that can be used as vaccines for H1, H2, H3, and H5 subtypes of influenza virus [13, 62, 65, 66, 68-71, 111, 123]. This next-generation antigen design approach allows the natural viral evolution to dictate antigen design, while at the same time incorporating antigenic epitopes from numerous simultaneously circulating strains isolated during the most recent influenza seasons to produce broadly reactive antigens [91, 111]. These broadly reactive HA antigens elicit antibodies capable of blocking HA-specific receptor binding, inhibiting viral infection, and limiting virus induced pathogenesis in influenza immunologically naive and influenza pre-immune animals [13, 65, 66, 68, 72-74, 111, 123].

The performance of influenza virus vaccines primarily depends on how well the vaccine antigen matches the viruses currently in circulation, but it also depends on the previous influenza virus exposure histories of a population through infection and vaccination [103, 119]. However, the impact of a lifetime of prior infections and vaccinations on vaccine effectiveness remains unclear [99, 102, 115]. Most humans are infected with influenza viruses by the time they are 3-4 years old, and early childhood exposures can profoundly impact how an individual responds to antigenically distinct strains later in life [5, 99, 113, 118]. Despite this, most broadly reactive influenza virus vaccine candidates are tested in animal models with no previous exposures to influenza [101, 124, 125]. Broadly reactive influenza virus vaccine candidates need to be evaluated in pre-immune animal models that more closely resemble human immunity to influenza in order to have a better understanding of their potential protective efficacy [124].

The H3 COBRA HA vaccine antigen, TJ5, which was designed using influenza A(H3N2) WT HA sequences from viruses isolated between 2008-2012, has been evaluated in both influenza naïve and pre-immune animal models [111, 123]. In these models, TJ5 induced sero-protective antibody titers against historical H3N2 vaccine isolates and co-circulating strains from 2005-2018, however it did not produce protective hemagglutination inhibition (HAI) antibody titers against the recently circulating A/Hong Kong/2671/2019 (HK/19) H3N2 vaccine strain isolate. This is not entirely unexpected, as influenza viruses will mutate though natural processes of antigenic drift, and the protection offered by broadly reactive vaccine candidates may eventually begin to decline due to the diversity of newly emerging HA surface epitopes present in the circulating viral population [76, 121]. A similar phenomenon was observed with the historic H1 COBRA HA antigens, which had trouble eliciting antibodies against newly emerged H1N1 isolates from 2013-2019 [126]. The H1 antigens were redesigned using a next generation COBRA design

methodology [111], and the newly synthesized Y2 antigen, designed from WT H1N1 input sequences from 2014-2016, had the ability to elicit sero-protective HAI antibodies against H1N1 isolates from 2009-2019 [126].

In this study, updated H3 COBRA antigens were designed using the next generation COBRA methodology [111] to enhance the vaccine derived antigenic breadth against newly emerging influenza A(H3N2) isolates by using WT H3N2 HA input sequences from 2012-2019. This process led to the development of 7 distinct COBRA HA vaccine candidates that were first evaluated in influenza virus naïve mice. Subsequently, two H3 COBRA HA candidates, J4 and NG2, were selected for further testing in an influenza pre-immune animal model, based on their ability to elicit HAI reactive antibodies against the HK/19 virus, as well as numerous other H3N2 historical isolates. In the pre-immune mouse model J4 and NG2 were both superior to WT vaccine antigens at eliciting antibodies against antigenically drifted strains of H3N2 viruses by inducing sero-protective antibodies against all of the H3N2 vaccine strain isolates from 2012-2019.

Commercial seasonal influenza vaccines in the United States, are typically composed of two influenza A WT strains representing the A(H1N1) and A(H3N2) subtypes, and one or two influenza B strains representing the Victoria and Yamagata lineages [6, 7]. In this study, bivalent formulations of COBRA Y2 H1 and the TJ5, J4 and NG2 COBRA H3 rHAs were tested in pre-immune mice for their ability to elicit broadly reactive antibodies against panels of H1N1 and H3N2 influenza viruses from 2007-2019. Since most humans have extensive pre-existing immune histories to both H1N1 and H3N2 influenza A virus subtypes, either through infection or vaccination, the bivalent vaccine candidates were evaluated in mice that are pre-immune to both H1N1 and H3N2 historical strains [102, 118, 124]. This is the first time that H1 and H3 COBRA antigens have been used in a bivalent vaccine formulation, and their performance was compared

to multiple bivalent mixtures of historical WT H1 and H3 rHA vaccine antigens. In this model, bivalent mixtures of COBRA H1+H3 rHA, Y2+J4 and Y2+NG2, outperformed WT H1+H3 bivalent rHA mixtures, by eliciting sero-protective HAI antibody titers against all H1N1 and H3N2 historical vaccine strain isolates from 2009-2019. They also elicited antibodies capable of neutralizing more live virus infections of H1N1 and H3N2 isolates from 2009-2019 at higher titers than any one mixture of WT rHA antigens in neutralization assays. Additionally, the bivalent COBRA rHAs elicited antibodies that protected vaccinated mice from H3N2 influenza virus challenge and these animals had no detectable virus in their lungs at day 3 post-infection. Overall, the newly generated H1 and H3 COBRA rHA antigens, Y2, J4, and NG2, had the ability to induce broadly reactive antibodies in influenza naïve and pre-immune populations using both monovalent and bivalent, H1+H3, formulations. Overall, these antigens outperformed H1 and H3 WT rHA vaccine antigens by eliciting sero-protective antibodies against panels of antigenically drifted historical H1N1 and H3N2 vaccine virus strains from 2009-2019.

Materials and Methods

Vaccine Design and Preparation

Full length wild-type (WT) influenza A(H3N2) HA protein amino acid sequences from 54,041 human H3N2 viruses collected from May 1, 2008 to September 30, 2019, were downloaded from the Global Initiative on Sharing Avian Influenza Data (GISAID) EpiFlu online database. Sequences were organized by their date of collection and used to produce consensus sequences based on the next-generation COBRA design methodology as previously described [111]. Briefly, the sequences from each influenza season were divided into clusters based on 95% similarity, and from each cluster a primary consensus sequence was generated. The

primary sequences were then clustered based on percent identity and used to produce secondary consensus sequences. The secondary consensus sequences were then input into 2 different COBRA consensus building scenarios as previously described [111] to generate the final H3 consensus sequences. This process generated 8 different COBRA HA sequences: TJ5 (designed using sequences isolated during May 2008 - September 2012), J1 (May 2013 - September 2015), J2 (September 2014 - April 2016), J3 (May 2014 - September 2016), J4 (May 2013 – April 2016), NG1 (May 2015 – April 2017), NG2 (May 2016 – April 2018), and NG3 (May 2017 – September 2019).

Additionally, full length WT influenza A(H1N1) HA protein amino acid sequences from 3,078 human H1N1 viruses collected from May 1, 2014 – September 30, 2016, were also downloaded from the GISAID Epiflu database. These sequences were also organized by their collection date, and put into the COBRA algorithm to generate the Y2 COBRA HA sequence as previously described [126].

Soluble rHA proteins, were generated by transfecting truncated COBRA and WT HA genes that were cloned into the pcDNA3.1^{+} plasmid, into HEK293T suspension cells (Thermo Fisher, Waltham, MA, USA) as previously described [127]. The truncated HA genes were generated by replacing the transmembrane domain with a T4 fold-on domain, an Avitag, and a 6x His-tag for purification by immobilized metal affinity chromatography (IMAC) [127]. The concentration of the soluble HA proteins was determined by conventional bicinchoninic acid assay (BCA) according to the manufacturer's instructions (Thermo Fisher, Waltham, MA, USA).

Viruses and HA antigens

Influenza A(H3N2) viruses were obtained through either the Influenza Reagents Resource (IRR), BEI Resources, the Centers for Disease Control (CDC), or provided by Virapur (San Diego, CA, USA). Viruses were passaged once in the same growth conditions as they were received, either embryonated chicken eggs or semi-confluent Madin-Darby canine kidney (MDCK) cell cultures as per the instructions provided by the WHO [82]. H3N2 virus lots were titered with 0.75% guinea pig erythrocytes in the presence of 20nM Oseltamivir, and made into aliquots for single-use applications. H1N1 virus lots were titered with 0.8% turkey erythrocytes, and made into aliquots for single use applications.

The A(H3N2) 2012-2019 historical influenza vaccine strain viral panel for HAI analysis included the 8 following viral strains: A/Texas/50/2012 (Tx/12) egg passage 4 (EP4), A/Switzerland/9715293/2013 (Switz/13) EP4, A/Hong Kong/4801/2014 (HK/14) EP11, and A/Singapore/IFNIMH-16-0019/2016 (Sing/16) EP3, A/Kansas/14/2017 (Kan/17) EP1, A/Texas/71/2017 (Tx/17) MDCK cell passage 1 (MDCKP1), A/Switzerland/8060/2017 (Switz/17) EP1, A/South Australia/34/2019 (SA/19) EP1, A/Hong Kong/2671/2019 (HK/19) EP1.

The A(H1N1) 2007-2019 historical influenza vaccine strain panel for HAI analysis included the 5 following viral strains: A/Brisbane/59/2007 (Bris/07) EP1, A/California/07/2009 (Cal/09) EP4, A/Michigan/45/2015 (Mich/15) EP1, A/Brisbane/02/2018 (Bris/18) EP1, and A/Guangdong-Maonan/SWL1536/2019 (Guang/19) EP1.

One historical H1N1 vaccine strain virus, A/Singapore/6/1986 (Sing/86) EP1, and one historical H3N2 vaccine strain virus, A/Panama/2007/1999 (Pan/99) EP4, were used to make mice pre-immune to H1N1 and H3N2 viruses. The preimmune mice were also challenged with an H3N2 influenza virus, A/Kansas/14/2017 (Kan/17) EP1 on day 86 of the pre-immune study.

Viral infection and COBRA rHA vaccination of mice.

BALB/c and DBA/2J mice (females, 6-8 weeks old) were purchased from The Jackson Laboratory (Bar Harbor, ME, USA). The mice were housed in microisolator units, and allowed free access to food and water. All animals were cared for under the USDA guidelines for laboratory animals, and all procedures were approved by the University of Georgia Institutional Animal Care and Use Committee (IACUC) (no. A2018 06-018-Y3-A16).

The 75 influenza naïve BALB/c mice were randomly divided into 15 groups (5 animals/group), and vaccinated intramuscularly with either 3ug of COBRA: TJ5, J1, J2, J3, J4, NG1, NG2, or NG3 rHA, 3ug of WT rHA from historical H3N2 vaccine strains: A/Switzerland/9715293/2013 (Switz/13), A/Hong Kong/4801/2014 (HK/14), A/Singapore/IFNIMH-16-0019/2016 (Sing/16), A/Kansas/14/2017 (Kan/17), A/Switzerland/8020/2017 (Switz/2017), A/South Australia/34/2019 (SA/19), or administered 25uL of phosphate-buffered saline (PBS, Corning, Tewksbury, MA, USA) alone as a mock vaccination. All vaccines (COBRA, WT, and mock) were formulated with an emulsified squalene-based oil-in-water emulsion adjuvant, Addavax (InvivoGen, San Diego, CA, USA), and the final concentration after mixing 1:1 with rHA was 2.5% squalene. Vaccines were administered into the hind leg of the animals on day 0, 28, and 56 in a homologous prime-boost-boost regimen. Blood was collected from the facial vein 14 days following each vaccination, on day 14, 42, and 70 (Fig 5.1). Sera was isolated from the blood by centrifugation at 2,500 rpm for 10 mins. Clarified serum was removed and frozen at −20 ± 5°C.

The 136-influenza naïve DBA/2J mice were randomly divided into 17 groups (8 animals/group) to be used in the pre-immune mouse experiment. 16 groups of mice were made pre-immune to both H1N1 and H3N2 influenza on day 0, by administering a mixture consisting

of equal concentrations of H1N1 (A/Singapore/6/1986 (Sing/86)) and H3N2 (A/Panama/2007/1999 (Pan/99)) at a final concentration of $5x10^5$ PFU/50uL in PBS, by administering 50uL to each mouse intranasally. Mock pre-immune animals were inoculated intranasally with 50uL of PBS. Following the pre-immune infection, animals were monitored twice daily, morning and evening, for weight loss and clinical signs (labored breathing, lethargy, hunched back, ruffled fur, failure to respond to stimuli, and severe respiratory distress), for 14 days post infection. During this time, none of the mice lost more than 5% of their original body weight, and exhibited no clinical signs. The animals were then allowed to rest for 30 days, at which point they were vaccinated with 3ug total of either monovalent formulations of COBRA rHA: Y2 (H1), TJ5 (H3), J4 (H3), or NG2 (H3); monovalent formulations of WT rHA: A/Brisbane/59/2007 (Bris/07) (H1), A/California/07/2009 (Cal/09) (H1), A/Switzerland/9715293/2013 (Switz/13) (H3), A/Singapore/IFNIMH-16-0019/2016 (Sing/16) (H3), or 3ug total (1.5ug H1 + 1.5ug H3) of COBRA rHA cocktails: Y2 + TJ5 (H1+H3), Y2 + J4 (H1 + H3), or Y2 + NG2 (H1 + H3), or 3ug total (1.5ug H1 + 1.5ug H3) of WT rHA cocktails: Bris/07 + Switz/13 (H1 + H3), Bris/07 + Sing/16 (H1 + H3), Cal/09 + Switz/13 (H1 + H3), Cal/09 + Sing/16 (H1 + H3); or mock vaccines consisting of 25uL of phosphate-buffered saline (PBS) (Corning, Tewksbury, MA, USA) alone. All vaccines (COBRA, WT, and mock) were formulated with Addavax adjuvant, and the final concentration after mixing 1:1 with rHA was 2.5% squalene. Vaccines were administered intramuscularly into the hind leg of the animals on day 30 and 58 in a homologous prime-boost regimen. Blood was collected from the facial vein 14 days following the pre-immune infection and each vaccination, on day 14, 44, and 72 (Fig 5.2). Sera was isolated from the blood by centrifugation at 2,500 rpm for 10 mins. Clarified serum was removed and frozen at −20 ± 5°C. All DBA/2J mice were then challenged with 50uL of live H3N2 influenza virus, A/Kansas/14/2107 (EP4), at a concentration

of $6.7x10^6$ PFU/50uL, intranasally on day 86. Following infection, animals were monitored twice daily, morning and evening, for weight loss and clinical signs (labored breathing, lethargy, hunched back, ruffled fur, failure to respond to stimuli, and severe respiratory distress), for 14 days post infection. On day 89, 3 animals from each group were sacrificed, and lungs were collected to assess the viral load. Lungs were frozen on dry ice, and stored at -80 ± 5°C until viral plaque assays were performed.

Hemagglutination-Inhibition (HAI) assay

The hemagglutination inhibition (HAI) assay was used to assess functional antibodies to the HA that are able to inhibit agglutination of guinea pig erythrocytes for H3N2 viruses, and turkey erythrocytes for H1N1 viruses. The protocols were adapted from the WHO laboratory influenza surveillance manual [82]. Guinea pig red blood cells are frequently used to characterize contemporary A(H3N2) influenza strains that have developed a preferential binding to alpha (2,6) linked sialic acid receptors [83, 84]. To inactivate nonspecific inhibitors, sera samples were treated with receptor-destroying enzyme (RDE) (Denka Seiken, Co., Japan) prior to being tested. Briefly, three parts of RDE was added to one part of sera and incubated overnight at 37°C. RDE was inactivated by incubation at 56°C for 30 min.

RDE-treated sera were diluted in a series of two-fold serial dilutions in v-bottom microtiter plates. An equal volume of each A(H3N2) virus, adjusted to approximately 8 hemagglutination units (HAU)/50µl in the presence of 20nM Oseltamivir carboxylate, was added to each well. The plates were covered and incubated at room temperature for 30 mins, and then 0.75% guinea pig erythrocytes (Lampire Biologicals, Pipersville, PA, USA) in PBS were added. Prior to use, the red blood cells (RBCs) were washed twice with PBS, stored at 4°C, and used within 24 h of

preparation. The plates were mixed by gentle agitation, covered, and the RBCs were allowed to settle for 1 h at room temperature. The HAI titer was determined by the reciprocal dilution of the last well that contained non-agglutinated RBCs. Positive and negative serum controls were included for each plate.

In separate assays RDE-treated sera were diluted in a series of two-fold serial dilutions in v-bottom microtiter plates. An equal volume of each A(H1N1) virus, adjusted to approximately 8 hemagglutination units (HAU)/50µl was added to each well. The plates were covered and incubated at room temperature for 20 mins, and then 0.8% turkey erythrocytes (Lampire Biologicals, Pipersville, PA, USA) in PBS were added. Prior to use, the RBCs were washed twice with PBS, stored at 4°C, and used within 24 h of preparation. The plates were mixed by gentle agitation, covered, and the RBCs were allowed to settle for 30 mins at room temperature. The HAI titer was determined by the reciprocal dilution of the last well that contained non-agglutinated RBCs. Positive and negative serum controls were included for each plate.

All mice were negative (HAI $\leq$ 1:10) for pre-existing antibodies to human influenza viruses prior to infection or vaccination, and for this study, a positive HAI reaction (HAI+), or "sero-protection", is defined as an HAI titer $\geq$1:40, and "seroconversion" refers to a 4-fold increase in titer compared to baseline, as per the WHO and European Committee for Medicinal Products to evaluate influenza vaccines [85].

Focus Reduction Assay (FRA)

The Focus Reduction Assay (FRA) used in this study was initially developed by the WHO collaborating Centre in London, U.K. and modified by U.S. Centers for Disease Control and Prevention (CDC) (Thomas Rowe, personal communication). MDCK-SIAT1 cells (Sigma, St.

Louis, MO, USA) were plated at 2.5 – 3 x 10^5 cells/ml (100uL/well in 96-well plate) one day prior to use in the assay. Cells were cultured in Dulbecco's Modified Eagle Medium (DMEM) containing 5% heat-inactivated fetal bovine serum and antibiotics in 96-well flat bottom plates overnight to form a 95-100% confluent monolayer. The following day, the cell monolayers are rinsed with 0.01M phosphate-buffered saline pH 7.2 (PBS, Gibco, Waltham, MA, USA), followed by the addition of 2-fold serially diluted RDE treated serum (50uL per well) starting with a 1:20 dilution in virus growth medium containing TPCK-treated trypsin (1µg/ml) (Thermo Fisher, Waltham, MA, USA), VGM-T, (DMEM containing 0.1% BSA, 1% Penicillin/Streptomycin (100 U/mL Penicillin, 100 ug/mL Streptomycin solution), and 1µg/ml TPCK-treated trypsin) (Sigma, St. Louis, MO, USA). 50uL of A(H3N2) influenza virus (1.2 x 10^4 focus forming units (FFU)/mL, which corresponds to 600 FFU/50µl) in VGM-T was added to the wells of each plate, or VGM-T only was added to cell control wells. Virus stocks were standardized by previous titration in the FRA [54, 55]. The A(H3N2) viruses used in this assay were the historical WHO selected vaccine strains A/Singapore/IFNIMH-16-0019/2016 EP3, A/Kansas/14/2017 EP1, and A/Hong Kong/2671/2019 EP1. The A(H1N1) viruses used in this assay were the historical WHO selected vaccine strains A/California/07/2009 EP4, A/Brisbane/2/2018 EP1, and A/Guangdong-Maonan/SWL1536/2019 EP1.

Following a 2 h incubation period at 37ºC with 5% CO_2, the cells in each well were then overlaid with 100uL of equal volumes of 1.2% Avicel RC/CL (Type: RC581 NF; FMC Health and Nutrition, Philadelphia, PA, USA) in 2X Modified Eagle Medium containing 1µg/ml TPCK-treated trypsin, 0.1% BSA and antibiotics [86]. Plates were incubated for 18-22 h at 37ºC, 5% CO_2. The overlays were then removed from each well and the monolayer was washed once with PBS to remove any residual Avicel. The plates were then fixed with ice-cold 4% formalin in PBS

for 30 min at 4ºC, followed by a PBS wash and permeabilization using 0.5% Triton-X-100 in PBS/glycine at room temperature for 20 min. Plates were washed three times with wash buffer (PBS, 0.1% Tween-20; PBST) and then incubated for 1 h with a monoclonal antibody against the influenza A nucleoprotein [54, 87, 88] obtained from the Influenza Reagent Resource (IRR) (Manassas, VA, USA) (FR-1217) (1mg/mL), diluted 1:2000 in ELISA buffer (PBS,10% horse serum, 0.1% Tween-80). Following washing (3X PBST), the cells were incubated with goat anti-mouse peroxidase-labelled IgG (Sera Care, Inc., Milford, MA, USA) (KPL 474-1802) (1mg/mL), diluted 1:2000 in ELISA buffer for 1 hour at RT. Plates were then washed again (3X PBST) and infectious foci were visualized using TrueBlue substrate (Sera Care, Inc., Milford, MA USA) containing 0.03% H_2O_2 incubated at room temperature (RT) for 10 min. The reaction was stopped by washing five times with dH_20. Plates were air dried and foci enumerated using a CTL BioSpot Analyser with ImmunoCapture 6.4.87 software (CTL, Shaker Heights, OH, USA). The FRA titer was reported as the reciprocal of the highest dilution of serum corresponding to 50% foci reduction compared to the virus control minus the cell control.

In order for a plate to pass quality control, both the average of the octuplet virus control wells (VC), as well as the average of the octuplet cell control wells (CC) must pass. The virus controls must fall between 200 and 1600 foci and the cell controls must be free of foci. Additionally, the positive control, A(H1N1) and A(H3N2) historical influenza vaccine strain viruses were run in triplicate plates in each individual assay and at least two out of three plates must pass VC and CC criteria. Homologous mouse antisera, previously generated through infection with homologously matched A(H1N1) and A(H3N2) influenza viruses at 1e6 FFU/mL, and collected 14 days post infection, must have the same titer across the plates [65]. Each assay plate (one virus per plate) contained a panel of mouse reference antisera, as well as a human

influenza vaccine serum control to assess overall assay consistency [13]. The percentage of infected cells reported in the assay is calculated by averaging the foci count from the positive control (virus and cell only) wells, and dividing the number of foci in each experimental well by the average of the positive control.

Influenza Viral Plaque Assay

MDCK cells (Sigma, St. Louis, MO, USA) were seeded into each well of a six-well plate at a concentration of 1×10^6 cells/well one day prior to performing the plaque assay. On the day of the assay, frozen Lung tissues were thawed on ice were weighed and homogenized in 1 ml of DMEM (Thermo Fisher, Waltham, MA, USA). The homogenate was centrifuged at 2,000 rpm for 5 min to remove tissue debris, and the supernatant was collected and subjected a serial 10-fold dilution in DMEM supplemented with 1% penicillin-streptomycin (DMEM + P/S) (Thermo Fisher, Waltham, MA, USA). When MDCK cells reached 90% confluency in each well, the plates were washed 2x with DMEM + P/S, and infected with 100uL of each dilution of homogenate supernatant. The plates were then shaken every 15 mins for 1 hour. After 1 hour of incubation, the supernatant was removed and cells were washed twice with fresh DMEM + P/S. Following the second wash, a solution of 2xMEM and 1.6% agarose (Thermo Fisher, Waltham, MA, USA) mixed 50:50 v/v, and supplemented with 1ug/mL of TPCK trypsin (Thermo Fisher, Waltham, MA, USA) was added into each well. Plates were then incubated at 37°C + 5% CO2 for 72 hours. After 72 hours, the gel overlays were removed from each well, and the cells were fixed with 10% buffered formalin for 10 mins and stained with 1% crystal violet (Thermo Fisher, Waltham, MA, USA) for 10 mins at room temperature. Plates were then rinsed thoroughly 5x with fresh water to remove excess crystal violet. Plates were allowed to air dry for 24 hours, and the viral plaques

were enumerated as the reciprocal of each dilution. The lung viral titers were calculated and presented as plaque forming units (PFU)/g of lung tissue.

Statistical Analysis

Data is presented as absolute mean values ± standard error of the mean (SEM). One-way ANOVA was used to analyze the statistical differences between groups using GraphPad Prism 9 software (GraphPad, San Diego, CA, USA). A "p" value less than 0.05 was defined as statistically significant (*, $P < 0.05$; **, $P < 0.01$; ***, $P < 0.001$; ****, $P < 0.0001$).

Results

COBRA Vaccination Enhances H3N2 HAI Breadth in Influenza Naïve Mice Compared to WT Vaccines

In order to determine the antibody breadth elicited by the newly generated H3 COBRA rHA antigens, influenza naïve BALB/c mice were vaccinated with either COBRA or WT rHAs in a prime-boost-boost regimen over a span of 56 days (Fig 5.1). Sera collected from these mice on day 70, 2 weeks after the final vaccination, were evaluated for HAI+ reactive antibodies against a panel of historical influenza A(H3N2) virus vaccine strains spanning 2012-2019 (Fig 5.2). Antibodies collected from mice vaccinated with the historical H3 COBRA HA, TJ5, had antibodies with sero-protective HAI+ titers against all of the H3N2 influenza viruses representing the time period between 2012-2019, except for the HK/19 virus, for which there were no detectable HAI titers (Fig 5.2A). Mice vaccinated with the J1 COBRA rHA had antibodies with HAI+ activity against the H3N2 influenza viruses isolated from 2012-2016 and the Switz/17 and SA/19 strains, but these antibodies failed to recognize the Kan/17, Tx/17, and HK/19 viruses (Fig 5.2B). J2 vaccinated mice had antibodies with HAI activity against Tx/12, HK/14, Sing/16, and Switz/17

(Fig 5.2C). Mice vaccinated with J3 rHA had antibodies with HAI+ activity against all of the H3N2 influenza virus strains isolated from 2012-2016, as well as Switz/17 and SA/19, with their highest antibody titer being directed against the Tx/12 isolate (Fig 5.2D). The J4 COBRA rHA induced antibodies with HAI+ activity against Tx/12, HK/14, Sing/16, Switz/17, and SA/19 in vaccinated mice, with their highest antibody titers detected against the HK/14 and Sing/16 strains (Fig 5.2E). Mice vaccinated with NG1 rHA sero-converted to all of the H3N2 strains isolated from 2012-2019, except for Kan/17 and HK/19 (Fig 5.2F). Mice vaccinated with NG2 rHA possessed sero-protective antibody titers against all of the H3N2 strains in the panel, with their highest antibody titers being directed against the SA/19 virus (Fig 5.2G). The NG3 rHA vaccine induced sero-conversion to Tx/12, Switz/13, Switz/17, and SA/19 (Fig 5.2H).

Animals vaccinated with Switz/13 only sero-converted to the homologously matched virus, Switz/13, and none of the other viruses in the H3N2 panel (Fig 5.2I). The HK/14 rHA vaccine induced antibodies with HAI+ activity against all of the viruses from 2012-2016, with its highest magnitude antibody titers being directed against the homologously matched HK/14 virus. The HK/14 rHA vaccine did not induce antibodies with HAI+ activity against any of the strains isolated during 2017-2019 (Fig 5.2J). Mice vaccinated with Sing/16 rHA had antibodies with HAI+ activity against all of the strains isolated from 2012-2019, with the exception of the Kan/17 and HK/19 viruses. The highest magnitude antibody response for these mice was against the homologously matched Sing/16 virus (Fig 5.2K). The Kan/17 rHA vaccine induced antibodies with HAI+ activity against all of the H3N2 isolates from 2012-2017, except against the Sing/16 virus. These mice also did not sero-convert to either of the 2019 isolates, SA/19 or HK/19, and the highest magnitude antibody response from this group was directed towards the homologously matched Kan/17 virus (Fig 5.2L). Mice vaccinated with Switz/17 rHA had antibodies with HAI+

activity against Tx/12, Tx/17, Switz/17, and SA/19; with the highest magnitude antibody response directed against the homologously matched Switz/17 virus (Fig 5.2M). The SA/19 rHA vaccine induced antibodies with HAI+ activity against the Tx/12, HK/14, Tx/17, Switz/17, and SA/19 virus. The highest titer of HAI antibodies for this group was directed against the homologously matched SA/19 virus (Fig 5.2N). The mock vaccinated mice did not have any detectable titers against any of the H3N2 viruses in the panel (Fig 5.2O).

H1 and H3 COBRA Vaccines Elicit Broader HAI Responses in Pre-immune Mice than Naïve Mice

In order to investigate the breadth of HAI directed antibodies generated by COBRA rHA vaccine antigens in pre-immune animals, influenza immunologically naïve DBA/2J mice were made pre-immune to both H1N1 and H3N2 historical influenza viruses. The mice were first infected with equal mixtures of A/Singapore/6/1986 (H1N1) and A/Panama/2007/1999 (H3N2) to establish pre-immunity, and were then vaccinated in a homologous prime-boost model with either COBRA (Y2, TJ5, J4, or NG2) or WT H1 and H3 rHA proteins. J4 was selected over the other J-series COBRA HA proteins based on its ability to elicit broad HAI responses across the 2012-2019 H3N2 historical vaccine strain panel, and the magnitude of antibody titer it generates against the 2019 WT H3N2 isolates in naïve mice (Fig 5.2E). Similarly, NG2 was chosen to study in the pre-immune model, as it was the only NG-series COBRA rHA vaccine antigen to elicit sero-protective HAI titers against all of the H3N2 strains from 2012-2019 (Fig 5.2G). Two WT H1 rHA vaccine antigens, Bris/07 and Cal/09, were chosen to serve as seasonal and pandemic H1N1 comparators. Likewise, two WT H3 rHA vaccine antigens, Switz/13 and Sing/16, were chosen to serve as the H3N2 comparators. In addition to monovalent formulations of each COBRA and WT

rHA vaccine antigens, bivalent mixtures (H1+H3) of each COBRA and WT rHA were also evaluated in the pre-immune model for their ability to enhance HAI reactive antibody breadth to both H1N1 and H3N2 WT historical vaccine virus strains (Fig 5.3).

Sera isolated 72 days after pre-immunization, 14 days following the second vaccination, were tested in HAI assays to determine the antibody breadth elicited by each monovalent rHA vaccine antigen against H1N1 and H3N2 WT historical vaccine strains from 2007-2019 (Fig 5.4). Pre-immune mice vaccinated with Bris/07 rHA only generated sero-protective HAI+ antibody responses to the homologously matched Bris/07 H1N1 virus isolate (Fig 5.4A). The Cal/09 rHA vaccine elicited antibodies with HAI+ activity against the H1N1 isolates from 2009-2018 (Fig 5.4B). Pre-immune mice vaccinated with the H1 COBRA rHA, Y2, had antibodies with HAI+ activity against all of the H1N1 strains isolated from 2009-2019 (Fig 5.4C). The HAI reactive antibody titer generated by the Y2 rHA vaccinated animals against the Guang/19 virus was significantly higher (~8 fold; $P<.0001$) than the titer generated by the Cal/09 rHA vaccine (Fig 5.4B and 5.4C).

Pre-immune mice vaccinated with the H3 Switz/13 rHA protein had antibodies with HAI+ activity against the Tx/12, Switz/13, Kan/17, Tx/17, and SA/19 H3N2 viral isolates, with the highest titers against the homologously matched Switz/13 virus (Fig 5.4D). The Sing/16 rHA vaccine induced antibodies with HAI+ activity against Tx/12, HK/14, Sing/16, Tx/17, Switz/17, SA/19, and HK/19 H3N2 isolates (Fig 5.4E). Mice that received the TJ5 COBRA rHA vaccine had antibodies with HAI+ activity against all of the H3N2 strains isolated from 2012-2019, with the exception of Tx/17 and HK/19. The TJ5 vaccinated mice generated their largest HAI reactive antibody response against the Tx/12 virus (Fig 5.4F). Pre-immune mice vaccinated with J4 had antibodies with HAI+ activity against all of the H3N2 historical vaccine strains isolated from 2012-

2019 (Fig 5.4G). Similarly, pre-immune mice vaccinated with NG2 also had antibodies with HAI+ activity against all of the H3N2 strains from 2012-2019 (Fig 5.4H). The pre-immune mice that received mock vaccinations did not sero-convert to any of the H1N1 or H3N2 viral strains in the panel (Fig 5.4I).

Bivalent H1+H3 COBRA Vaccination Enhances H3N2 HAI Breadth in Pre-immune Mice compared to Bivalent WT H1+H3 Mixtures

Sera isolated 72 days after pre-immunization, 14 days following the second vaccination, was tested in HAI assays to determine the antibody breadth elicited by bivalent rHA vaccine antigen mixtures (H1+H3) against H1N1 and H3N2 WT historical vaccine strain isolates from 2007-2019 (Fig 5.5). The WT bivalent mixture of Bris/07+Switz/13 induced antibodies with HAI+ activity against the Bris/07 H1N1 influenza strain and the Tx/12, Switz/13, Kan/17, Tx/17, and SA/19 H3N2 influenza strains. The highest antibody response from this group was directed towards the homologously matched Bris/07 H1N1 and Switz/13 H3N2 strains (Fig 5.5A). Similarly, the group of pre-immune mice vaccinated with the bivalent mixture of Bris/07+Sing/16 only had antibodies with HAI+ activity against the Bris/07 H1N1 influenza strain, but had antibodies with HAI+ activity against the Tx/12, HK/14, Sing/16, Switz/17, and SA/19 H3N2 strains (Fig 5.5B). Mice vaccinated with Cal/09+Switz/13 had antibodies with HAI+ activity against the H1N1 influenza strains isolated from 2009-2018 and the homologously matched Switz/13 H3N2 strain (Fig 5.5C). Similarly, the bivalent mixture of Cal/09+Sing/16 rHA induced sero-conversion to all of the H1N1 influenza strains from 2009-2018, but had a broader HAI+ response to the H3N2 influenza viruses, inducing antibodies with HAI+ activity against the Tx/12, HK/14, Sing/16, Switz/17, SA/19, and HK/19 strains (Fig 5.5D). This is in contrast to the pre-

immune mice vaccinated with the bivalent mixture of Y2+TJ5 COBRA rHA antigens, which had antibodies with HAI+ activity against all of the H1N1 isolates from 2009-2019, as well as the H3N2 isolates from 2012-2016, Kan/17, and SA/19 (Fig 5.5E). The bivalent mixture of Y2+J4 also induced antibodies with HAI+ activity against all of the H1N1 strains from 2009-2019, but they possessed antibodies with HAI activity against all of the H3N2 strains from 2012-2019 (Fig 5.5F). Similarly, the mixture of Y2+NG2 induced antibodies with HAI+ activity against all of the H1N1 strains from 2009-2019, and the H3N2 strains from 2012-2019 (Fig 5.5G). The influenza naïve mice that received mock vaccinations did not sero-convert to any of the H1N1 or H3N2 viral strains in the panel (Fig 5.5H).

COBRA Vaccines Enhance Neutralizing Antibody Responses Against Modern Pandemic-like H1N1 Viruses

Influenza virus focal reduction assays (FRAs) were used to determine the ability of vaccine elicited antibodies to neutralize live virus infections against a panel of 3 historical influenza A(H1N1) vaccine strain isolates from 2009-2019 from sera collect 72 days after pre-immunization (Fig 5.6). Pre-immune mice vaccinated with the monovalent formulation of COBRA Y2 rHA had antibodies that neutralized Cal/09 viral infections with an average titer greater than the Log2 80% neutralization ($PRNT_{80}$) mark at every dilution (Fig 5.6A). Likewise, mice vaccinated with Cal/09 rHA also generated antibodies capable of neutralizing Cal/09 viral infection at every dilution tested at a titer greater than the $PRNT_{80}$ (Fig 5.6A). All other monovalent rHA vaccinated mice did not have neutralizing antibodies against the Cal/09 virus with titers similar to the mock vaccinated pre-immune animals (Fig 5.6A). Sera collected from influenza naïve mice that received mock vaccinations were unable to neutralize the Cal/09 virus at any dilution (Fig 5.6A). The pre-immune

mice vaccinated with the Y2 rHA also had antibodies that neutralized Bris/18 viral infections at a titer >$PRNT_{80}$ at every dilution (Fig 5.6B). Sera collected from mice vaccinated with Cal/09 rHA also neutralized Bris/18 viral infection at every dilution with a titer >$PRNT_{80}$ (Fig 5.6B). All other monovalent rHA vaccine groups had antibodies that prevented fewer than ~20% of the cells from being infected with Bris/18, similar to the mock vaccinated pre-immune animals, at the lowest serum dilution (Fig 5.6B). Sera collected from influenza naïve mice that received mock vaccinations were unable to neutralize the Bris/18 virus at any sera dilution (Fig 5.6B). The pre-immune mice vaccinated with Y2 rHA had the highest neutralizing titers of any of the monovalent groups against the Guang/19 virus, with an average Log2 50% neutralization ($PRNT_{50}$) titer of 10.14 (Fig 5.6C). Mice vaccinated with Cal/09 rHA had antibodies that neutralized Guang/19 at an average $PRNT_{50}$ titer of 7.75; a titer ~6-fold lower than the titer elicited in Y2 rHA vaccinated animals (Fig 5.6C). All other monovalent rHA vaccine groups had antibodies that prevented ~10% of the cells from Guang/19 virus infections, similar to the mock vaccinated pre-immune animals (Fig 5.6C). Sera from influenza naïve mice that received mock vaccinations were unable to neutralize the Guang/19 virus (Fig 5.6C).

Mice vaccinated with bivalent rHA formulations containing the COBRA Y2 antigen, Y2+TJ5, Y2+J4, and Y2+NG2, all had antibodies with similar neutralizing capabilities against the Cal/09 virus, with an average $PRNT_{80}$ titers of 11.08, 11.35, and 11.61 respectively (Fig 5.6D). Similarly, pre-immune mice vaccinated with mixtures containing the Cal/09 rHA (Cal/09+Switz/13 and Cal/09+Sing/16) had high $PRNT_{80}$ titers between 11.96 - 12.32 against the homologously matched Cal/09 virus (Fig 5.6D). Mice that were vaccinated with mixtures that contained the Bris/07 H1 rHA (Bris/07+Switz/13 and Bris/07+Sing/16) prevented ~25% of the cells from being infected Cal/09 virus infections at the lowest serum dilution, similar to the mock

vaccinated pre-immune animals (Fig 5.6D). Mice that were vaccinated with mixtures containing the Cal/09 rHA (Cal/09+Switz/13 and Cal/09+Sing/16) also produced high $PRNT_{80}$ titers that ranged between 11.35 - 11.73 against the Bris/18 virus, which were slightly lower than the values generated against the Cal/09 virus (Fig 5.6E). Mice vaccinated with mixtures containing the COBRA Y2 rHA antigen (Y2+TJ5, Y2+J4, and Y2+NG2) all had antibodies with similar neutralizing capabilities against the Bris/18 virus, with $PRNT_{80}$ titers that ranged between 11.75 - 12.13, which were slightly higher than the titers produced by Cal/09 vaccine mixtures (Fig 5.6E). Animals vaccinated with mixtures that contained the Bris/07 rHA prevented ~20% of the cells from being infected with Bris/18 virus infections at the lowest serum dilution, similar to the mock vaccinated pre-immune animals (Fig 5.6E). Mice vaccinated with bivalent formulations containing the Cal/09 rHA (Cal/09+Switz/13 and Cal/09+Sing/16) produced $PRNT_{50}$ titers of 6.59 - 6.78 respectively against the Guang/19 virus (Fig 5.6F). In contrast, pre-immune animals vaccinated with mixtures containing the COBRA Y2 H1 rHA antigen (Y2+TJ5, Y2+J4, and Y2+NG2) all had antibodies with similar neutralizing capabilities against the Guang/19 virus, with $PRNT_{50}$ titers ~4-fold higher than those elicited in the Cal/09 rHA vaccinated animals with Log2 titers between 8.34 - 8.44 respectively (Fig 5.6F). Mice vaccinated with mixtures that contained the Bris/07 rHA prevented ~10% of the cells from being infected with Guang/19 virus at the lowest serum dilution, similar to the mock vaccinated pre-immune animals (Fig 5.6E).

COBRA Vaccines Enhance Neutralizing Antibody Responses Against Recently Circulating H3N2 Viruses

Serum samples collected from mice 72 days after pre-immunization were also assessed for antibodies with the ability to neutralize live virus infections against a panel of 3 historical influenza

A(H3N2) vaccine strain isolates from 2016-2019 (Fig 5.7). Pre-immune mice vaccinated with the monovalent formulation of the COBRA TJ5, J4, or NG2 rHAs had antibodies with high $PRNT_{80}$ titers against the Sing/16 virus, that ranged between 10.92 - 11.76 (Fig 5.7A). These titers were similar to those generated by the monovalent Sing/16 rHA vaccinated group, which had an average $PRNT_{80}$ titer of 12.46 against the homologously matched Sing/16 virus (Fig 5.7A). The mice vaccinated with the Switz/13 rHA had ~6-fold lower neutralization titers than the other H3 rHA vaccine antigens, but still produced an average $PRNT_{80}$ titer of 7.47 against the Sing/16 virus (Fig 5.7A). Mice that received monovalent H1 rHA vaccines, Y2, Bris/07, or Cal/09 had antibodies that neutralized ~10% of Sing/16 virus infections, similar to that of the pre-immune mice that received mock vaccinations (Fig 5.7A). The influenza naïve mock vaccinated mice did not have antibodies that could neutralize Sing/16 infections at any dilution (Fig 5.7A). Mice vaccinated with the monovalent COBRA TJ5, J4, or NG2 H3 rHAs generated antibodies with $PRNT_{50}$ titers against the Kan/17 virus that ranged between 7.56 - 7.82 (Fig 5.7B). Mice vaccinated with Switz/13 rHA had the highest neutralizing antibodies against Kan/17 with a $PRNT_{50}$ titer of 8.71 (Fig 5.7B). The Sing/16 rHA vaccinated mice had an average $PRNT_{50}$ titer of 6.34, which was ~2-fold lower than those vaccinated with the COBRA H3 rHAs and ~4-fold lower than Switz/13 rHA vaccinated animals (Fig 5.7B). The animals that received H1 rHA or mock vaccines had antibodies that neutralized ~10% of the Kan/17 infections and influenza naïve animals that were mock vaccinated were unable to neutralize the Kan/17 virus (Fig 5.7B). Pre-immune mice that were vaccinated with either J4 or NG2 rHA had $PRNT_{50}$ titers that ranged between 9.64 - 9.89 against the HK/19 virus, which was the highest neutralizing antibody response against this H3N2 strain (Fig 5.7C). Mice vaccinated with TJ5 and Sing/16 had similar $PRNT_{50}$ titers that ranged between 7.55 - 7.8 against the HK/19 virus, but their titers were ~4-fold lower than the neutralizing antibody

titers generated by J4 and NG2 (Fig 5.7C). The mice vaccinated with Switz/13 rHA had a slightly lower average $PRNT_{50}$ titer of 7.12, which was lower than any other group of H3 rHA vaccinated animals (Fig 5.7C). Groups that received H1 rHA or mock vaccines generated antibodies that neutralized ~15% of the HK/19 infections (Fig 5.7C). Influenza naïve animals that were mock vaccinated were unable to neutralize the HK/19 virus at any serum dilution (Fig 5.7C).

Pre-immune mice vaccinated with bivalent, H1+H3, rHA formulations containing any of the H3 COBRA antigens (Y2+TJ5, Y2+J4, and Y2+NG2) had antibodies with similar neutralizing capabilities against the Sing/16 virus, with average $PRNT_{50}$ titers that ranged between 12.34 - 12.48 (Fig 5.7D). These neutralizing antibody titers were similar, albeit slightly lower, than those elicited by the homologously matched rHA vaccine, Sing/16, in which both bivalent formulations Bris/07+Sing/16 and Cal/09+Sing16, produced $PRNT_{50}$ titers of 12.75 and 12.99 respectively (Fig 5.7D). This is in contrast to mice vaccinated with bivalent combinations containing the Switz/13 rHA, Bris/07+Switz/13 and Cal/09+Switz/13, which had ~10-fold lower $PRNT_{50}$ titers of 7.49 and 7.74 respectively against the Sing/16 virus (Fig 5.7D). However, mice vaccinated with bivalent vaccines containing the Switz/13 rHA, Bris/07+Switz/13 and Cal/09+Switz/13, generated the highest neutralizing antibody titers against the Kan/17 virus, with average $PRNT_{50}$ titers that ranged between 7.93 – 8.0 (Fig 5.7E). Mice vaccinated with bivalent protein formulations containing the Sing/16 H3 rHA, Bris/07+Sing/16 and Cal/09+Sing16, had the lowest average neutralizing antibody titers of any bivalent vaccinations against the Kan/17 virus with $PRNT_{50}$ titers ranging between 5.21 - 5.45 (Fig 5.7E). Animals vaccinated with rHA formulations containing the H3 COBRA antigens (Y2+TJ5, Y2+J4, and Y2+NG2) all had antibodies with average $PRNT_{50}$ titers between 6.92 - 7.51 against the Kan/17 virus (Fig 5.7E). Mice vaccinated with either Y2+J4 or Y2+NG2 generated the highest neutralizing antibody response against the

HK/19 virus, with $PRNT_{50}$ titers of 8.41 and 8.52 respectively (Fig 5.7F). Pre-immune animals vaccinated with Y2+TJ5 or either of the vaccines containing the Sing/16 rHA, Bris/07+Sing/16 and Cal/09+Sing16, produced similar neutralizing antibody responses against the HK/19 virus, but these titers were ~4-fold lower than those generated by either Y2+J4 or Y2+NG2 (Fig 5.7F). Mice vaccinated with the Switz/13 rHA (Bris/07+Switz/13 and Cal/09+Switz/13) had the lowest neutralizing antibody titers against the HK/19 virus with identical $PRNT_{50}$ titers of 5.64 (Fig 5.7F).

H3 COBRA rHA Vaccines Provide Protection against H3N2 Viral Challenge and Prevent Viral Replication in the Lung

On day 86, the pre-immune mice were challenged with the influenza A(H3N2) vaccine strain virus, A/Kansas/14/2017. Following challenge, the mice were monitored for weight loss for 14 consecutive days (Fig 5.8). The influenza naïve mock vaccinated animals lost more weight than any other group; peaking at 10% body weight loss at day 2 post infection (Fig 5.8A). This trend was also observed in all of the other vaccine groups; where weight loss peaked at day 2 post infection, but then began to steadily rise until day 7 post infection, after which the weight gain plateaued (Fig 5.8A-B). Overall, this H3N2 influenza viral challenge was relatively mild and none of the mice succumbed to the disease over the course of the 14 days, and no significant differences in weight loss were observed between the different vaccine groups.

Lungs were collected from 3 mice/group on day 3 post-infection in order to quantify the amount of virus replicating in the respiratory tissue of these animals following H3N2 challenge (Fig 5.9). The influenza naïve mock vaccinated animals had the most virus present in their lungs (~$1x10^4$ PFU/g of lung tissue). This was significantly higher than pre-immune animals vaccinated with either monovalent COBRA J4 or NG2 rHA, as well as the bivalent formulations of Y2+J4 or

Y2+NG2 rHA, in which there were no detectable virus present in the lung tissue at day 3 post-infection (Fig 5.9). In contrast, mice vaccinated with monovalent H1 rHAs, Y2, Bris/07, or Cal/09 had similar lung titers to those of the pre-immune animals that received mock vaccinations (~$1x10^3$ PFU/g of lung tissue) (Fig 5.9). Animals vaccinated with either monovalent or bivalent vaccines containing TJ5, Switz/13, or Sing/16 had similar levels of virus replicating in their lungs (~$1x10^1$ PFU/g of lung tissue) (Fig 5.9).

Discussion

Developing a broadly reactive vaccine that can offer protection against antigenically drifted H3N2 influenza strains is of great clinical importance, as these influenza viruses remain a major public health threat [98]. The COBRA HA design approach offers a solution to this problem as it utilizes sequence data from recent influenza seasons, obtained from influenza surveillance databases to generate broadly reactive vaccine candidates [111]. In this manuscript, WT H3N2 HA sequences from 2013-2019 were used to generate new H3 COBRA HA sequences and used to elicit antibodies with HAI titers against recently emerging antigenically drifted strains of influenza. Using WT H3N2 sequences isolated from 2016-2018, this process resulted in the generation of the NG2 HA COBRA sequence. The NG2 rHA was the only newly generated COBRA HA vaccine antigen to elicit sero-protective antibody titers against all of the strains in the H3N2 viral panel from 2012-2019, including the antigenically drifted HK/19 virus, in influenza naïve animals (Fig 5.2G). This response was superior to those generated by all of the WT rHA antigens used in this study, including the HA from the SA/19 virus, the Southern Hemisphere WHO vaccine selection in 2020, which circulated during the same year as HK/19, the Northern Hemisphere WHO vaccine selection for the 2020-2021 influenza season [128, 129] (Fig 5.2). The elicitation of broadly

reactive antibodies by NG2 HA is likely due to differences in antigenic site A of the HA protein, where NG2 and HK/19 share a 147T mutation, while SA/19 possesses a 147K at this position. Changes in residue 145 in antigenic site A influence HAI assays by modulating receptor binding avidity, so amino acid substitutions at neighboring site 147 may play a role in the observed differences in reactivity [100]. Differences in antigenic site D could also play a significant role, as NG2 and HK/19 share a 235S mutation, while SA/19 possesses a 235F at this position. All of the other amino acid differences in the antigenic sites between NG2 and HK/19 are shared between NG2 and SA/19, therefore they are not likely to contribute to the expanded breadth of reactivity by NG2 HA compared to SA/19 HA. H3N2 influenza viruses routinely acquire amino acid substitutions in all 5 HA antigenic sites and single point mutations in the HA protein can alter the immunogenicity of the antigenic sites [100]. Therefore, future site directed mutagenesis studies aimed towards these two positions, 147 and 235, can be explored to determine if one or both of these substitutions are necessary to induce seroconversion to the HK/19 influenza virus strain.

The lead COBRA H1 and H3 vaccine candidates, Y2, TJ5, J4, and NG2, were also evaluated in mice previously exposed to influenza A(H1N1) and A(H3N2) viruses. The impact of pre-immunity on influenza vaccination has been understudied, however this evaluation is critical, as most humans are infected with influenza viruses before the age of five [97, 109]. Therefore, the majority of the targeted vaccine population will already possess an immune history to one or both of these subtypes prior to vaccination [97]. In the pre-immune model, J4 had improved HAI reactive antibody breadth compared to other vaccine candidates in the influenza naïve model (Fig 5.4G). Pre-immune mice vaccinated with J4 had antibodies with HAI activity against Switz/13, Kan/17, Tx/17, and HK/19, which were not present in the influenza naïve J4 HA vaccinated mice. A similar expansion of breadth occurred in the pre-immune mice vaccinated with Sing/16, which

had antibodies with HAI activity against HK/19 in the pre-immune model that were not present in the influenza naïve mice (Fig 5.4E). Seasonal influenza vaccination in the context of pre-existing immunity is strongly biased by contributions from the immune memory compartment and primarily stimulates memory B cells leading to a transient surge in the number of antibody-secreting plasmablasts [98, 105]. Therefore, the observed expansion of HA reactive antibody breadth is likely the result of memory B cell responses that recognize shared epitopes between the rHA vaccine antigens and the HA protein of H3N2 priming strain, Pan/99, as broad HA group-level immune memory arises when lymphocytes target conserved HA epitopes [114]. Furthermore, pre-immune imprinting induces immune memory to both conserved and variable sites on different influenza virus antigens [102, 114]. Therefore, these shared HA epitopes between vaccine antigen and the priming strain may also be present on the H3N2 viruses in the historical HAI panel and upon vaccine induced immune recall, specific memory B cells are stimulated to produce HAI reactive antibodies that are not elicited by the vaccine in the absence of influenza pre-immunity. To help confirm this hypothesis, future studies will be aimed at deciphering the differences in antigen specific memory B cell responses that are elicited by COBRA and WT rHA vaccines between influenza naïve and pre-immune animal models.

Commercial vaccines are typically formulated as mixtures of H1N1, H3N2, and B influenza virus antigens, and are administered to adults possessing complex immune histories to multiple subtypes of influenza [100]. Using the pre-immune mouse model, bivalent mixtures of H1 and H3 COBRA and WT rHA proteins were evaluated for their ability to induce HAI reactive and neutralizing antibody breadth across panels of H1N1 and H3N2 viral isolates from 2007-2019. In this model, bivalent mixtures of COBRA Y2+J4 and Y2+NG2 rHAs were superior to any one mixture of H1 and H3 WT rHA vaccines at eliciting HAI reactive sero-protective antibody breadth

across H1 and H3 viruses isolated from 2009-2019 (Fig 5.5F, 5.5G). In comparison, mixtures of Cal/09+Sing/16 did not induce sero-conversion to the Guang/19 H1N1, Switz/13 H3N2, or Kan/17 H3N2 strains from the same time period (Fig 5.5D). The H1 rHA sequences of Cal/09 and Y2 differ by 4 amino acids in antigenic sites, Sa (E171K, K180Q), Ca1 (S220T), and Ca2 (G239D) respectively and Y2 shares its amino acid motifs in these positions with Guang/19. Point mutations in a single antigenic site can abolish the binding of most monoclonal antibodies that are specific to that site [100, 102, 121]. Therefore, it is likely that these specific epitopes are supporting the antibody cross-reactivity between Y2 and Guang/19, causing a decrease in the observed HAI reactivity between Cal/09 elicited antibodies and the Guang/19 virus. The H3N2 viruses Switz/13 and Kan/17 both belong to clade 3c3.a, while the other viruses in the H3N2 panel, including Sing/16, belong to clade 3c2 or its subclades 3c2.a and 3c2.a1 [122]. Viruses belonging to clade 3c2.and are antigenically distinct from 3c3.a H3N2 viruses [104, 120]. This antigenic distinction may be due to the HA protein of 3c2.a viruses, which possess a T160 mutation located in antigenic site B that results in the addition of an N-linked glycosylation motif, N X S/T, where X represents any amino acid other than P, at site 160 [104]. Viruses from clade 3c3.a possess a K160 mutation at this site and lack the glycosylation which may be covering up epitopes present on 3c2.a HA proteins necessary to generate neutralizing antibody responses against 3c.3a viruses [5, 113]. Similar to 3c3.a viruses the J4 COBRA HA possesses a K160 at this site, lacking this glycosylation motif, and is able to generate HAI reactive antibodies against the 3c3.a viruses in the pre-immune animal model (Fig 5.5F). However, this glycosylation may not fully explain the differences in observed HAI reactivity, as the NG2 COBRA HA possesses a T160 mutation, containing a glycosylation motif at site 160, but is able to induce sero-conversion against both Switz/13 and Kan/17 (Fig 5.5G). Consequently, the differences in reactivity may be also driven by another

mutation in site B at position 175, where the Switz/13, Kan/17, J4, and NG2 HA proteins all possess an N175, but Sing/16 possesses K175. From 1968 to 2003, the major antigenic changes in H3N2 viruses have occurred as a result of single amino acid substitutions in antigenic site B [120]. Therefore, it is likely that the differences in the amino acids at these positions in antigenic site B are driving the observed differences in antibody reactivity. Future studies will focus on performing site directed mutagenesis at these sites, 160 and 175, to determine if certain amino acid substitutions in these positions can cause antibodies generated by the Sing/16 rHA, a 3c2.a virus, to cross-react with 3c3.a viruses in the HAI assay.

The bivalent COBRA rHA vaccine mixtures of Y2+J4 and Y2+NG2 also elicited higher broadly neutralizing antibody titers across panels of H1N1 and H3N2 viruses from 2009-2019 than any one WT bivalent rHA vaccine mixture (Fig 5.6, 5.7). However, in both the HAI and FRA, the antibody titers generated by the bivalent mixtures were lower for both COBRA and WT rHA vaccine antigens when compared to those generated by the monovalent rHA formulations. This reduction in HAI reactive antibody titers between monovalent and bivalent antigen formulations was larger against the H1N1 panel, ~3.9-fold, than the ~2.6-fold drop observed against the H3N2 panel. In the FRA, the $PRNT_{50}$ antibody titers also declined for the bivalent antigen mixtures compared to those generated by monovalent vaccines, and this decrease was also larger for the H1N1 neutralizing antibody titers, ~3.36-fold, compared to the H3N2 neutralizing antibody titers which fell ~1.86-fold. These observations are not unexpected, as polyvalent influenza vaccines in humans tend to have decreased effectiveness compared to monovalent formulations against homologously matched influenza infections [130, 131]. In this study, there was also an observed difference in the magnitude of the HAI reactive antibody responses generated by the individual H1 and H3 rHA components of the bivalent vaccines against the H1N1 and H3N2 virus panels

respectively, and this appeared to be more pronounced for the H3 reactive antibodies, which were on average ~2-fold lower in magnitude than those generated by the H1 component, despite both antigens being administered in equal concentrations. This observation may indicate some level of immunodominance of the H1 rHA vaccine antigens over the H3 rHA antigens. Studies investigating the human immune response to seasonal influenza vaccination also revealed that antibody responses to H3N2 were reduced in magnitude when compared to the other vaccine components [132, 133]. Polyvalency can alter antigen immunogenicity due to a multitude of factors, such as competition between vaccine antigens that can create an immunogenic hierarchy, or cross-reactive epitopes that may also be present between previously encountered antigens and those present in the vaccine that preferentially drive differential immune responses [132-135]. This immunodominance phenomenon has also been observed in other polyvalent vaccines, such as those for human papillomavirus, *Streptococcus pnuemoniae*, and dengue fever virus [136]. However, the impact of heterosubtypic immunodominance between influenza virus vaccine strains has not been extensively studied, but increasing the dose of the least immunogenic HA subtype could help overcome the limitations observed in immune responses generated in polyvalent vaccine formulations [132, 133]. Therefore, future multivalent COBRA vaccine studies will focus on determining the proper dose to mix the COBRA H1 and H3 antigens to optimize the host immune response to both components following vaccination.

There are some limitations to the pre-immune animal model presented in this study. First, this model establishes pre-immunity with one mixed infection of both H1N1 and H3N2, that is followed by no other exposures to influenza prior to rHA vaccination. The effects of priming individuals simultaneously with H1N1 and H3N2 through infection or vaccination remain unknown and this model does not accurately depict the immune histories of most adult humans

who are generally exposed to one subtype of influenza at a time, and throughout their lives encounter other subtypes of influenza virus, such as influenza B [102, 106, 118, 124]. Most individuals will also likely receive seasonal influenza virus vaccines over the course of their lives, which makes their immune histories even more complex [101, 109]. The immune responses generated by influenza virus infections are generally broader and more persistent than those elicited through vaccination, as live virus infections typically stimulate antibody and T-cell mediated immunity [103, 108, 109, 137]. The experimental timeline of 30 days between infection and vaccination in our model was also much shorter than the typical human exposure timeline of months to years [103]. However, no animal models currently exist that quantitatively reproduce the responses of different human populations to vaccination, but useful qualitative information may be gained from certain animal studies [138]. Therefore, the use of animal models in which the subjects are exposed to more influenza virus antigens, such as infection followed by vaccinations from different eras, will be the focus of future studies in order to better recapitulate the immune responses of older individuals to broadly reactive vaccine candidates. Furthermore, this model only evaluated the performance of influenza A bivalent vaccines containing H1 and H3 rHA antigens. The majority of commercial vaccines in the United States are either trivalent or quadrivalent mixtures that include multiple influenza A and B antigens [5, 100]. Future studies will focus on the addition of COBRA influenza B rHA proteins, as well as COBRA rNA proteins, to the mixture of H1 and H3 rHA antigens to vaccinate both influenza naïve and pre-immune animals. Lastly, the age, gender, and immune status of the mice used in this study may also be a confounding factor, as all of the mice were 6–8 week old females, representing healthy young adult animals [124]. However, young and elderly individuals rely differently on their immunological memory compartments to generate specific immune responses following

vaccination [99, 102]. This study also did not include any obese, diabetic, elderly, or other high-risk groups which all respond differentially to infection and vaccination [73, 105]. Future studies will focus on evaluating broadly reactive COBRA rHA vaccine candidates in different genders as well as various high-risk animal models. These are important models to study, as ideal universal influenza vaccine candidates should produce broadly reactive antibodies in all populations, regardless of gender or their particular immune status [101].

Balb/c	Bleed/Vax	Bleed	Vax	Bleed	Vax	Bleed
Group	Day 0	Day 14	Day 28	Day 42	Day 56	Day 70
1	TJ5		TJ5		TJ5	
2	J1		J1		J1	
3	J2		J2		J2	
4	J3		J3		J3	
5	J4		J4		J4	
6	NG1		NG1		NG1	
7	NG2		NG2		NG2	
8	NG3		NG3		NG3	
9	Switz/13		Switz/13		Switz/13	
10	HK/14		HK/14		HK/14	
11	Sing/16		Sing/16		Sing/16	
12	Kan/17		Kan/17		Kan/17	
13	Switz/17		Switz/17		Switz/17	
14	SA/19		SA/19		SA/19	
15	Mock		Mock		Mock	

Figure 5.1. Influenza Naïve Mouse Experimental Group Outline. Groups (N=5) of influenza naïve Balb/c mice were vaccinated in a prime-boost-boost regimen with 3ug of either H3 COBRA rHA (TJ5, J1, J2, J3, J4, NG1, NG2, or NG3), WT H3 rHA (Switz/13, HK/14, Sing/16, Kan/17, Switz/17, SA/19), or mock (PBS) vaccines on day 0, 28, and 56. Blood was collected from each group on day 0, 14, 42, and 70 for serological analysis.

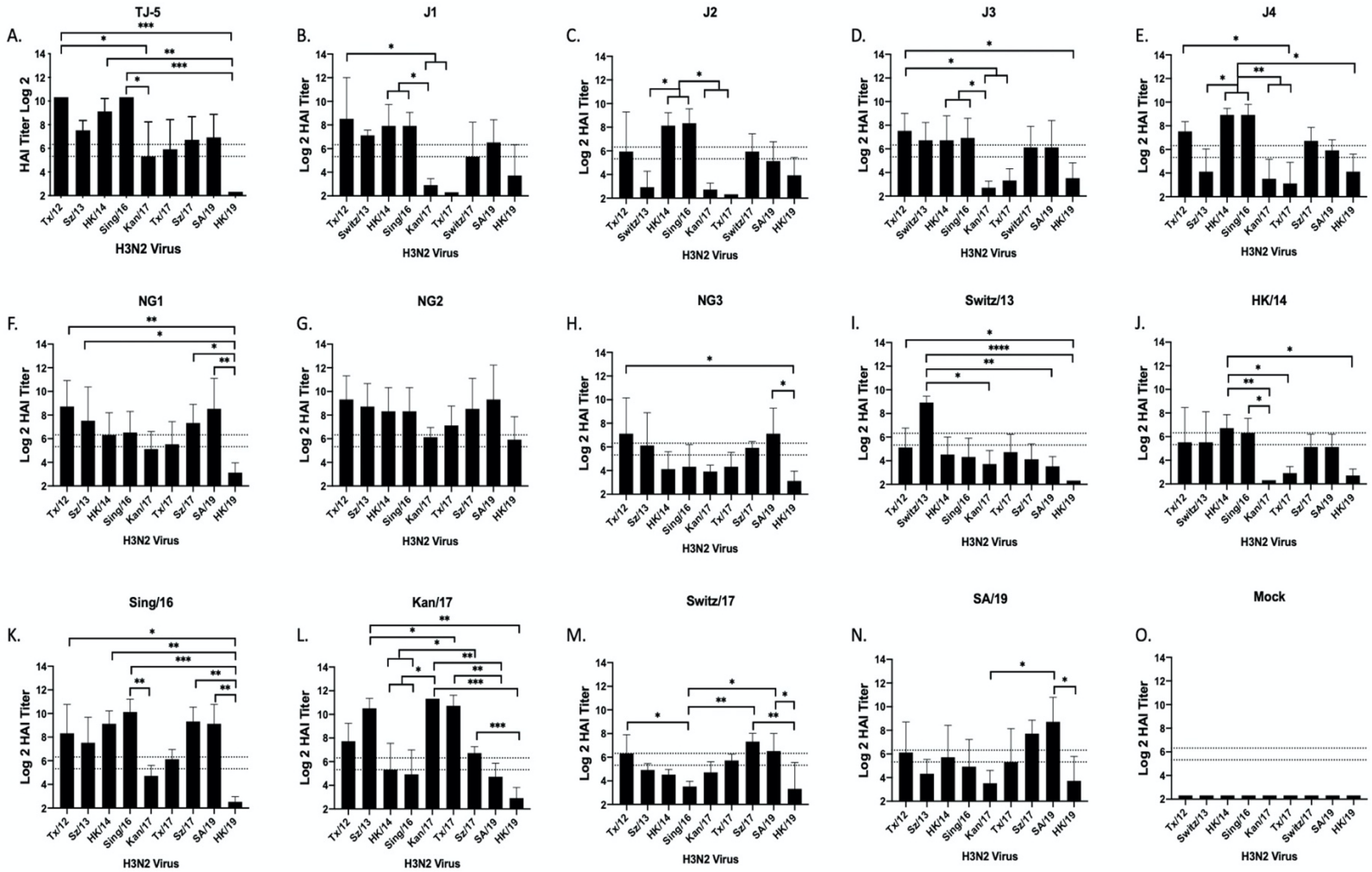
A.
TJ-5
HAI Titer Log 2
H3N2 Virus
B.
J1
Log 2 HAI Titer
H3N2 Virus
C.
J2
Log 2 HAI Titer
H3N2 Virus
D.
J3
Log 2 HAI Titer
H3N2 Virus
E.
J4
Log 2 HAI Titer
H3N2 Virus
F.
NG1
Log 2 HAI Titer
H3N2 Virus
G.
NG2
Log 2 HAI Titer
H3N2 Virus
H.
NG3
Log 2 HAI Titer
H3N2 Virus
I.
Switz/13
Log 2 HAI Titer
H3N2 Virus
J.
HK/14
Log 2 HAI Titer
H3N2 Virus
K.
Sing/16
Log 2 HAI Titer
H3N2 Virus
L.
Kan/17
Log 2 HAI Titer
H3N2 Virus
M.
Switz/17
Log 2 HAI Titer
H3N2 Virus
N.
SA/19
Log 2 HAI Titer
H3N2 Virus
O.
Mock
Log 2 HAI Titer
H3N2 Virus

Figure 5.2. Influenza Naïve Mice: Day 70 HAI H3N2 2012-2019 Historical Vaccine Strain Panel. Serum collected from 75 influenza naïve Balb/c mice (n=5/group) on day 70 post initial vaccination were assessed for HAI activity against a panel of historical H3N2 vaccine strains isolated during 2012-2019 (X-axis). Log2 HAI titers are reported as absolute mean values ± SEM (Y-axis). The lower dotted line represents an HAI titer of 1:40 and the upper dotted line represents an HAI titer of 1:80. Mice were vaccinated with 3ug rHA: TJ5 (A), J1 (B), J2 (C), J3 (D), J4 (E), NG1 (F), NG2 (G), NG3 (H), Switz/13 (I), HK/14 (J), Sing/16 (K), Kan/17 (L), Switz/17 (M), SA/19 (N), mock (O). HAI titers were statistically analyzed using nonparametric one-way ANOVA by GraphPad Prism 9 software (GraphPad, San Diego, CA, USA). A p value of less than 0.05 was defined as statistically significant (*, $p < 0.05$; **, $p < 0.01$; ***, $p < 0.001$; ****, $p < 0.0001$).

DBA/2J	Pre-immunity	Bleed/Vaccinate	Bleed	Vax	Bleed	Challenge	Harvest Lungs	Terminate
Group	Day 0	Day 30	Day 44	Day 58	Day 72	Day 86	Day 89	Day 100
1	Pan/99, Sing/86	Y2 (H1)		Y2 (H1)		A/Kansas/14/2017 H3N2	N=3	N=5
2	Pan/99, Sing/86	TJ5 (H3)		TJ5 (H3)		A/Kansas/14/2017 H3N2	N=3	N=5
3	Pan/99, Sing/86	J4 (H3)		J4 (H3)		A/Kansas/14/2017 H3N2	N=3	N=5
4	Pan/99, Sing/86	NG2 (H3)		NG2 (H3)		A/Kansas/14/2017 H3N2	N=3	N=5
5	Pan/99, Sing/86	Y2, TJ5 (H1+H3)		Y2, TJ5 (H1+H3)		A/Kansas/14/2017 H3N2	N=3	N=5
6	Pan/99, Sing/86	Y2, J4 (H1+H3)		Y2, J4 (H1+H3)		A/Kansas/14/2017 H3N2	N=3	N=5
7	Pan/99, Sing/86	Y2, NG2 (H1+H3)		Y2, NG2 (H1+H3)		A/Kansas/14/2017 H3N2	N=3	N=5
8	Pan/99, Sing/86	Bris/07 (H1)		Bris/07 (H1)		A/Kansas/14/2017 H3N2	N=3	N=5
9	Pan/99, Sing/86	Cal/09 (H1)		Cal/09 (H1)		A/Kansas/14/2017 H3N2	N=3	N=5
10	Pan/99, Sing/86	Switz/13 (H3)		Switz/13 (H3)		A/Kansas/14/2017 H3N2	N=3	N=5
11	Pan/99, Sing/86	Sing/16 (H3)		Sing/16 (H3)		A/Kansas/14/2017 H3N2	N=3	N=5
12	Pan/99, Sing/86	Bris/07 + Switz/13 (H1+H3)		Bris/07 + Switz/13 (H1+H3)		A/Kansas/14/2017 H3N2	N=3	N=5
13	Pan/99, Sing/86	Bris/07 + Sing/16 (H1+H3)		Bris/07 + Sing/16 (H1+H3)		A/Kansas/14/2017 H3N2	N=3	N=5
14	Pan/99, Sing/86	Cal/09 + Switz/13 (H1+H3)		Cal/09 + Switz/13 (H1+H3)		A/Kansas/14/2017 H3N2	N=3	N=5
15	Pan/99, Sing/86	Cal/09 + Sing/16 (H1+H3)		Cal/09 + Sing/16 (H1+H3)		A/Kansas/14/2017 H3N2	N=3	N=5
16	Pan/99, Sing/86	Mock		Mock		A/Kansas/14/2017 H3N2	N=3	N=5
17	Mock	Mock		Mock		A/Kansas/14/2017 H3N2	N=3	N=5

Figure 5.3. H1+H3 Pre-immune Mouse Experimental Group Outline. On day 0, 136 influenza naïve DBA/2J mice (n=8/group) were infected with mixtures of H1N1 (A/Singapore/6/1986) and H3N2 (A/Panama/2007/1999) influenza virus at a concentration of $5x10^5$ PFU/50uL in PBS, by administering 50uL to each mouse intranasally. Mock pre-immune animals were inoculated intranasally with 50uL of PBS. On day 30 and 58, the mice were vaccinated with 3ug total of either monovalent formulations of COBRA rHA: Y2 (H1), TJ5 (H3), J4 (H3), or NG2 (H3); WT rHA: Bris/07 (H1), Cal/09 (H1), Switz/13 (H3), or Sing/16 (H3); or 3ug total of COBRA rHA cocktails: Y2 + TJ5, Y2 + J4, or Y2 + NG2; or 3ug total of WT rHA cocktails: Bris/07 + Switz/13, Bris/07 + Sing/16, Cal/09 + Switz/13, Cal/09 + Sing/16; or mock vaccines (PBS). Blood was collected from each group on day 0, 30, 44, and 72 for serological analysis. On day 86, the mice were challenged intranasally with $6.7x10^6$ PFU/50uL of A/Kansas/14/2017 (H3N2). Following challenge mice were monitored for weight loss for 14 consecutive days. On day 89 lungs were harvested from n=3 mice per group. On day 100 all animals were humanely euthanized.

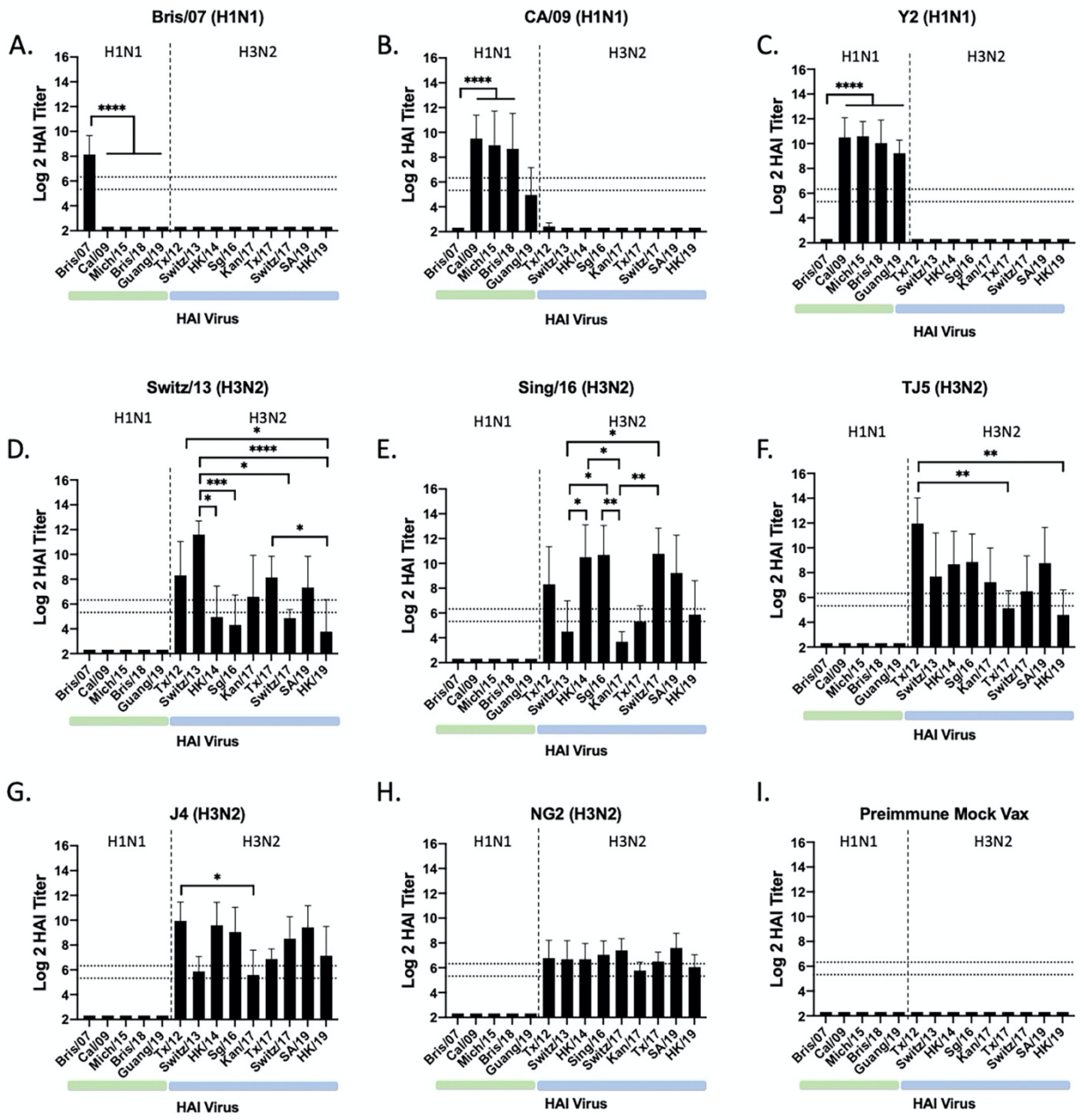

Figure 5.4. Pre-immune Mice Day 72 HAI titers: Monovalent Vaccine Groups. Serum collected from 72 H1+H3 pre-immune DBA/2J mice (n=8/group) that were vaccinated with monovalent formulations of COBRA or WT rHA, on day 72 post initial infection were assessed for HAI activity against a panel of historical H1N1 vaccine strains from 2007-2019 (green bar) and H3N2 vaccine strains from 2012-2019 (blue bar) (separated by vertical dotted line) (X-axis). Log2 HAI

titers are reported as absolute mean values ± SEM (Y-axis). The lower dotted line represents an HAI titer of 1:40 and the upper dotted line represents an HAI titer of 1:80. Mice were vaccinated with 3ug rHA: Bris/07 (A), Cal/09 (B), Y2 (C), Switz/13 (D), Sing/16 (E), TJ5 (F), J4 (G), NG2 (H), mock (I). The green bar below the Y-axis denotes H1N1 viruses, and the blue bar denotes H3N2 viruses. HAI titers were statistically analyzed using nonparametric one-way ANOVA by GraphPad Prism 9 software (GraphPad, San Diego, CA, USA). A p value of less than 0.05 was defined as statistically significant (*, $p < 0.05$; **, $p < 0.01$; ***, $p < 0.001$; ****, $p < 0.0001$).

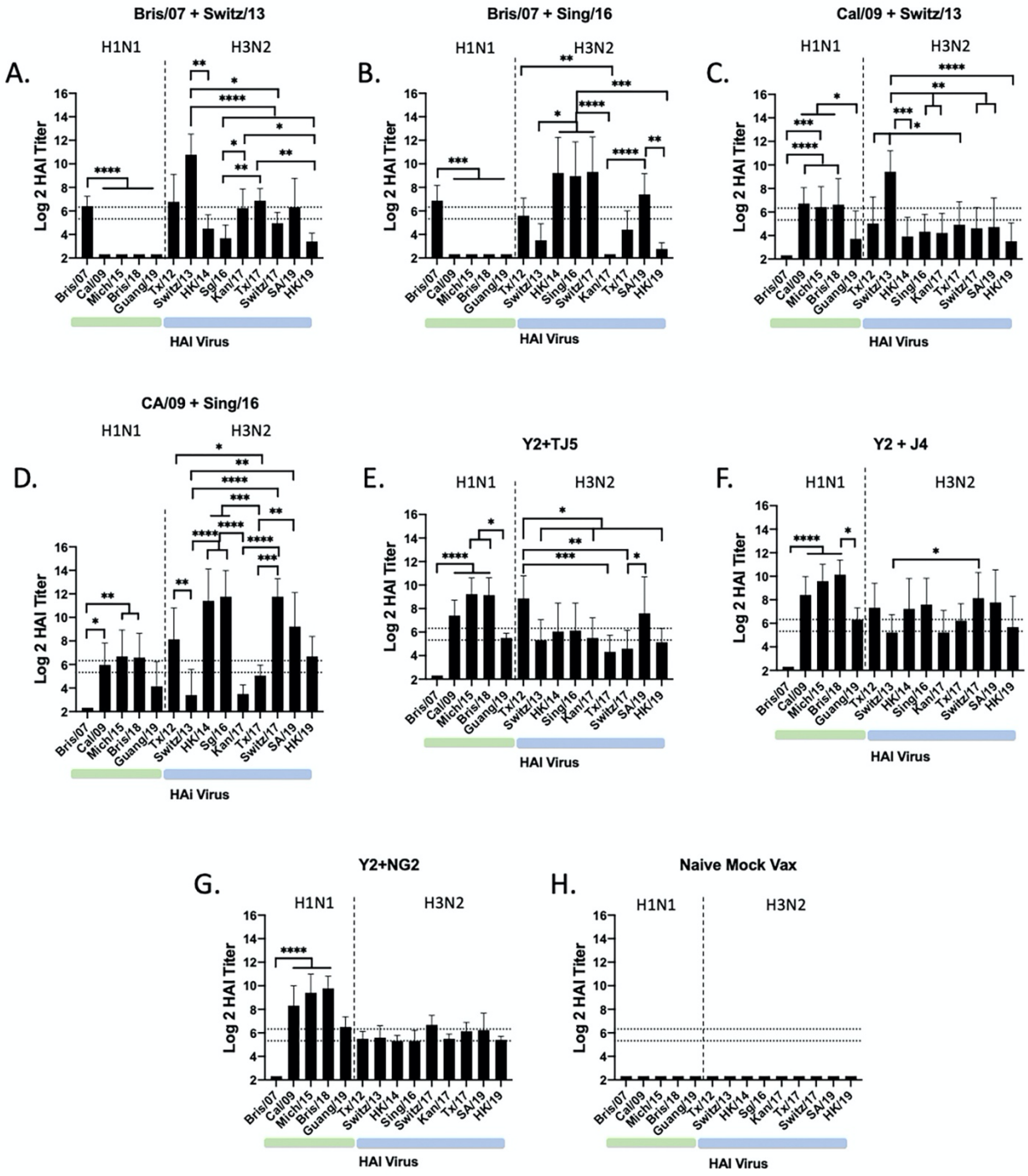

Figure 5.5. Pre-immune Mice Day 72 HAI titers: Bivalent Cocktail Vaccine Groups. Serum collected from 64 H1+H3 pre-immune DBA/2J mice (n=8/group) that were vaccinated with bivalent cocktail formulations of H1+H3 COBRA or WT rHA, on day 72 post initial infection

were assessed for HAI activity against a panel of historical H1N1 vaccine strains from 2007-2019 (green bar) and H3N2 vaccine strains from 2012-2019 (blue bar) (separated by vertical dotted line) (X-axis). Log2 HAI titers are reported as absolute mean values ± SEM (Y-axis). The lower dotted line represents an HAI titer of 1:40 and the upper dotted line represents an HAI titer of 1:80. Mice were vaccinated with 3ug total rHA: Bris/07+Switz/13 (A), Bris/07+Sing/16 (B), Cal/09+Switz/13 (C), Cal/09+Sing/16 (D), Y2+TJ5 (E), Y2+J4 (F), Y2+NG2 (G), Mock (H). The green bar below the Y-axis denotes H1N1 viruses, and the blue bar denotes H3N2 viruses. HAI titers were statistically analyzed using nonparametric one-way ANOVA by GraphPad Prism 9 software (GraphPad, San Diego, CA, USA). A p value of less than 0.05 was defined as statistically significant (*, $p < 0.05$; **, $p < 0.01$; ***, $p < 0.001$; ****, $p < 0.0001$).

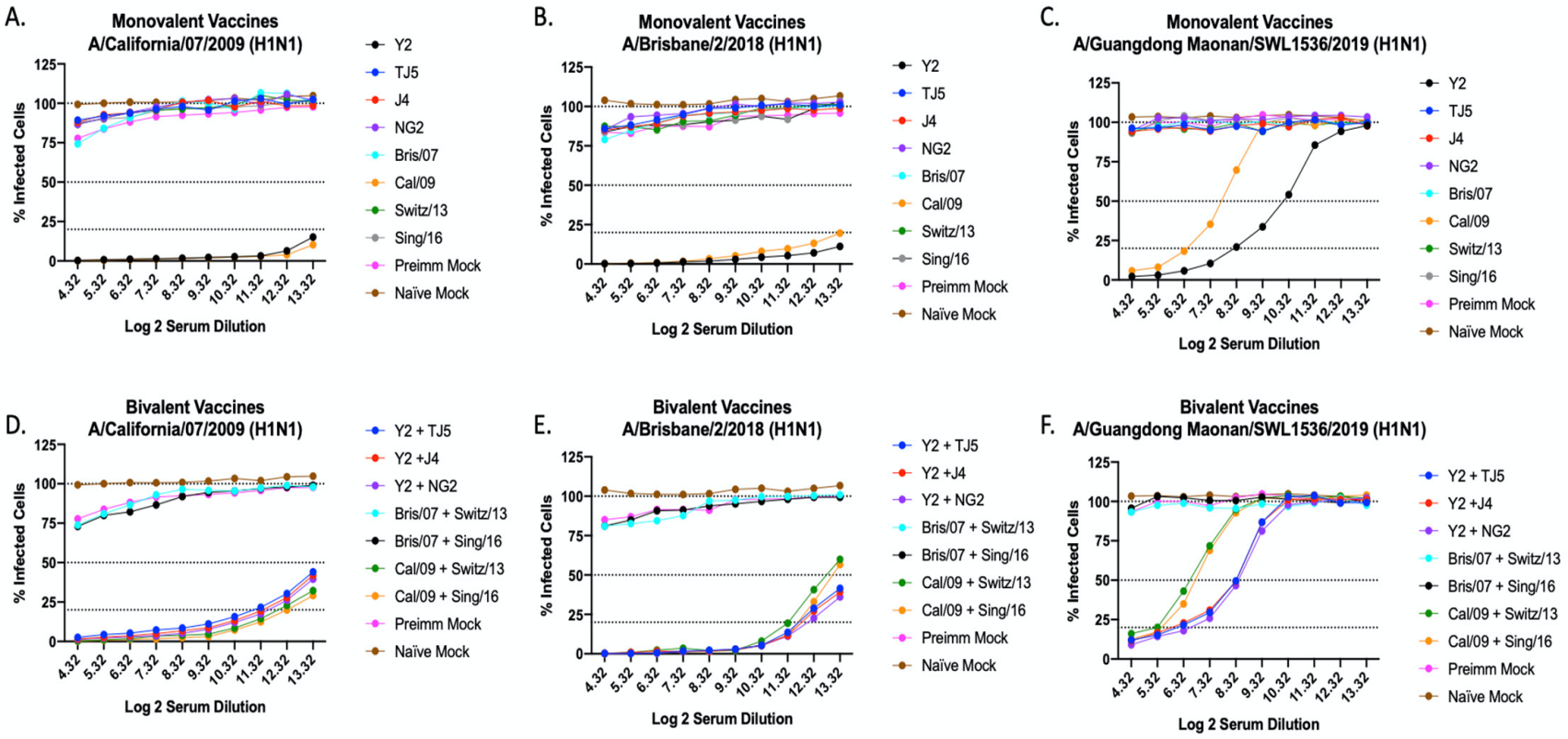
A.
Monovalent Vaccines
A/California/07/2009 (H1N1)
B.
Monovalent Vaccines
A/Brisbane/2/2018 (H1N1)
C.
Monovalent Vaccines
A/Guangdong Maonan/SWL1536/2019 (H1N1)
D.
Bivalent Vaccines
A/California/07/2009 (H1N1)
E.
Bivalent Vaccines
A/Brisbane/2/2018 (H1N1)
F.
Bivalent Vaccines
A/Guangdong Maonan/SWL1536/2019 (H1N1)
% Infected Cells
Log 2 Serum Dilution
4.32
5.32
6.32
7.32
8.32
9.32
10.32
11.32
12.32
13.32
Y2
TJ5
J4
NG2
Bris/07
Cal/09
Switz/13
Sing/16
Preimm Mock
Naïve Mock
Y2 + TJ5
Y2 +J4
Y2 + NG2
Bris/07 + Switz/13
Bris/07 + Sing/16
Cal/09 + Switz/13
Cal/09 + Sing/16

Figure 5.6. Pre-immune Mice Day 72 FRA titers: H1N1 Virus Panel. Serum collected from 136 H1+H3 pre-immune DBA/2J mice (n=8/group) that were vaccinated with monovalent and bivalent formulations of H1+H3 COBRA or WT rHA, on day 72 post initial infection were pooled and assessed for FRA neutralization against a panel of historical H1N1 vaccine strains from 2009-2019. Sera from mice vaccinated with monovalent antigens were tested against H1N1 viruses: A/California/07/2009 (A), A/Brisbane/2/2018 (B), A/Guangdong Maonan/SWL1536/2109 (C). Sera from mice vaccinated with cocktails of bivalent H1+H3 antigens were tested against H1N1 viruses: A/California/07/2009 (D), A/Brisbane/2/2018 (E), A/Guangdong Maonan/SWL1536/2019 (F). The lower dotted line represents an 80% neutralization ($Neut_{80}$), middle dotted line represents a 50% neutralization ($Neut_{50}$), and the upper dotted line represents no neutralization of viral infection.

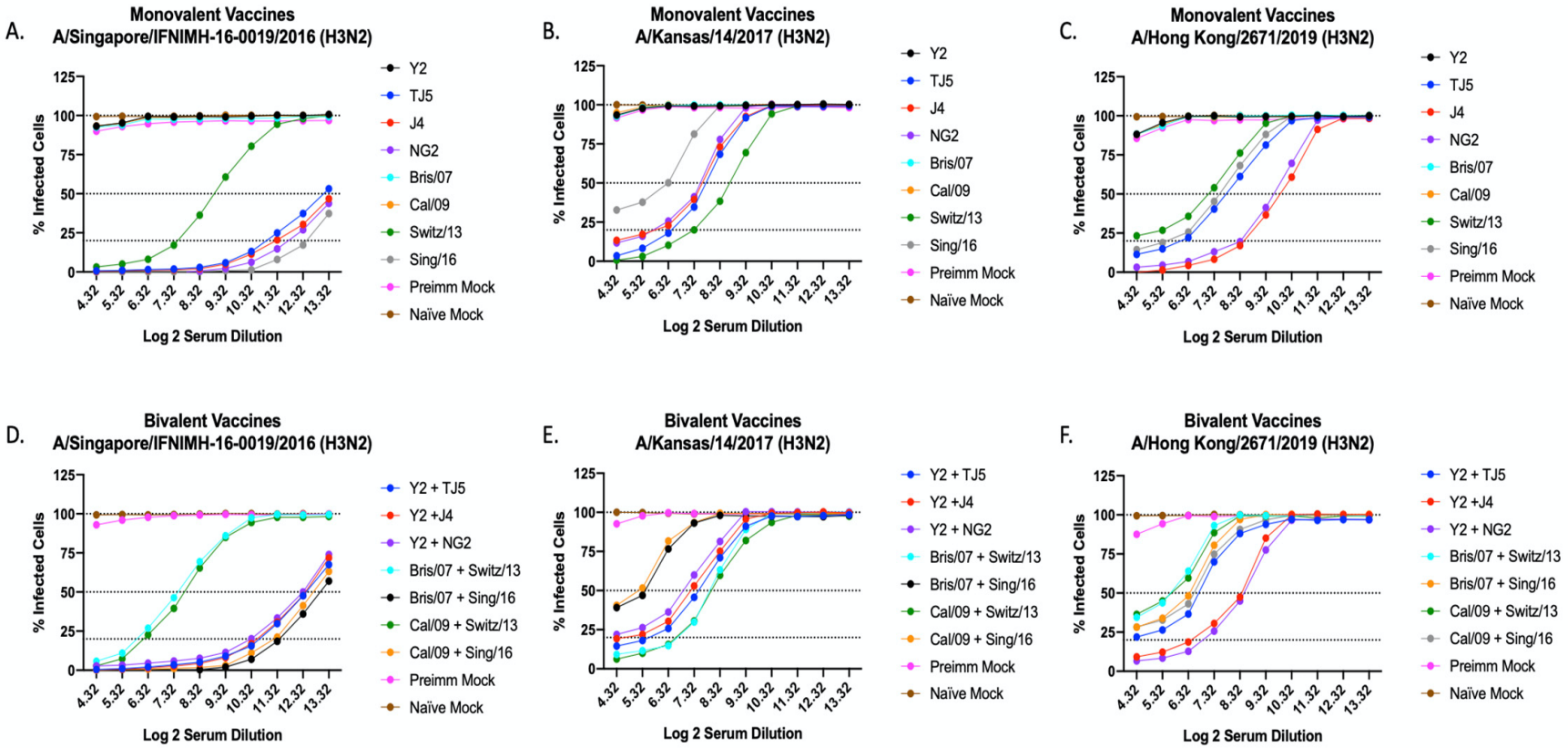
A.
Monovalent Vaccines
A/Singapore/IFNIMH-16-0019/2016 (H3N2)
B.
Monovalent Vaccines
A/Kansas/14/2017 (H3N2)
C.
Monovalent Vaccines
A/Hong Kong/2671/2019 (H3N2)
D.
Bivalent Vaccines
A/Singapore/IFNIMH-16-0019/2016 (H3N2)
E.
Bivalent Vaccines
A/Kansas/14/2017 (H3N2)
F.
Bivalent Vaccines
A/Hong Kong/2671/2019 (H3N2)
% Infected Cells
Log 2 Serum Dilution
4.32
5.32
6.32
7.32
8.32
9.32
10.32
11.32
12.32
13.32
Y2
TJ5
J4
NG2
Bris/07
Cal/09
Switz/13
Sing/16
Preimm Mock
Naïve Mock
Y2 + TJ5
Y2 +J4
Y2 + NG2
Bris/07 + Switz/13
Bris/07 + Sing/16
Cal/09 + Switz/13
Cal/09 + Sing/16

Figure 7.7. Pre-immune Mice Day 72 FRA Titers: H3N2 Virus Panel. Serum collected from 136 H1+H3 pre-immune DBA/2J mice (n=8/group) that were vaccinated with monovalent and bivalent formulations of H1+H3 COBRA or WT rHA, on day 72 post initial infection were pooled and assessed for FRA neutralization against a panel of historical H3N2 vaccine strains from 2016-2019. Sera from mice vaccinated with monovalent antigens were tested against H1N1 viruses: A/Singapore/IFNIMH-16-0019/2016 (A), A/Kansas/14/2017 (B), A/Hong Kong/2671/2019 (C). Sera from mice vaccinated with cocktails of bivalent H1+H3 antigens were tested against H1N1 viruses: A/Singapore/IFNIMH-16-0019/2016 (D), A/Kansas/14/2107 (E), A/Hong Kong/2671/2019 (F). The lower dotted line represents an 80% neutralization ($Neut_{80}$), middle dotted line represents a 50% neutralization ($Neut_{50}$), and the upper dotted line represents no neutralization of viral infection.

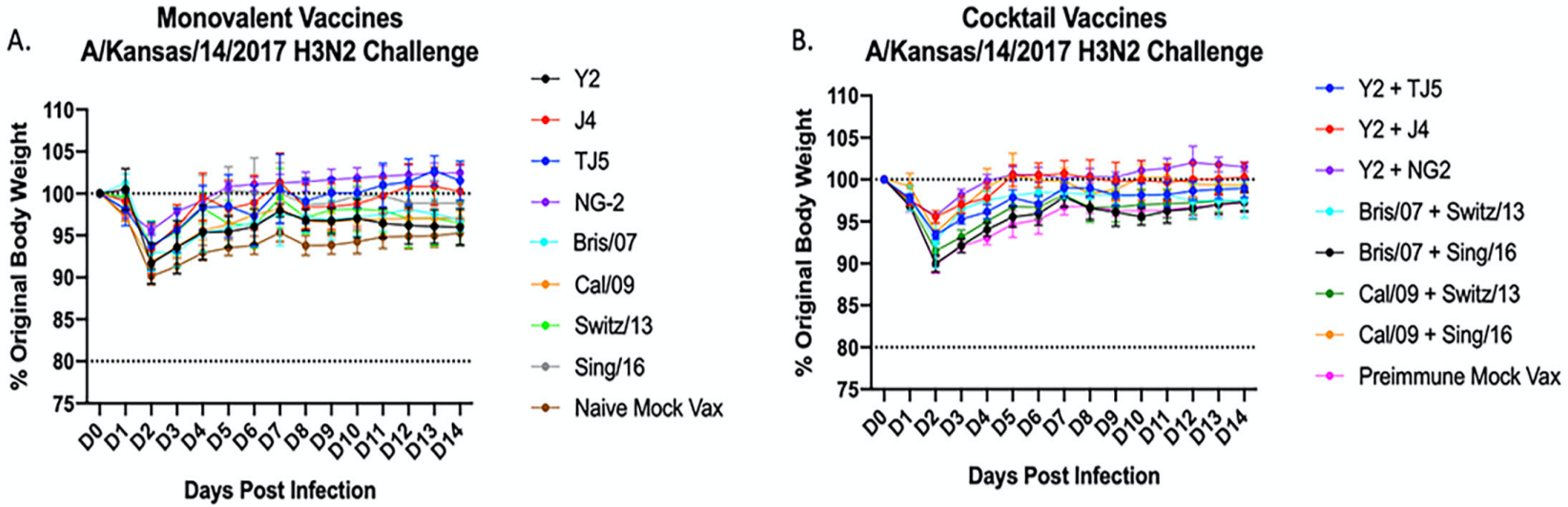
A.
Monovalent Vaccines
A/Kansas/14/2017 H3N2 Challenge
% Original Body Weight
110
105
100
95
90
85
80
75
D0 D1 D2 D3 D4 D5 D6 D7 D8 D9 D10 D11 D12 D13 D14
Days Post Infection
Y2
J4
TJ5
NG-2
Bris/07
Cal/09
Switz/13
Sing/16
Naive Mock Vax
B.
Cocktail Vaccines
A/Kansas/14/2017 H3N2 Challenge
% Original Body Weight
110
105
100
95
90
85
80
75
D0 D1 D2 D3 D4 D5 D6 D7 D8 D9 D10 D11 D12 D13 D14
Days Post Infection
Y2 + TJ5
Y2 + J4
Y2 + NG2
Bris/07 + Switz/13
Bris/07 + Sing/16
Cal/09 + Switz/13
Cal/09 + Sing/16
Preimmune Mock Vax

Figure 5.8. D86 H3N2 Viral Challenge Weight Loss. 136 Pre-immune DBA/2J mice (n=8/group) were infected on day 86 with $6.7x10^6$ PFU/50uL of A/Kansas/14/2017 (H3N2) influenza virus. The mice were tracked for 14 consecutive days (D1-D14) following challenge (X-axis), and the percentage of their original body weight lost was is reported (Y-axis). Data is separated by mice vaccinated with monovalent vaccine antigens (A), and those vaccinated with cocktails of bivalent rHA antigens. The lower dotted line represents the weight loss associated with the humane end point (80% original body weight), and the upper dotted line represents 100% original body weight.

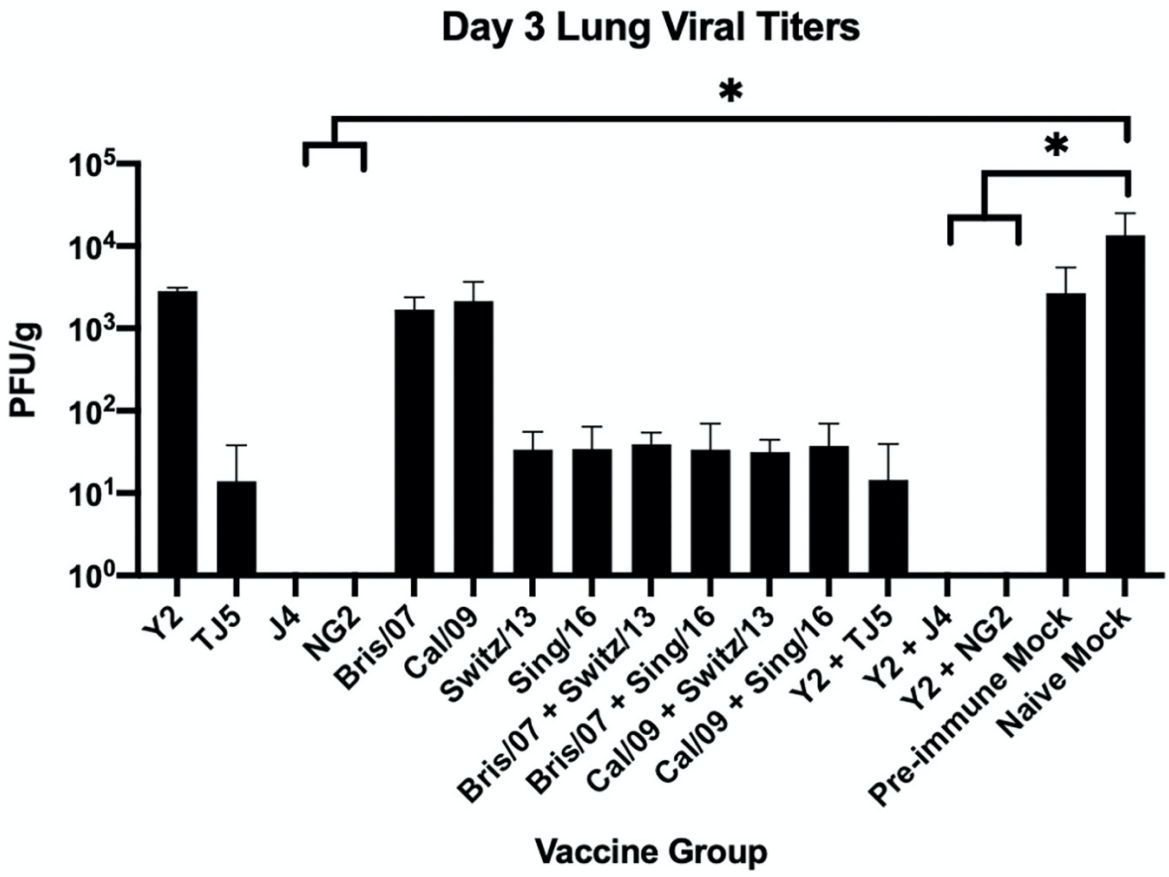

Figure 5.9. Day 89 Lung Viral Titers. Lungs were collected from N=3 mice per group on day 89 (3 days post A/Kansas/14/2017 challenge) to assess the viral load present in the lung tissue. Vaccine groups are listed on the x-axis, and plaque forming units per gram (PFU/g) of lung tissue are reported on the Y-axis. A nonparametric one-way ANOVA was used to analyze statistical differences between groups using GraphPad Prism 9 software (GraphPad, San Diego, CA, USA). A p value less than 0.05 was defined as statistically significant (*, $P < 0.05$; **, $P < 0.01$; ***, $P < 0.001$; ****, $P < 0.0001$).

CHAPTER 6

CONCLUSIONS

The goal of this project was to develop a new COBRA design methodology capable of producing influenza H3 HA vaccine antigens using WT H3N2 HA sequences from H3N2 influenza viruses isolated from recent circulating seasons. These HA protein vaccines should be suitable for individuals with diverse influenza pre-immune backgrounds, effective against 75% of influenza strains in a given season, and induce durable protection that lasts at least one year into the future against antigenically drifted isolates. The newly developed next-generation COBRA design methodology was used to generate H3 HA antigens on a seasonal basis from WT H3N2 sequences isolated during 2002-2019. From this process, 16 different H3 HA antigens were developed and tested in influenza naïve mice for their ability to induce broadly reactive antibodies against panels of antigenically diverse H3N2 viruses that were in circulation from 1995-2020. The hypothesis was that COBRA H3 HA antigens generated through the next generation design methodology would elicit broadly reactive antibodies capable of inducing more robust HAI and infection neutralizing titers than historical WT vaccine strains when tested against a panel of co-circulating influenza A(H3N2) viruses across multiple flu seasons and in a variety of influenza pre-immune backgrounds.

To test this hypothesis, the following specific aims were investigated:

Specific Aim 1: Design, generate, and evaluate next generation H3 COBRA HA influenza vaccines designed for 2002-2015 in an influenza naïve mouse model. The working hypothesis was that the next-generation COBRA H3 VLP vaccinated mice would generate broadly reactive

hemagglutination inhibition positive (HAI+) sero-protective antibodies against more H3N2 strains in circulation during 2004-2016 than those vaccinated with wild-type (WT) H3N2 antigens.

Nine next-generation H3 COBRA HA sequences, TJ1-TJ9 were generated from 22,144 human H3N2 WT HA sequences collected from January 1, 2002 to December 31, 2015. The HA antigen sequences were cloned into the pTR600 expression vector and amplified to produce VLPs in HEK 293-T cells expressing the COBRA HA on their surface. The VLPs expressing TJ1-TJ9 along with historical H3N2 WT VLP vaccines were used to vaccinate influenza naïve BALB/c mice in a homologous prime, boost, boost regimen. After the third and final vaccination sera from each mouse was assessed in the HAI assay for broadly reactive HAI+ antibodies against a panel of historical H3N2 vaccine strains from 1995-2016, as well as antigenically drifted co-circulating H3N2 strains from 2004-2016. The H3 COBRA HA antigens designed using the next-generation methodology were able to broadly elicit both HAI+ and neutralizing antibodies against historical, co-circulating, and future drifted strains of H3N2 influenza viruses at a level that was equivalent or greater than wild-type antigens from the same era. Two of the vaccine candidates, TJ-2 and TJ-5, in particular, outperformed the WT HA vaccine antigens and elicited the broadest and most robust anti-influenza antibody responses against the era for which they were designed, 2002-2005 and 2008-2012 respectively, as well as against future antigenically drifted H3N2 influenza strains. These results show that the next-generation H3 COBRA HA design methodology described herein is an effective approach for designing broadly reactive influenza antigens capable of eliciting anti-HA directed virus neutralizing antibodies against historical, co-circulating, and future drifted seasonal H3N2 influenza strains.

Specific Aim 2: Evaluate H3 COBRA HA vaccines, TJ2 and TJ5, in ferrets that are both naïve and pre-immune to H3N2 viruses from specific antigenic eras. The working hypothesis was that pre-immune animals that received next generation COBRA H3 vaccinations would elicit antibodies against more strains in an H3N2 HAI virus breadth panel than those that receive WT vaccines, and these responses would vary based on the animal's prior H3N2 antigenic exposure.

Immunologically influenza naïve ferrets were first made pre-immune by infecting them with one of three historical H3N2 vaccine strain viruses isolated during the 1970s, 1980s, or 1990s. The animals were then vaccinated with VLPs expressing either COBRA TJ2, TJ5, or one of two WT H3N2 HA proteins. After one vaccination with VLPs expressing either TJ2 or TJ5 HAs the COBRA immunized animals elicited HAI+ antibodies against more of the historical H3N2 vaccine strain isolates from 1968-2019 than WT vaccinated animals regardless of the H3N2 priming virus. However, differences were observed between the various pre-immune groups, as ferrets primed with the genetically distant PC/73 virus had HAI+ antibodies to ~36% fewer strains in the historical H3N2 panel compared to the ferret's that were pre-immune to either Sich/87 or Pan/99. In general, VLPs expressing H3 HA vaccine antigens that were more genetically similar to the specific priming virus induced the highest level of HAI breadth across the panel of historical A(H3N2) influenza vaccine strains. The HA protein of the TJ5 vaccines shares ~92% genetic similarity to Pan/99 and Sich/87, and after one vaccination, it elicited sero-protective HAI titers to ~80% viruses in the historical vaccine strain panel. In comparison the HA protein of TJ5 shares ~87% similarity to the PC/73 priming strain, and following one vaccination in this model the vaccine only induced sero-protective HAI antibody titers to ~20% of the strains in the historical H3N2 panel. In this study it appeared that when the genetic distance between priming strain and vaccine antigen is greater ~87%, the ability of the HA vaccine antigens to elicit broadly-reactive

antibodies against the panel drops considerably. These results were in contrast to the immunologically naïve animals that required two homologous vaccinations of TJ5 to sero-convert to ~20% of the strains in the panel, and did not have HAI+ antibodies against any of the historical H3N2 strains after one vaccination. This was likely due to the number of shared antigenic epitopes between the chosen vaccine strain and those present in the priming virus. The initial priming infection likely established a pool of HA reactive memory B cells that are recalled when exposed to common epitopes that are shared between the priming strain and the vaccine antigens. The next-generation COBRA design methodology aims to maximize these shared epitopes by producing an optimized antigen that contains multiple antigenic epitopes from a number of different recently circulating viruses, in order to maximize the cross-reactive potential of the induced antibody pool. These results show that the H3 COBRA HA antigens were better at eliciting broader HA-reactive antibody responses in pre-immune animals than in influenza naïve animal models, and highlight the importance of fully vetting broadly reactive vaccine candidates in both pre-immune and naïve animals before making determinations on their potential efficacy in a target population that likely possesses immunological memory to influenza viruses. These results also showed that the COBRA HA vaccines were better at eliciting HAI+ antibodies against historical vaccine strains than WT HA antigens after a single vaccination regardless of the immune history of the animal; demonstrating that the COBRA methodology for designing influenza vaccine candidates would be highly advantageous for vaccine manufacturers who want their products to generate potent cross-reactive antibody responses populations with diverse immune backgrounds.

Specific Aim 3: Evaluate bivalent mixtures of H1 and H3 COBRA HA vaccine antigens for expansion of immunologic breadth in mice that are pre-immune to both H1N1 and H3N2 influenza

viruses. The working hypothesis was that pre-immune animals vaccinated with bivalent formulations of H1 and H3 COBRA HAs will elicit broadly reactive antibodies against more H1N1 and H3N2 historical vaccine strains in an HAI breadth panel and in neutralization assays than those that receive bivalent mixtures of WT HA vaccine antigens.

The COBRA TJ5 H3 vaccine antigen, which was designed from H3 WT HA sequences in circulation from 2008-2012, did not elicit HAI+ antibodies against the antigenically drifted HK/19 H3N2 virus. As a result, 7 new HA antigens were designed from sequences in circulation during 2013-2019 using the next generation COBRA design methodology. These 7 candidate HA vaccine antigens were evaluated in influenza naïve BALB/c mice to determine their antigenic reactivity against historical H3N2 vaccine strains from 2012-2019. The results showed that one of the sequences, NG2, was particularly effective at generating broadly reactive antibody responses, and was the only vaccine antigen to elicit HAI+ antibody titers against all of the H3N2 vaccine strains from 2012-2019, but other COBRA HA proteins were also effective at generating HAI reactive antibodies against HK/19.

As most commercial vaccines are administered as polyvalent mixtures of influenza antigens from different subtypes, the two newly generated COBRA HA sequences that elicited the highest HAI titers against the HK/19 virus, J4 and NG2, were selected for further testing in pre-immune animals to determine if their antigenic breadth would be diminished by mixing them with H1 COBRA HA antigens. In order to test this, influenza naïve DBA/2J mice were made pre-immune to both H1N1 and H3N2 influenza viruses. The pre-immune mice were then vaccinated with bivalent formulations of COBRA H1, Y2, and H3, J4 or NG2, HA antigens for their ability to elicit broadly reactive antibodies against panels of historical H1N1 and H3N2 influenza viruses from 2007-2019. This investigation was the first time that H1 and H3 COBRA antigens were

administered as a bivalent mixture and evaluated in influenza pre-immune animals. The results showed that bivalent vaccine mixtures of COBRA H1+H3 rHA, Y2+J4, and Y2+NG2, outperformed WT H1+H3 bivalent rHA mixtures by eliciting HAI+ antibody responses against H1N1 and H3N2 influenza vaccine strain isolates from 2009-2019. These polyvalent COBRA H1+H3 vaccines also elicited antibodies capable of neutralizing more live virus infections with recently circulating H1N1 and H3N2 isolates at higher titers than any one bivalent mixture of WT rHA antigens in neutralization assays. Both of the bivalent COBRA rHA antigens also elicited antibodies that protected mice from an H3N2 influenza virus challenge, and the animals had no detectable virus in their lungs three days post infection. Overall, these results showed that the H1 and H3 COBRA HA antigens, Y2, J4, and NG2, produced using the next-generational methodology all had the ability to induce broadly reactive antibodies in influenza naïve and pre-immune animals in both monovalent and bivalent formulations, and these antigens outperformed H1 and H3 WT rHA vaccine antigens by eliciting HAI+ antibodies against panels of antigenically drifted historical H1N1 and H3N2 vaccine strains from 2009-2019.

Additional Experiments: Determine which HA epitopes are responsible for the expansion of HAI breadth observed in COBRA NG2 rHA vaccinated animals. The working hypothesis is that point mutations at amino acid site 147 and 235 can be made to the NG2 HA sequence to make it lose its ability to generate HAI+ antibodies against the HK/19 H3N2 isolate. The SA/19 WT HA does not induce HAI+ antibodies to the antigenically drifted HK/19 strain, and possesses a lysine at position 147, while NG2 and HK/19 share a 147T at this location. Changes in residue 145 in antigenic site A can influence HAI assays by modulating the receptor binding avidity of the influenza virus, so amino acid substitutions at neighboring site 147 may play a role in the observed

differences in reactivity between NG2 and SA/19 [100]. Similarly, differences in antigenic site D could also play a role, as the NG2 and HK/19 HA sequences share a 235S mutation within this site, while SA/19 possesses a 235F. All of the other amino acid differences in the antigenic sites between NG2 and HK/19 are shared between NG2 and SA/19, therefore they are not likely to contribute to the expanded breadth of reactivity by NG2 HA compared to SA/19 HA. H3N2 influenza viruses routinely acquire amino acid substitutions in their antigenic sites, and single point mutations in the HA protein at these sites can alter their immunogenicity [100]. Through site directed mutagenesis the NG2 sequence can be made to express 147K and/or 235F to determine if one or both of the amino acid substitutions causes the NG2 rHA antigen to no longer elicit HAI+ antibodies against the HK/19 isolate. The results of this analysis could provide information on which epitopes are necessary to elicit broadly reactive immune responses to modern H3N2 viruses.

Additional experiments could also be conducted to optimize the subtype specific antibody responses generated by the individual H1 and H3 rHA vaccine components. The working hypothesis is that by increasing the concentration of the H3 rHA relative to the H1 rHA component of the bivalent vaccine, the H3 specific antibody response will be stronger than when the components are mixed in equal concentrations. In the bivalent vaccine study from specific aim 3, differences were observed in the magnitude of the HAI reactive antibody responses generated by the individual H1 and H3 rHA components of the multivalent vaccines for both COBRA and WT rHA against the H1N1 and H3N2 virus panels respectively. This difference in antibody titer appeared to be more pronounced for the H3 reactive antibodies, which were on average ~2-fold lower in magnitude than those generated by the H1 components, despite both antigens being administered to the mice in equal concentrations. This may indicate some level of immunodominance of the H1 rHA vaccine antigens over the H3 rHA antigens. This result is not

unexpected, as multiple studies that investigated the human immune response to seasonal influenza vaccination also revealed that antibody responses to H3N2 were reduced in magnitude when compared to the other vaccine components [132, 133]. Increasing the dose of the H3 component relative to the H1 component in the bivalent vaccine mixture should strengthen the antibody response against the H3N2 viruses and weaken those directed against H1N1 viruses. The results of this study would provide a better understanding of how to optimize the relative concentrations of the vaccine components in order to generate a more balanced immune response against multiple subtypes of influenza viruses.

The next-generation COBRA design methodology described in this manuscript could also be applied to other subtypes of human influenza antigens, such as influenza B HA, or other immunostimulatory viral proteins such as NA (N1, N2, and NB), to generate more broadly reactive antigens for use in seasonal vaccines. The working hypothesis would be that COBRA recombinant B (rB) HA and recombinant neuraminidase (rNA) vaccine antigens would elicit more broadly reactive antibodies against antigenically drifted H1N1, H3N2, and influenza B viruses than WT rB HAs or rNAs. The majority of commercial vaccines in the United States are either trivalent or quadrivalent mixtures that include multiple influenza A and/or B antigens from different viral subtypes [5, 100]. The addition of COBRA influenza B rHA proteins, as well as COBRA rNA proteins, to the mixture of H1 and H3 rHA antigens would be used to vaccinate both influenza naïve and pre-immune animals to determine the antigenic breadth generated against antigenically drifted influenza viruses from multiple subtypes, H1N1, H3N2 and B, in populations with varying immune histories to influenza. The results from this analysis would provide insight as to how a multivalent COBRA recombinant protein vaccine would compare to a multivalent standard of care

vaccine, and the potential benefits of using a broadly reactive vaccine candidate as opposed to a WT vaccine to fight human influenza viruses on a seasonal basis.

Lastly, experiments could also be performed to evaluate the next-generation H1 and H3 COBRA HA vaccine antigens in animal populations modeling individuals that have the greatest risk of developing severe complications from influenza infections (*i.e.*, young, elderly, obese, diabetic, and the immunocompromised). The working hypothesis would be that COBRA HA vaccine antigens would generate more broadly reactive antibody responses in these high-risk animal models than individuals that receive WT HA vaccine antigens. Young, elderly, and other high-risk individuals rely differently on their immunological memory compartments to generate specific immune responses following influenza vaccination [99, 102]. Consequently, it is probable that these various populations will respond differentially to influenza infection and vaccination [73, 105]. However, the results from these studies will shed light on how broadly reactive influenza vaccine candidates perform in different populations. This is highly important, as an ideal universal vaccine candidate should produce broadly reactive antibodies in everyone, regardless of their specific immune state.

The goal of this work was to develop a COBRA HA design methodology such that it would be advantageous for both influenza vaccine manufacturers and consumers, in comparison to the production process and immunogenicity of WT vaccine antigens. The use of broadly reactive antigens in seasonal influenza vaccines would help reduce the need to update vaccine antigens on a bi-annual basis, while simultaneously increasing the protection offered by vaccine candidates against multiple co-circulating strains in a given influenza season. Current vaccine manufacturing processes take about 6-8 months from strain selection to vaccine availability, and delays in strain recommendation or antigenic characterization can lead to significant reductions in the vaccine

supply [11, 75]. In contrast, COBRA vaccine antigens can be designed in real time based on recently circulating viral isolates, and rapidly characterized in animal models before the strain selection process ever takes place. Therefore, having a broadly reactive vaccine candidate on the shelf that has been previously antigenically characterized and optimized for production would save manufacturers a considerable amount of stress and time, allowing them to make more doses of vaccine, while at the same time reducing the chances of having a mismatch between circulating viruses and the chosen vaccine antigen.

Earlier COBRA HA designs focused on developing antigens using influenza sequences from previous viral outbreak groups or antigenic eras, and were tested against historical vaccine strain isolates to determine their immunologic breadth against past strains [13, 68, 71]. However, because A(H3N2) viruses evolve so quickly through antigenic drift, it is likely that the protection offered by a broadly reactive vaccine candidate designed in such a manner will eventually begin to decline due to the diversity of newly emerging isolates in the viral population [76]. Therefore, there is a need for a method of updating broadly reactive influenza vaccine candidates on a seasonal basis to mirror the diversity present in the population of circulating viruses. The next-generation COBRA design methodology presented herein, differs from its predecessors by utilizing seasonal viral surveillance information, in combination with unique layered consensus-based sequence building approaches to provide a method for keeping vaccine antigens up to date with the ever-changing viral landscape. This method keeps the vaccine antigens current by allowing the natural evolution of influenza viruses to dictate the antigen design process, and places an emphasis on current drifted strains rather than historical strains or outbreak groups, allowing the next-generation COBRA HA antigens to retain highly immunogenic and cross-reactive epitopes present in the viral population.

The HA proteins generated through the next-generation COBRA design methodology likely elicit broadly reactive antibodies similarly to those generated by the historical COBRA antigens, whereby the HA proteins stimulate diverse B cell responses that target conserved HA surface epitopes present on the vaccine antigens and co-circulating influenza variants [91]. Many other universal influenza vaccine candidates drive their induced antibody responses toward the conserved stem regions of the HA protein, but COBRA HA antigens preferentially direct antibody responses toward conserved regions of the HA globular head, such as the receptor binding site, which tends to remain unchanged in order to successfully bind to host sialic acids [75, 91]. Vaccine antigens capable of inducing antibodies directed against the head region of the HA are advantageous because they are induced at much higher titers than those directed against the stalk region of the HA protein [92, 93]. This is not to say that the next-generation COBRA HA antigens only generate head-based antibody responses. These antigens also generate antibodies against the HA stalk, as they are full length HA protein sequences that express both HA head and stem regions [126]. However, it is still unknown if the broadly reactive antibody responses generated by the COBRA HA antigens are the result of multiple antibodies working together to target various conserved HA epitopes, or if they are the product of a highly specific monoclonal antibody response targeting a single conserved epitope [91]. Future studies will be aimed at answering these questions by generating monoclonal antibodies, and assessing them in competition ELISAs, as well as solving antibody-antigen co-crystal structures to determine which HA epitopes these COBRA HA elicited antibodies are actually binding.

Elucidating the interactions of COBRA HA proteins with antigen specific B cell populations would also provide great insight as to how these antigens are likely to perform in humans with pre-existing influenza immunity. Currently, the antigen specific B cell response to

COBRA HA vaccination in influenza naïve and pre-immune models is unknown. Seasonal influenza vaccination in humans primarily stimulates pre-existing memory B cells to secrete HA specific antibodies, but it can also induce germinal center reactions in the draining lymph node, where B cells targeting novel HA epitopes are likely to be recruited [98, 102]. Additionally, vaccine formulations that promote vigorous germinal center reactions are more likely to induce a more diverse antibody response against circulating and emerging influenza isolates [98]. Therefore, understanding the COBRA HA elicited B cell response is of great importance, as generating an influenza vaccine antigen that can stimulate the pre-existing memory B cell populations as well the naive B cell compartment would be highly beneficial for designing antigens that produce broadly reactive antibody responses.

While there is still much to learn about the specific immunogenic epitopes and B cell responses stimulated by COBRA HA vaccination, the results from this project demonstrate that the next-generation COBRA HA design methodology is capable of producing influenza HA antigens that elicit broadly reactive antibodies against historical, co-circulating, and future emerging influenza A(H3N2) drift variants. The newly designed COBRA HA antigens elicited these broadly reactive antibodies in animals that were influenza naïve and pre-immune to H3N2 viruses from different decades, and they maintained their cross-reactive breadth when mixed with an H1 COBRA HA that was also generated using the next-generation COBRA design methodology. Overall, the next-generation COBRA HA antigens described in this dissertation elicited more broadly reactive and neutralizing antibodies than WT HA vaccine antigens against panels of antigenically drifted H1N1 and H3N2 viruses from 2009-2019 and these vaccines can be used as effective influenza vaccines in people with diverse immunological backgrounds.

References

1. Vemula, S.V., et al., *Current approaches for diagnosis of influenza virus infections in humans.* Viruses, 2016. **8**(4): p. 96.
2. Garten, R., et al., *Update: influenza activity in the United States during the 2017–18 season and composition of the 2018–19 influenza vaccine.* Morbidity and Mortality Weekly Report*,* 2018. **67**(22): p. 634.
3. Xu, X., et al., *Update: influenza activity in the United States during the 2018–19 season and composition of the 2019–20 influenza vaccine.* Morbidity and Mortality Weekly Report, 2019. **68**(24): p. 544.
4. Alymova, I.V., et al., *Glycosylation changes in the globular head of H3N2 influenza hemagglutinin modulate receptor binding without affecting virus virulence.* Scientific Reports, 2016. **6**(1): p.1-15.
5. Gouma, S., E.M. Anderson, and S.E. Hensley, *Challenges of making effective influenza vaccines.* Annual Review of Virology, 2020. **7**(1): p. 495.
6. Doyle, J.D., et al., *Relative and absolute effectiveness of high-dose and standard-dose influenza vaccine against influenza-related hospitalization among older adults - United States, 2015-2017.* Clinical Infectious Diseases : an official publication of the Infectious Diseases Society of America, 2020: p. ciaa160.
7. Duwe, S., *Influenza viruses - antiviral therapy and resistance.* GMS infectious diseases, 2017. **5**: p. Doc04-Doc04.

8. Bosaeed, M., D.J.H.v. Kumar. *Seasonal influenza vaccine in immunocompromised persons.* Human Vaccines and Immunotherapeutics, 2018. **14**(6): p. 1311-1322.

9. Shao, W., et al., *Evolution of influenza a virus by mutation and re-assortment.* International Journal of Molecular Sciences, 2017. **18**(8): p. 1650.

10. Lin, Y., et al., *The characteristics and antigenic properties of recently emerged subclade 3C. 3a and 3C. 2a human influenza A (H3N2) viruses passaged in MDCK cells.* Influenza and Other Respiratory Viruses, 2017. **11**(3): p. 263-274.

11. Chen, J.-R., et al., *Better influenza vaccines: an industry perspective.* Journal of Biomedical Science, 2020. **27**(1): p. 1-11.

12. Flannery, B., et al., *Spread of antigenically drifted influenza A (H3N2) viruses and vaccine effectiveness in the United States during the 2018–2019 season.* Journal of Infectious Diseases, 2020. **221**(1): p. 8-15.

13. Wong, T.M., et al., *Computationally optimized broadly reactive hemagglutinin elicits hemagglutination inhibition antibodies against a panel of H3N2 influenza virus cocirculating variants.* Journal of Virology, 2017. **91**(24): p. e01581-17.

14. Shim, J.M., et al., *Influenza Virus Infection, Interferon Response, Viral Counter-Response, and Apoptosis.* Viruses, 2017. **9**(8): p. 223.

15. Yang, J., et al., *A new role of neuraminidase (NA) in the influenza virus life cycle: implication for developing NA inhibitors with novel mechanism of action.* Reviews in medical virology, 2016. **26**(4): p. 242-250.

16. Melidou, A., et al., *Influenza A (H3N2) genetic variants in vaccinated patients in northern Greece.* Journal of Clinical Virology, 2017 **94**: p.29-32.

17. Blackburne, B.P., A.J. Hay, and R.A. Goldstein, *Changing selective pressure during antigenic changes in human influenza H3.* PLoS Pathogens, 2008. **4**(5): p. e1000058.

18. Chambers, B.S., et al., *Recent H3N2 influenza virus clinical isolates rapidly acquire hemagglutinin or neuraminidase mutations when propagated for antigenic analyses.* Journal of Virology, 2014. **88**(18): p. 10986-10989.

19. Pavlova, S., et al., *Workshop report: Immunoassay standardisation for "universal" influenza vaccines.* Influenza and Other Respiratory Viruses, 2017. **11**(3): p. 194-201.

20. Zhu, X., et al., *Influenza virus neuraminidases with reduced enzymatic activity that avidly bind sialic acid receptors.* Journal of Virology, 2012. **86**(24): p. 13371-13383.

21. Lin, Y.P., et al., *Neuraminidase receptor binding variants of human influenza A (H3N2) viruses resulting from substitution of aspartic acid 151 in the catalytic site: a role in virus attachment?* Journal of Virology, 2010. **84**(13): p. 6769-6781.

22. Bouvier, N.M. and P. Palese, *The biology of influenza viruses.* Vaccine, 2008. **26**: p. D49-D53.

23. Westgeest, K.B., et al., *Genomewide analysis of reassortment and evolution of human influenza A (H3N2) viruses circulating between 1968 and 2011.* Journal of Virology, 2014. **88**(5): p. 2844-2857.

24. Huang, Z.-Z., et al., *Charged amino acid variability related to N-glyco-sylation and epitopes in A/H3N2 influenza: Hem-agglutinin and neuraminidase.* PloS One, 2017. **12**(7): p. e0178231.

25. Peng, W., et al., *Recent H3N2 viruses have evolved specificity for extended, branched human-type receptors, conferring potential for increased avidity.* Cell Host & Microbe, 2017. **21**(1): p. 23-34.

26. Ushirogawa, H., et al., *Re-emergence of H3N2 strains carrying potential neutralizing mutations at the N-linked glycosylation site at the hemagglutinin head, post the 2009 H1N1 pandemic.* BMC Infectious Diseases, 2016. **16**(1): p. 380.

27. Shao, W., et al., *Evolution of Influenza A Virus by Mutation and Re-Assortment.* International Journal of Molecular Sciences, 2017. **18**(8): p. 1650.

28. Hooper, K.A., J.E. Crowe, and J.D. Bloom, *Influenza viruses with receptor-binding N1 neuraminidases occur sporadically in several lineages and show no attenuation in cell culture or mice.* Journal of Virology, 2015. **89**(7): p. 3737-3745.

29. Medeiros, R., et al., *Hemagglutinin residues of recent human A (H3N2) influenza viruses that contribute to the inability to agglutinate chicken erythrocytes.* Virology, 2001. **289**(1): p. 74-85.

30. Yang, H., et al., *Structure and receptor binding preferences of recombinant human A (H3N2) virus hemagglutinins.* Virology, 2015. **477**: p. 18-31.

31. Yokoyama, M., et al., *Molecular dynamics simulation of the influenza A (H3N2) hemagglutinin trimer reveals the structural basis for adaptive evolution of the recent epidemic clade 3C. 2a.* Frontiers in Microbiology, 2017. **8**.

32. Van Poucke, S., et al., *Role of Substitutions in the Hemagglutinin in the Emergence of the 1968 Pandemic Influenza Virus.* Journal of Virology, 2015. **89**(23): p. 12211-12216.

33. Koel, B.F., et al., *Substitutions near the receptor binding site determine major antigenic change during influenza virus evolution.* Science, 2013. **342**(6161): p. 976-979.

34. Kobayashi, Y. and Y. Suzuki, *Compensatory evolution of net-charge in influenza A virus hemagglutinin.* PloS One, 2012. **7**(7): p. e40422.

35. Asaoka, N., et al., *Low growth ability of recent influenza clinical isolates in MDCK cells is due to their low receptor binding affinities.* Microbes and Infection, 2006. **8**(2): p. 511-519.

36. Parker, L., et al., *Effects of egg-adaptation on receptor-binding and antigenic properties of recent influenza A (H3N2) vaccine viruses.* Journal of General Virology, 2016. **97**(6): p. 1333-1344.

37. Hervé, P.-L., et al., *Addition of N-glycosylation sites on the globular head of the H5 hemagglutinin induces the escape of highly pathogenic avian influenza A H5N1 viruses from vaccine-induced immunity.* Virology, 2015. **486**: p. 134-145.

38. Harvala, H., et al., *Emergence of a novel subclade of influenza A (H3N2) virus in London, December 2016 to January 2017.* Eurosurveillance, 2017. **22**(8).

39. Park, A.W., et al., *Quantifying the impact of immune escape on transmission dynamics of influenza.* Science, 2009. **326**(5953): p. 726-728.

40. Skowronski, D.M., et al., *Mutations acquired during cell culture isolation may affect antigenic characterisation of influenza A (H3N2) clade 3C. 2a viruses.* Eurosurveillance, 2016. **21**(3).

41. Chambers, B.S., et al., *Identification of hemagglutinin residues responsible for H3N2 antigenic drift during the 2014–2015 influenza season.* Cell Reports, 2015. **12**(1): p. 1-6.

42. Wu, N.C., et al., *A structural explanation for the low effectiveness of the seasonal influenza H3N2 vaccine.* PLoS Pathogens, 2017. **13**(10): p. e1006682.

43. Wang, B., et al., *Single radial haemolysis compared to haemagglutinin inhibition and microneutralization as a correlate of protection against influenza A H3N2 in children and adolescents.* Influenza and Other Respiratory Viruses, 2017. **11**(3): p. 283-288.

44. Trombetta, C.M., et al., *Overview of serological techniques for influenza vaccine evaluation: past, present and future.* Vaccines, 2014. **2**(4): p. 707-734.

45. Gulati, S., et al., *Human H3N2 influenza viruses isolated from 1968 to 2012 show varying preference for receptor substructures with no apparent consequences for disease or spread.* PloS One, 2013. **8**(6): p. e66325.

46. Lin, Y.P., et al., *Evolution of the receptor binding properties of the influenza A (H3N2) hemagglutinin.* Proceedings of the National Academy of Sciences, 2012. **109**(52): p. 21474-21479.

47. Barr, I.G., et al., *Epidemiological, antigenic and genetic characteristics of seasonal influenza A (H1N1), A (H3N2) and B influenza viruses: basis for the WHO recommendation on the composition of influenza vaccines for use in the 2009–2010 Northern Hemisphere season.* Vaccine, 2010. **28**(5): p. 1156-1167.

48. Oh, D.Y., et al., *MDCK-SIAT1 cells show improved isolation rates for recent human influenza viruses compared to conventional MDCK cells.* Journal of Clinical Microbiology, 2008. **46**(7): p. 2189-2194.

49. Matrosovich, M., et al., *Overexpression of the α-2, 6-sialyltransferase in MDCK cells increases influenza virus sensitivity to neuraminidase inhibitors.* Journal of Virology, 2003. **77**(15): p. 8418-8425.

50. Matrosovich, M.N., et al., *Neuraminidase is important for the initiation of influenza virus infection in human airway epithelium.* Journal of Virology, 2004. **78**(22): p. 12665-12667.

51. Mishin, V.P., et al., *The effect of the MDCK cell selected neuraminidase D151G mutation on the drug susceptibility assessment of influenza A (H3N2) viruses.* Antiviral Research, 2014. **101**: p. 93-96.

52. Colman, P.M., J. Varghese, and W. Laver, *Structure of the catalytic and antigenic sites in influenza virus neuraminidase.* Nature, 1983. **303**(5912): p. 41-44.

53. van Baalen, C.A., et al., *ViroSpot microneutralization assay for antigenic characterization of human influenza viruses.* Vaccine, 2017. **35**(1): p. 46-52.

54. Lin, Y., Y. Gu, and J.W. McCauley, *Optimization of a Quantitative Micro-neutralization Assay.* Journal of visualized experiments: JoVE, 2016(118).

55. Sullivan, K., et al., *High throughput virus plaque quantitation using a flatbed scanner.* Journal of Virological Methods, 2012. **179**(1): p. 81-89.

56. Chen, J.-R., et al., *Better influenza vaccines: an industry perspective.* Journal of Biomedical science, 2020. **27**(1): p. 1-11.

57. Iuliano, A.D., et al., *Estimates of global seasonal influenza-associated respiratory mortality: a modelling study.* The Lancet, 2018. **391**(10127): p. 1285-1300.

58. Castro, L., T. Bedford, and L.J.B. Meyers, *Early Prediction of Antigenic Transitions for Influenza A H3N2.* PLoS Computational Biology, 2019: p. 558577.

59. McLean, H.Q. and E.A. Belongia, *Influenza Vaccine Effectiveness: New Insights and Challenges.* Cold Spring Harbor Perspectives in Medicine, 2020: p. a038315.

60. Chung, J.R., et al., *Effects of Influenza Vaccination in the United States during the 2018–2019 Influenza Season.* Clinical Infectious Diseases, 2020.

61. Loiacono, M.M., et al., *Patient and practice level factors associated with seasonal influenza vaccine uptake among at-risk adults in England, 2011 to 2016: An age-stratified retrospective cohort study.* Vaccine: X, 2020. **4**: p. 100054-100054.

62. Reneer, Z.B. and T.M. Ross, *H2 influenza viruses: designing vaccines against future H2 pandemics.* Biochemical Society Transactions, 2019. **47**(1): p. 251-264.

63. Dowdle, W.J.B.o.t.W.H.O., *Influenza A virus recycling revisited.* Bulletin of the World Health Organization, 1999. **77**(10): p. 820.

64. Wei, C.-J., et al., *Next-generation influenza vaccines: opportunities and challenges.* Nature Reviews Drug Discovery, 2020: p. 1-14.

65. Allen, J.D., et al., *Elicitation of protective antibodies against 20 years of future H3N2 cocirculating influenza virus variants in ferrets preimmune to historical H3N2 influenza viruses.* 2019. Journal of Virology, **93**(3): p. e00946-18.

66. Giles, B.M. and T.M.J.V. Ross, *A computationally optimized broadly reactive antigen (COBRA) based H5N1 VLP vaccine elicits broadly reactive antibodies in mice and ferrets.* 2011. The Journal of Immunology, **29**(16): p. 3043-3054.

67. Giles, B.M., et al., *Antibody breadth and protective efficacy are increased by vaccination with computationally optimized hemagglutinin but not with polyvalent hemagglutinin-based H5N1 virus-like particle vaccines.* Clinical and Vaccine Immunology, 2012. **19**(2): p. 128-139.

68. Giles, B.M., et al., *A computationally optimized hemagglutinin virus-like particle vaccine elicits broadly reactive antibodies that protect nonhuman primates from H5N1 infection.* 2012. The Journal of Infectious Diseases, **205**(10): p. 1562-1570.

69. Crevar, C.J., et al., *Cocktail of H5N1 COBRA HA vaccines elicit protective antibodies against H5N1 viruses from multiple clades.* Human Vaccines and Immunotherapeutics, 2015. **11**(3): p. 572-583.

70. Carter, D.M., et al., *Elicitation of protective antibodies against a broad panel of H1N1 viruses in ferrets preimmune to historical H1N1 influenza viruses.* Journal of Virology, 2017. **91**(24): p. e01283-17.

71. Carter, D.M., et al., *Design and characterization of a computationally optimized broadly reactive hemagglutinin vaccine for H1N1 influenza viruses.* Journal of Virology, 2016. **90**(9): p. 4720-4734.

72. Carter, D.M., et al., *Sequential seasonal H1N1 influenza virus infections protect ferrets against novel 2009 H1N1 influenza virus.* 2013. Journal of Virology, **87**(3): p. 1400-1410.

73. Kirchenbaum, G.A., D.M. Carter, and T.M. Ross, *Sequential infection in ferrets with antigenically distinct seasonal H1N1 influenza viruses boosts hemagglutinin stalk-specific antibodies.* Journal of Virology, 2016. **90**(2): p. 1116-1128.

74. Kirchenbaum, G.A. and T.M. Ross, *Eliciting broadly protective antibody responses against influenza.* Current Opinion in Immunology, 2014. **28**: p. 71-76.

75. Ostrowsky, J., et al., *Tracking progress in universal influenza vaccine development.* Current Opinion in Virology, 2020. **40**: p. 28-36.

76. Elliott, S.T., et al., *A synthetic micro-consensus DNA vaccine generates comprehensive influenza A H3N2 immunity and protects mice against lethal challenge by multiple H3N2 viruses.* Human Gene Therapy, 2018. **29**(9): p. 1044-1055.

77. Agor, J.K. and O.Y. Özaltın, *Models for predicting the evolution of influenza to inform vaccine strain selection.* Human Vaccines & Immunotherapeutics, 2018. **14**(3): p. 678-683.

78. Wilson, I.A. and N.J. Cox, *Structural basis of immune recognition of influenza virus hemagglutinin.* Annual Review of Immunology, 1990. **8**(1): p. 737-787.

79. Ross, T.M., et al., *C3d enhancement of antibodies to hemagglutinin accelerates protection against influenza virus challenge.* Nature Immunology, 2000. **1**(2): p. 127.

80. Green, T.D., D.C. Montefiori, and T.M. Ross, *Enhancement of antibodies to the human immunodeficiency virus type 1 envelope by using the molecular adjuvant C3d.* Journal of Virology, 2003. **77**(3): p. 2046-2055.

81. Tan, G.S., et al., *Characterization of a broadly neutralizing monoclonal antibody that targets the fusion domain of group 2 influenza A virus hemagglutinin.* Journal of Virology, 2014. **88**(23): p. 13580-13592.

82. World Health Organization, G., Switzerland, *WHO global influenza surveillance network: manual for the laboratory diagnosis and virological surveillance of influenza.* World Health Organization, 2011, **252**.

83. Katz, J.M., K. Hancock, and X. Xu, *Serologic assays for influenza surveillance, diagnosis and vaccine evaluation.* Expert Review of Anti-infective Therapy, 2011. **9**(6): p. 669-683.

84. Oh, D.Y., et al., *MDCK-SIAT1 cells show improved isolation rates for recent human influenza viruses compared to conventional MDCK cells.* Journal of Clinical Microbiology, 2008. **46**(7): p. 2189-2194.

85. EMA/CHMP/VWP/457259/2014, *Guideline on influenza vaccines. Non-clinical and Clinical module.* Committee for Medicinal Products for Human Use, 2014. **44**: p. 1-31.

86. Matrosovich, M., et al., *New low-viscosity overlay medium for viral plaque assays.* Virology Journal, 2006. **3**(1): p. 63.

87. Walls, H.H., et al., *Characterization and evaluation of monoclonal antibodies developed for typing influenza A and influenza B viruses.* Journal of Clinical Microbiology, 1986. **23**(2): p. 240-245.

88. van Baalen, C.A., et al., *ViroSpot microneutralization assay for antigenic characterization of human influenza viruses.* Vaccine, 2017. **35**(1): p. 46-52.

89. Choi, A., A. García-Sastre, and M. Schotsaert, *Host immune response-inspired development of the influenza vaccine.* Annals of Allergy, Asthma & Immunology, 2020 **125**(1): p28-35.

90. Buckland, B.C., *The development and manufacture of influenza vaccines.* Human Vaccines & Immunotherapeutics, 2015. **11**(6): p. 1357-1360.

91. Sautto, G.A., et al., *A Computationally Optimized Broadly Reactive Antigen Subtype–Specific Influenza Vaccine Strategy Elicits Unique Potent Broadly Neutralizing Antibodies against Hemagglutinin.* The Journal of Immunology, 2020. **204**(2): p. 375-385.

92. Kubo, M. and K. Miyauchi, *Breadth of Antibody Responses during Influenza Virus Infection and Vaccination.* Trends in Immunology, 2020 **41**(5): p.394-405.

93. Corti, D., et al., *Tackling influenza with broadly neutralizing antibodies.* Current Opinion in Virology, 2017. **24**: p. 60-69.

94. Ansaldi, F., et al., *New A/H3N2 influenza variant: a small genetic evolution but a heavy burden on the Italian population during the 2004-2005 season.* Journal of Clinical Microbiology, 2005. **43**(6): p. 3027-3029.

95. Beer, K., et al., *Characterization of neutralizing epitopes in antigenic site B of recently circulating influenza A (H3N2) viruses.* The Journal of General Virology, 2018. **99**(8): p. 1001.

96. Henry, C., et al., *From original antigenic sin to the universal influenza virus vaccine.* Trends in Immunology, 2018. **39**(1): p. 70-79.

97. Guzmán, C.A., *Next Generation Influenza Vaccines: Looking into the Crystal Ball*. Multidisciplinary Digital Publishing Institute, 2020. **464**.

98. Turner, J.S., et al., *Human germinal centres engage memory and naive B cells after influenza vaccination.* Nature, 2020. **586**(7827): p. 127-132.

99. Arevalo, C.P., et al., *Original antigenic sin priming of influenza virus hemagglutinin stalk antibodies.* Proceedings of the National Academy of Sciences, 2020. **117**(29): p. 17221-17227.

100. Hensley, S.E., *Challenges of selecting seasonal influenza vaccine strains for humans with diverse pre-exposure histories.* Current Opinion in Virology, 2014. **8**: p. 85-89.

101. Hatta, Y., et al., *Novel influenza vaccine M2SR protects against drifted H1N1 and H3N2 influenza virus challenge in ferrets with pre-existing immunity.* Vaccine, 2018. **36**(33): p. 5097-5103.

102. Knight, M., et al., *Imprinting, immunodominance, and other impediments to generating broad influenza immunity.* Immunological Reviews, 2020. **296**(1): p. 191-204.

103. Hay, J.A., et al., *Characterising antibody kinetics from multiple influenza infection and vaccination events in ferrets.* PLoS Computational Biology, 2019. **15**(8): p. e1007294.

104. Gouma, S., M. Weirick, and S.E. Hensley, *Antigenic assessment of the H3N2 component of the 2019-2020 Northern Hemisphere influenza vaccine.* Nature Communications, 2020. **11**(1): p. 1-5.

105. Zhang, A., et al., *Original antigenic sin: how first exposure shapes lifelong anti–influenza virus immune responses.* The Journal of Immunology, 2019. **202**(2): p. 335-340.

106. Worobey, M., S. Plotkin, and S.E. Hensley, *Influenza vaccines delivered in early childhood could turn antigenic sin into antigenic blessings.* Cold Spring Harbor Perspectives in Medicine, 2020. **10**(10): p. a038471.

107. Francis, T., *On the doctrine of original antigenic sin.* Proceedings of the American Philosophical Society, 1960. **104**(6): p. 572-578.

108. Monto, A.S., et al., *The doctrine of original antigenic sin: separating good from evil.* The Journal of Infectious Diseases, 2017. **215**(12): p. 1782-1788.

109. Le Sage, V., et al., *Pre-existing heterosubtypic immunity provides a barrier to airborne transmission of influenza viruses.* PLoS Pathogens, 2021. **17**(2): p. e1009273.

110. Dong, W., et al., *Cross-protective immune responses induced by sequential influenza virus infection and by sequential vaccination with inactivated influenza vaccines.* Frontiers in Immunology, 2018. **9**: p. 2312.

111. Allen, J.D. and T.M. Ross, *Next generation methodology for updating HA vaccines against emerging human seasonal influenza A (H3N2) viruses.* Scientific Reports, 2021. **11**(1): p. 1-14.

112. Yewdell, J.W. and J.J. Santos, *Original antigenic sin: how original? How sinful?* Cold Spring Harbor Perspectives in Medicine, 2020. **11**(5): p. a038786.

113. Gouma, S., et al., *Middle-aged individuals may be in a perpetual state of H3N2 influenza virus susceptibility.* Nature Communications, 2020. **11**(1): p. 1-8.

114. Gostic, K.M., et al., *Childhood immune imprinting to influenza A shapes birth year-specific risk during seasonal H1N1 and H3N2 epidemics.* PLoS Pathogens, 2019. **15**(12): p. e1008109.

115. McLean, H.Q., et al., *Impact of repeated vaccination on vaccine effectiveness against influenza A (H3N2) and B during 8 seasons.* Clinical Infectious Diseases, 2014. **59**(10): p. 1375-1385.

116. Brandenburg, B., et al., *Mechanisms of hemagglutinin targeted influenza virus neutralization.* PloS One, 2013. **8**(12): p. e80034.

117. Haq, K. and J.E. McElhaney, *Immunosenescence: influenza vaccination and the elderly.* Current Opinion in Immunology, 2014. **29**: p. 38-42.

118. Gostic, K.M., et al., *Potent protection against H5N1 and H7N9 influenza via childhood hemagglutinin imprinting.* Science, 2016. **354**(6313): p. 722-726.

119. Xie, H., et al., *Differential effects of prior influenza exposures on H3N2 cross-reactivity of human postvaccination sera.* Clinical Infectious Diseases, 2017. **65**(2): p. 259-267.

120. Korsun, N., et al., *Genetic characterisation of the influenza viruses circulating in Bulgaria during the 2019–2020 winter season.* Virus Genes, 2021: p. 1-12.

121. Li, C., et al., *Selection of antigenically advanced variants of seasonal influenza viruses.* Nature Microbiology, 2016. **1**(6): p. 1-10.

122. Pando, R., et al., *Diversity in the Circulation of Influenza A (H3N2) Viruses in the Northern Hemisphere in the 2018–19 Season.* Vaccines, 2021. **9**(4): p. 375.

123. Allen, J.D. and T.M. Ross, *Evaluation of next-generation H3 influenza vaccines in ferrets pre-immune to historical H3N2 viruses.* Frontiers in Immunology, 2021 **12**: p. 3147.

124. Skarlupka, A.L. and T.M. Ross, *Immune imprinting in the influenza ferret model.* Vaccines, 2020. **8**(2): p. 173.

125. Ellebedy, A., et al., *Impact of prior seasonal influenza vaccination and infection on pandemic A (H1N1) influenza virus replication in ferrets.* Vaccine, 2011. **29**(17): p. 3335-3339.

126. Huang, Y., et al., *Next Generation of Computationally Optimized Broadly Reactive HA Vaccines Elicited Cross-Reactive Immune Responses and Provided Protection against H1N1 Virus Infection.* Vaccines, 2021. **9**(7): p. 793.

127. Ecker, J.W., et al., *High-Yield Expression and Purification of Recombinant Influenza Virus Proteins from Stably-Transfected Mammalian Cell Lines.* Vaccines (Basel), 2020. **8**(3): p. 462.

128. Epperson, S., et al., *Update: Influenza activity—United States and worldwide, May 19–September 28, 2019, and composition of the 2020 southern hemisphere influenza vaccine.* Morbidity and Mortality Weekly Report, 2019. **68**(40): p. 880.

129. Grohskopf, L.A., et al., *Prevention and control of seasonal influenza with vaccines: recommendations of the Advisory Committee on Immunization Practices—United States, 2020–21 influenza season.* MMWR Recommendations and Reports, 2020. **69**(8): p. 1.

130. Bashe Jr, W.J., et al., *Failure of polyvalent vaccine to provide clinical protection against Asian influenza.* New England Journal of Medicine, 1964. **270**(17): p. 870-874.

131. Maynard, J., et al., *Evaluation of monovalent and polyvalent influenza vaccines during an epidemic of type A2 and B influenza.* American Journal of Epidemiology, 1968. **87**(1): p. 148-57.

132. Abreu, R.B., et al., *Preexisting subtype immunodominance shapes memory B cell recall response to influenza vaccination.* JCI insight, 2020. **5**(1).

133. Lee, H., E.H. Shim, and S. You, *Immunodominance hierarchy of influenza subtype-specific neutralizing antibody response as a hurdle to effectiveness of polyvalent vaccine.* Human Vaccines & Immunotherapeutics, 2018. **14**(10): p. 2537-2539.

134. Guess, H.A., *Combination vaccines: issues in evaluation of effectiveness and safety.* Epidemiologic Reviews, 1999. **21**(1): p. 89-95.

135. Smith, J., M. Lipsitch, and J.W. Almond, *Vaccine production, distribution, access, and uptake.* The Lancet, 2011. **378**(9789): p. 428-438.

136. Robbins, J., et al., *Considerations for formulating the second-generation pneumococcal capsular polysaccharide vaccine with emphasis on the cross-reactive types within groups.* The Journal of Infectious Diseases, 1983. **148**(6): p. 1136-1159.

137. Houser, K.V., et al., *Impact of prior seasonal H3N2 influenza vaccination or infection on protection and transmission of emerging variants of influenza A (H3N2) v virus in ferrets.* Journal of Virology, 2013. **87**(24): p. 13480-13489.

138. McLaren, C., et al., *Effect of priming infection on serologic response to whole and subunit influenza virus vaccines in animals.* Journal of Infectious Diseases, 1977. **136**(Supplement_3): p. S706-S711.